UNIVERSITÀ DEGLI STUDI DI TRIESTE

XXVIII CICLO DEL DOTTORATO DI RICERCA IN BIOMEDICINA MOLECOLARE

Epigenetic regulation of telomeres: TERRA non-coding RNA and chromatin structure

Settore scientifico-disciplinare: **BIO11**

DOTTORANDA
ELEONORA PETTI

COORDINATORE
PROF. GUIDALBERTO MANFIOLETTI

SUPERVISORE DI TESI
PROF. STEFAN SCHOEFTNER

ANNO ACCADEMICO 2014 / 2015

UNIVERSITÀ DEGLI STUDI DI TRIESTE

XXVIII CICLO DEL DOTTORATO DI RICERCA IN BIOMEDICINA MOLECOLARE

Epigenetic regulation of telomeres: TERRA non coding RNA and chromatin structure

Settore scientifico-disciplinare: **BIO11**

DOTTORANDA
ELEONORA PETTI

COORDINATORE
PROF. GUIDALBERTO MANFIOLETTI

SUPERVISORE DI TESI
PROF. STEFAN SCHOEFTNER

ANNO ACCADEMICO 2014 / 2015

To you…

ACAB box, Cajal body-specific localization signal

ALT, Alternative Lengthening of Telomeres

APB, ALT-associated promyelocytic leukaemia (PML) body

ATM, Ataxia Telangiectasia mutated

ATR, ATM and rad3-related

ATRIP, ATR interacting protein

ATRX, alpha thalassemia/mental retardation syndrome X-linked

BIR, break-induced replication

BLM, Bloom syndrome protein, RecQ helicase-like

BRCA1/2, breast cancer type 1/2 susceptibility protein

53BP1, p53 binding protein

EXOSC 3/10, exoribonuclease exosome component 3/10

CDC proteins, cell-division cycle

CDK, cyclin-dependent kinase

CFS, common fragile site

CHK1, checkpoint kinase 1

CHK2, checkpoint kinase 2

CO-FISH, chromosome orientation fluorescence in situ hybridization

CTE, C-terminal domain

DDR, DNA damage response

D-loop, displacement loop

DAXX, Death domain-associated protein 6

DSB, double strand break

dsDNA, double-stranded DNA

DKC, Dyskerin

DNMT, DNA methyltransferase

ECTR, extra chromosomal telomeric repeat

ERF, early replicating fragile site

FANC, Fanconi anemia

FEN1, Flap endonuclease 1

ERCC1, DNA excision repair protein ERCC-1Fbx4, F-box protein 4

G4, G-quadruplex

GAR, Gly/Arg rich domain

GBM, glioblastoma multiforme

HAT, histone acethyltransferase

HDAC, histone deacetylase

HMT, histone methyltransferase

HP, heterochromatin protein

HR, homologous recombination

ICF syndrome, immunodeficiency, centromeric instability, facial anomalies

iDDR domain, inhibitor of DNA damage response domain

LSD1, lysine-specific demethylase 1

MDC1, mediator of DNA damage checkpoint protein 1

MEF, mouse embryonic fibroblast

MLL, mixed-lineage leukaemia

MRN complex, MRE11-RAD50-NBS1

MTS, multitelomeric signal

NER, nucleotide excision repair

NHEJ, non-homologous end joining

NMD, nonsense-mediated RNA decay

NONO, non-POU domain containing octamer binding

PIKK, phosphatidylinositol 3-kinase-like-protein kinase

PML bodies, promyelocytic leukaemia nuclear bodies

POT1, protection of telomeres 1

PSF, polypyrimidine tract-binding protein-associated splicing factor

P53, tumor suppressor p53

P54nrb, nuclear RNA-binding protein 54kDa

ORC1, origin recognition complex

RAD21, radiation-sensitive 21

RAP1, repressor-activator protein 1

RAD50/51 family, DNA repair proteins

RH1, RNase H1

RNP, ribonucleoprotein

RPA, replication protein A

RTEL, regulator of telomere length

scaRNA, small Cajal-body specific RNA

SFPQ, splicing factor proline/glutamine-rich

snoRNA, small Nucleolar RNA

Sp1, specific protein 1

ssDNA, single-stranded DNA

Suv39h1, suppressor of variegation 3-9 homolog 1

TCAB1, telomerase Cajal Body protein 1

TDM, double-minute chromosome

TEN, N-terminal domain

TERC, telomerase RNA component

TERRA, telomeric repeat-containing RNA

TERT, telomerase reverse transcriptase

TIF, telomere dysfunction induced DNA damage foci

TIN2, TERF1-interacting nuclear factor 2

TMM, telomere maintenance mechanism

TOP1, topoisomerase 1

TOPOIIα, topoisomerase II α

TPE, telomere position effect

TPP1, POT1 and TIN2-interacting protein

TRBD, telomerase RNA-binding Domain

TRF1, telomere Repeat binding Factor 1

TRF2, telomere Repeat binding Factor 2

TSA, trichostatin A

T-SCE, telomere sister chromatid exchange

UFB, ultrafine bridge

WRN, Werner syndrome ATP-dependent helicase

ABSTRACT

Telomeres are nucleoprotein structures located at the physical ends of eukaryotic chromosomes that ensure genome integrity. Dynamic changes in telomere length and structure play key roles in replicative aging, genome stability and cancer. A repressive chromatin structure is a common feature of telomeric repeats from yeast to man and plays an important role in the control of telomere length homeostasis and telomeric recombination. The chromatin structure of telomeric repeats is defined by the H3K9 specific histone methyltransferases (HMTases) Suv39h1 and Suv39h2. The imposition of H3K9me3 provides a high-affinity binding site for HP1 and the sequential recruitment of the Suv4-20h1 and Suv4-20h2 HTMases to establish constitutive heterochromatin at telomeres. Notably, the heterochromatin at telomeres and subtelomeres remains still permissive for transcription. DNA methylation sensitive subtelomeric promoters recruit RNA polymerase II that gives rise to 0.1 – 9kb UUAGGG repeat containing long non-coding RNAs (TERRA, telomeric repeat-containing RNA). TERRA is a nuclear RNA that associates with telomeric chromatin and contributes to heterochromatin formation. In addition, TERRA has been connected to pathways of telomere homeostasis including telomere length regulation, replication, recombination and the DNA damage response. Providing an assembly platform for a variety of proteins, TERRA may sustain additional pathways of telomere regulation.

My PhD thesis aimed to define the impact of Suv39h1 overexpression on telomere homeostasis and carcinogenesis using a transgenic mouse model (**project 1**) and to obtain new insights into the molecular function of TERRA in telomere regulation by identifying novel proteins with binding specificity for TERRA (**project 2**).

Project 1: Altered telomere homeostasis and resistance to carcinogenesis in Suv39h1 transgenic mice

We use a transgenic mouse model system to study the impact of Suv39h1 on telomere homeostasis and carcinogenesis *in vivo*. Suv39h1 overexpression enhances the imposition of H3K9me3 levels at constitutive heterochromatin at telomeres in primary mouse embryonic fibroblasts and is linked with telomere shortening. We further show that increased Suv39h1 levels results in an impaired clonogenic potential of transgenic

epidermal stem cells and Ras/E1A transduced transgenic primary mouse embryonic fibroblasts. Importantly, Suv39h1 overexpression confers resistance to skin carcinogenesis. Our results provide evidence that Suv39h1 controls telomere homeostasis and mediates resistance to oncogenic stress *in vivo*.

Project 2: Identification of novel TERRA interactors that control mammalian telomeres

An RNA pull-down approach followed by mass spectrometry identified two novel TERRA interacting proteins that belong to the Drosophila behavior human splicing family (DBHS): polypyrimidine tract-binding protein-associated splicing factor (PSF) and the nuclear RNA-binding protein 54 kDa (p54nrb). PSF and p54nrb form a complex and are multifunctional regulators of RNA metabolism, transcription and DNA damage repair.

We demonstrated that the PSF/p54nrb complex locates at telomeres and prevents telomere fragility and telomeric recombination by suppressing telomere:TERRA DNA-RNA hybrids formation. In particular, we found that depletion of p54nrb and PSF correlates with an accumulation of nuclear TERRA foci and activation of DNA damage response at telomeres. Elucidating the mechanism by which p54nrb and PSF depletion leads to dysfunctional telomeres, we found an increased loading of RPA32pSer33 to telomeres, demonstrating replicative stress at chromosome ends. This effect is caused by an increased amount of telomere:TERRA DNA-RNA hybrids that results the exposure of the TTAGGG containing, telomeric lagging strand. This type of structure is named R-loop and represents an obstacle for the replication machinery; consequently telomeric R-loops could impede correct replication of chromosome ends and induce telomere fragility. In line with this, Chromosome Orientation FISH (CO-FISH) analysis revealed that depletion of p54nrb selectively increases lagging strand telomere fragility in U2-OS. Unexpectedly, PSF RNAi causes reduced lagging strand telomere fragility compared to control cells. However, this effect is paralleled by a drastic increase of Telomeric Sister Chromatid Exchange (T-SCE) frequency. Essentially, loss of PSF unleashes the Homologous Recombination (HR) machinery at telomeres, allowing the rescue of telomere fragility and promoting telomere elongation in ALT cells. Altogether, we demonstrate that PSF/p54nrb complex is essential to suppress telomere:TERRA DNA-RNA hybrids formation thereby preventing telomeres fragility and recombination. This represents a new molecular mechanism that is essential to safeguard telomere stability in human cancer cells.

1. Introduction

1.1 Telomeres: general features

1.1.1 Historic background of telomere biology

Telomeres are nucleoprotein structures located at the physical ends of eukaryotic chromosomes. Their unique role in the maintenance of genome integrity was revealed by the pioneering studies of the geneticists Hermann J. Muller and Barbara McClintock in 1930s. Hermann J. Muller working with *Drosophila melanogaster*, observed that the ends of irradiated chromosomes differently from the rest of the genome did not present alterations such as deletions or inversions. This observation suggested the existence of a protective cap essential for chromosome integrity. He decided to name these caps "telomeres", meaning: *telos* (end) and *meros* (part) (Muller H.J. et al. 1938). Independently, Barbara McClintock, who used corn (*Zea mays*) for her studies on genetics, described that the rupture of the chromosomes induced by X-ray irradiation resulted in the fusion of their ends giving rise to dicentric chromosomes (McClintock B. et al. 1939). According to their conclusions, telomeres play a crucial role in chromosome end protection, genome stability and faithful segregation of chromosomes during cell division.

About 30 years after Muller and McClintock, new evidences in the field of molecular and cellular biology contributed to define the role of telomeres. In the early 1960s, Leonard Hayflick described that human primary fibroblasts have a limited proliferative potential in cell culture. Fibroblasts were found to divide between 60 and 80 times before entering in a state, called senescence, in which the cells are arrested in the cell cycle but remain metabolically active (Hayflick L. 1965). Ten years later, when the mechanisms subjacent to the replication of the deoxyribonucleic acid (DNA) were revealed, James Watson identified the "end replication problem". The end replication problem describes the incapacity of eukaryotic cells to completely replicate the linear ends of the DNA: DNA polymerases synthesize DNA in the 5′→ 3′ direction using a 8-12 base segment of RNA as a primer. The leading strand can be continuously synthesized while the lagging strand is synthesized in short RNA-primed Okazaki fragments. After extension, the RNA primers are removed and resulting gaps are filled by DNA polymerase priming from upstream DNA 3′

ends. Removal of the most distal RNA primer located at the very end of the chromosome generates a gap of 8-12nt that cannot be filled up (Figure 1.1)(Watson J.D. 1972). In that way, proliferating human somatic cells show progressively shorter telomeres after each round of cell division.

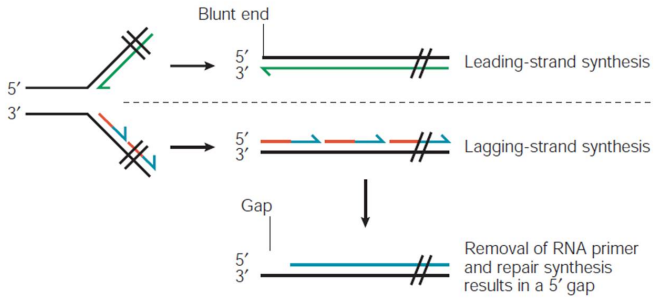

Figure 1.1. Semi-conservative DNA synthesis implicates the end-replication problem. Failure to fill in the gap resulting from the removal of the most distal RNA primer leads to a small loss of DNA in each round of DNA replication (taken from Vega L.R. et al. 2003).

The russian scientist Alexsei Olovnikov linked the so called "Hayflick limit" and the problem of terminal replication. He proposed that the "end replication problem" causes the progressive telomere shortening and it acts as an internal clock to determine the number of divisions that a cell could experience throughout its life thereby controlling organismal aging (Olovnikov A.M. 1973). These evidences also suggested that the cells might have a strategy to maintain their telomeric length during normal DNA replication. A key step to understand this strategy consisted in the identification of telomeric DNA sequence and the telomerase reverse transcriptase. The first chromosome terminal DNA sequence was identified in *Ciliates* such as *Tetrahymena* or *Oxytricha* that show a distinct organization of genomic DNA than other eukaryotic organisms. In particular, *Tetrahymena* and *Oxytricha* contain a micronucleus with normal chromosomes and a macronucleus that contains fragmented chromosomes consisting of multiple small segments of DNA that encode ribosomal RNA (rDNA) (Blackburn E.H and Gall J.G. 1978; Gall J.G 1974). The ends of these DNA molecules were found to contain multiple repetitions of a hexanucleotid CCCCAA/GGGGTT, that were subsequently also identified at the end of chromosomes located in the micronucleous (Yao M.C. et al. 1981). Importantly, Jack W. Szostak and Elizabeth H. Blackburn were able to demonstrate that repetitive sequences of *Tetrahymena* located at the end of a linear plasmid stabilize DNA

fragment in *S. cerevisiae,* thus acting as telomere (Szostak J.W. and Blackburn E.H. 1982). Similar results were also obtained removing one *Tetrahymena* telomere by restriction enzyme digestion and adding the yeast telomeres to the ends of *Tetrahymena* chromosomes (Shampay J. et al. 1984). This provided strong evidence for a high evolutionary conservation of the telomeric sequence and function. Using similar strategy human telomeres were joined to artificial chromosome in *S. cerevisiae*. As expected, the chimeric yeast-human chromosomes propagated like linear chromosomes (Riethman H.C. et al. 1989). The study of telomere sequences of diverse species revealed that telomeres consist of TG-rich tandem repeats that can have a size range from several hundreds base pairs in yeast to tens of kilobases in mammals (Meyne J. et al. 1989) (Table 1).

Species	Telomere length	Telomere sequence
Ciliates		
Protozoan (*T. thermophila*)	120–420 bp	T_2G_4
Yeast		
Baker's yeast (*S. cerevisiae*)	200–300 bp	$TG_{2-3}(TG)_{1-6}$
Vertebrates		
Humans	5–15 kb	T_2AG_3
Mice	Up to 150 kb	T_2AG_3
Rats	20–100 kb	T_2AG_3
Birds	5–20 kb	T_2AG_3
Invertebrate		
Ants	9–13 kb	T_2AG_2
Plants		
Thale cress (*A. thaliana*)	2–5 kb	T_3AG_3

Table 1. Telomere length and telomere sequence in different species (taken from Oeseburg H. et al. 2010).

In 1985, Elizabeth Blackburn and Carol Greider discovered the molecular mechanism that maintains telomere length in eukaryotic cells. They used extracts of cells of *T. thermophila* and synthetic telomeric primers. Their results demonstrated *de novo* synthesis of tandem TTGGGG repeats, which were added to the oligonucleotide primers. The enzyme executing this function was defined as telomere terminal transferase, or telomerase (Greider C.W. and Blackburn E.H. 1985).

1.1.2 Vertebrate telomere sequence and structure

In mammals, chromosome ends are composed of 5′-TTAGGG-3′ tandem repeats (G-rich strand) and a complementary sequence 3′-AATCCC-5′, defined as C-rich strand (Figure

1.2A). Human telomere length is typically 10–15 kilobases (kb) at birth, whereas the telomeres of laborarory mice and rats are 20-50 kb (Palm W. and de Lange T. 2008). The terminus of mammalian telomeres is not blunt-ended, but consists of a single-stranded protrusion of the G-strand, reffered to as the "G-overhang" that varies between 50-500 nt (Figure.1.2A) (McElligott R. and Wellinger R.J. 1997). Experiments focussing on the physical structure of chromosome ends in mouse and human revealed that protein-free DNA is organized in a large, looped structure called "t-loop" (Griffith J.D. et al. 1999) (Figure 1.2B-C). In fact, the 3′-end of G-strand telomere (G-overhang) invades a region of telomeric double-stranded DNA (dsDNA) to form a displacement-loop (D-loop) and a looped region of double stranded telomere repeats (T-loop) (Nikitina T. and Woodcock C.L. 2004). On the functional level the T-loop structure masks the DNA terminus from DNA double-stranded break (DSB) repair machinery and limits the access of telomerase (Griffith J.D. et al. 1999).

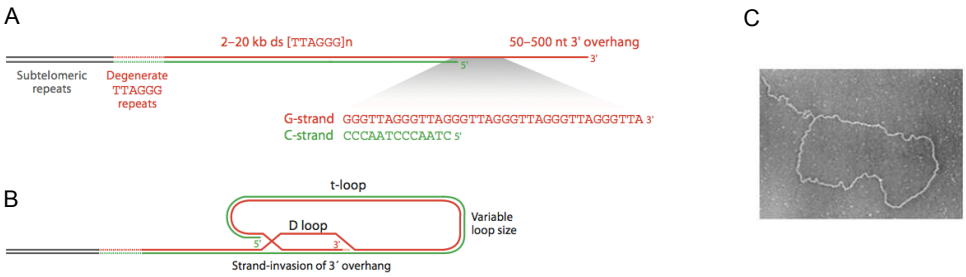

Figure 1.2. The structure of human telomeres. A. Human chromosomes ends consist of an array of TTAGGG repeats that varies in length. Proximal to the telomeric repeats is a segment of degenerate repeats and subtelomeric repetitive elements. The telomere terminus contains a long G-strand overhang. **B**. Telomeric 3′-overhang folds up and invades the double-stranded DNA forming D-loop and T-loop structure. **C**. Representative image of T-loop structure captured by electron microscope. (taken from Palm W. and de Lange T. 2008).

1.1.3 Protein complexes that regulate telomere homeostasis

1.1.3.1 The Telomerase complex

Normal somatic cells can perform a limited number of cell division before entering senescence. In contrast, stem cells or cancer cells can proliferate indefinitely due to the activity of a reverse transcriptase named "telomerase" that compensates telomere attrition caused by the end replication problem. Telomerase complex core components are the telomerase reverse transcriptase catalytic subunit (TERT in mouse and human) and the

RNA component (TERC in mouse, hTR in human) (Smogorzewska A. and de Lange T. 2004). The telomerase catalytic subunit (TERT) recognizes the 3'OH of the G-overhang and synthesizes TTAGGG repeats using the RNA component (TERC) as a template. In addition to TERT and TERC, other proteins that regulate the biogenesis and correct assembly of telomerase *in vivo* are part of the telomerase complex: TCAB1, dyskerin and its associated proteins NHP2, NOP10, GAR1 (Chan S.R. and Blackburn E.H. 2004, Smogorzewska A. and de Lange T. 2004).

Human telomerase consists of two subunits of TERT and two TERC molecules (Cohen S.B. et al. 2007) (Figure.1.3A). The catalytic subunit is a 127kDa protein that contains four functional domains: N-terminal domain (TEN), a RNA binding domain (TRBD), the reverse transcriptase domain (RT) and the conserved C-terminal domain (CTE) (Figure. 1.3B). Thanks to the TEN domain, the enzyme binds to the single-stranded G-overhang and performs the catalytic reaction using the RT domain (Chen J.L. and Greider C.W. 2003; Lai C.K. et al. 2003; Jacobs S.A. et al. 2006; Mitchell M. et al. 2010). The TRBD is essential for ribonucleoprotein assembly (Rouda S. and Skordalakes E. 2007; Mitchell M. et al 2010), while the CTE is especially implicated in DNA-RNA binding and processivity (Gillis A.J. et al. 2008; Mitchell M. et al 2010).

The second key telomerase component TERC is transcribed by RNA polymerase II and has a size of 451 nucleotides in humans (Feng J. et al. 1995). TERC contains a core domain that includes the template for reverse transcription (5'-CUAACCCUAAC-3') and conserved regions (CR3, CR4, CR6, CR7, CR8) that are used as anchor points for the sequence alignment. Remarkably, telomerase RNA contains a H/ACA box and a CAB box motif that define two classes of non-coding RNAs: the Small nucleolar RNAs (snoRNAs) and the Small Cajal-body specific RNAs (scaRNAs), respectively (Chen J.L. et al. 2000) (Figure 1.3A). The H/ACA box represents a binding site for dyskerin, an RNA-binding protein that together with three associated proteins (NHP2, NOP10, GAR1) controls the stability of TERC (Meier U.T. 2005; Pogacic V. et al. 2000; Artandi S.E. and DePinho R.A. 2009). Differently, the CAB box of TERC is a binding site for the Cajal body protein TCAB1 that ensures maturation of the complex in the Cajal bodies (Venteicher A.S. et al. 2009).

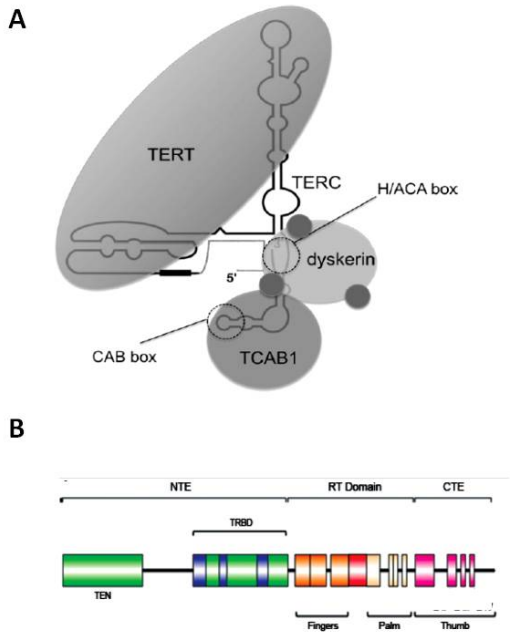

Figure 1.3. Telomerase complex. A. Telomerase is a large RNP. Catalytic subunit TERT and RNA component TERC with associated telomerase factors : TCAB1, dyskerin and its three associated proteins NHP2, NOP10 and GAR (shown as small grey spheres) (Taken from Artandi S.E. and DePinho R.A. 2009). **B**. Predicted linear architecture of human TERT. NTE, RT and CTE domains are indicated (taken from Wyatt H.D.M. et al. 2010).

Important evidence that demonstrates the importance of telomerase in development and disease comes from the generation of Terc knockout mice. Terc knockout mice do not show telomerase activity and are subjected to telomere shortening in successive generations (Blasco M.A. et al. 1997). This finally leads to an anticipated onset of aging related pathologies such as such as alopecia, intestinal atrophy, hair graying, infertility, heart dysfunction, bone marrow aplasia, kidney dysfunction, defective bone marrow and proliferative defects of neural stem cells (Lee H.W. et al. 1998; Herrera E. et al. 1999; Samper E. et al. 2002; Leri A. et al. 2003; Ferron S. et al. 2004; Blasco M.A. 2005; Garcia-Cao I. et al. 2006). Interestingly, in Terc deficient mice critically short telomeres became dysfunctional and are detected as damaged DNA triggering cell cycle arrest or apoptosis at the cellular level (Leri A. et al. 2003; Samper E. et al. 2002; Gonzalez-Suarez E. et al. 2000; d'Adda di Fagagna F. et al. 2003; Takai H. et al. 2003). In line with this, Terc deficient mice are resistant to both induced and spontaneous tumorigenesis (Gonzalez-Suarez E. et al. 2000). This indicates that short telomeres are potent suppressors of cancer. Conversely, overexpression of the telomerase reverse transcriptase in Tert over-expressing mice results in an augmented proliferation of the skin cells that increases susceptibility to skin carcinogenesis (Gonzalez-Suarez E. et al. 2001; Cayuela M.L. et al. 2005; Flores I. et

al. 2005). Telomerase overexpression in mice engineered to be cancer resistant (enhanced expression of the tumor suppressors p53, p16, and p19ARF) demonstrated the impact of telomerase overexpression on organismal aging. In this mouse model, median lifespan was increased of 40% demonstrating an anti-aging activity of Tert in the context of a mammalian organism (Tomas-Loba A. et al. 2008).

1.1.3.2 The Shelterin complex

Telomeric DNA is specifically bound by the multi-protein complex shelterin, that consists of six core components: Telomere Repeat Binding Factors 1 and 2 (TRF1 and TRF2), Protection Of Telomeres 1 (POT1), TRF2- and TRF1-Interacting Nuclear protein 2 (TIN2), TPP1 (known as TINT1, PTOP, or PIP1) and RAP1 (the human ortholog of the yeast Repressor/Activator Protein 1). Shelterin enables cells to distinguish their natural chromosome ends from DNA breaks, thereby suppressing DNA repair reactions at chromosome end (Diotti R. and Loayza D. 2011). In addition, Shelterin regulates telomere replication and recombination as well as telomere length homeostasis.
Shelterin binding specificity for telomeric DNA is mediated by TRF1 and TRF2 that specifically bind to double stranded TTAGGG repeats as homo-dimers or –tetramers (Figure 1.4). POT1 is associated with the single-stranded TTAGGG repeats present at the telomeric 3′-overhang. Mouse genome contains two POT1 orthologs, Pot1a and Pot1b. The other three shelterin proteins: TIN2, TPP1 and RAP1 are indirectly associated to telomeric DNA (De Lange T. 2005). In addition to Shelterin, accessory factors interact dynamically with mammalian telomeres influencing its stability (Diotti R. and Loayza D. 2011).

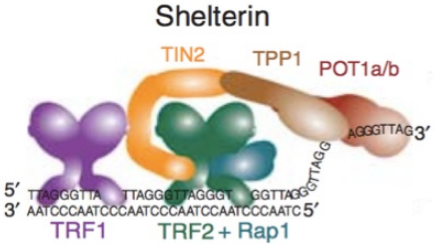

Figure 1.4. Shelterin complex. Schematic of the interactions among the six components of Shelterin and their interaction with telomeric DNA (taken from Doksani Y. and de Lange T. 2014).

Important insights into shelterin function come from mouse model systems. In line with the high relevance of telomeres, single abrogation of TRF1, TRF2, POT1a, TPP1 or TIN2 results in early embryonic lethality (Karlseder J. et al. 2003; Celli G.B. and de Lange T. 2005; Lazzerini Denchi E. et al. 2006; Hockemeyer D. et al. 2006; Wu L. et al. 2006; Kibe T. et al. 2010; Chiang Y.J. et al. 2004). Remarkably, abrogation of RAP1 does not affect mouse viability (Sfeir A. et al. 2010; Martinez P. et al. 2010). Conditional deletion of Trf1 correlates with the induction of senescence and an increase of DNA damage response at telomeres. The abrogation of p53 and pRB pathways in Trf1-deleted cells allows cell proliferation and leads to an increased telomere fragility and chromosomal instability (Martinez et al. 2009; Sfeir A. et al. 2009). Conditional deletion of mouse Trf2 in $p53^{-/-}$ context correlates with a strong damage response at telomeres and the loss of 3'overhang at telomeres, leading to chromosome end to end fusion by the non-homologous end-joining pathway (Celli G.B. and de lange T. 2005). Differently, TRF1 or TRF2 overexpression correlates with telomere shortening and increased chromosomal instability (Munoz P. et al. 2009, Munoz P. et al. 2005). Altogether data from mouse models demonstrate that TRF1 and TRF2 are essential for the survival of the organism and play a critical role in telomere replication, length regulation and protection from DNA damage response and repair.

The role of POT1 in telomere function *in vivo* has been studied using POT1 deficient mouse models. Conditional deletion of Pot1a has been demonstrated to elicit a DNA damage response at telomeres leading to senescence (Wu L. et al. 2006). In addition, Pot1a-deficient cells exhibit an increase in telomere length and telomeric 3' overhang elongation and also show aberrant homologous recombination (HR) at telomeres. Together these results demonstrate the critical role of POT1 in telomere length regulation, suppression of DNA damage response and homologous recombination. Importantly, deletion of TPP1 from mouse embryonic fibroblasts resulted in a release of POT1a and POT1b from telomere (Kibe T. et al. 2010). Furthermore, the telomere dysfunction phenotypes associated with deletion of TPP1 were identical to those of POT1a/POT1b knockdown cells, specifically: suppression of DNA damage response at telomere and 3'overhang elongation.

TIN2 links TPP1/POT1a (and POT1b) to TRF1 and TRF2 on the double-stranded telomeric DNA and its deletion in mouse cells led to the loss of TPP1/POT1a at telomeres causing

accumulation of RPA and the induction of ATR pathway (Takai K.K. et al. 2011). In contrast to other shelterin components, RAP1 is not essential for telomere protection but is important to repress homology-directed repair (HDR) at telomere as observed in Rap1 deficient mouse (Sfeir A. et al. 2010). In addition, RAP1 has been demonstrated to bind to telomeric and extratelomeric sequences in proximity of genes, thus suggesting a role in transcriptional regulation (Martinez P. et al. 2010).
Together these studies demonstrated a well-established role of shelterin complex in the control of telomere length and in the suppression of DNA damage response and repair, but also in telomere replication and recombination.

1.1.4 Telomeres in aging and diseases

Although telomeres represent the part of the genome dedicated to genomic protection, they are sensitive to damage by several mechanisms. As mentioned before, adult human cells have very low or undetectable telomerase activity whereby they encounter telomere attrition during cell divisions that leads to critically short or deprotected telomeres (Blackburn E.H et al. 2006). In addition, telomeric G-rich sequence is more susceptible to oxidative damage reactions (Petersen S. et al. 1998) and DNA replication stress (Sen D. and Gilbert W. 1988; Maizels N. and Gray L.T. 2013). Importantly, telomerase and shelterin complexes play a crucial role in maintenance of telomere length homeostasis and telomere protection and replication, thus ensuring telomere stability.
An inadequate telomere maintenance can cause aging phenotypes as demonstrated by laboratory model systems (see Terc deficient mice in par. 1.1.3.1) and monogenetic "inherited telomere syndromes" (Armanios M. and Blackburn E.H 2012). To date, single-gene inactivating mutations are reported in 11 human genes that encode proteins with a well-established role in telomere maintenance. These include components of telomerase complex (TERC, TERT, DKC1, NOP10, WRAP53) or telomere binding proteins with a protective role (TINF2, RTEL, POT1, CTC1, TPP1) (Armanios M. and Blackburn E.H 2012; Glousker G. et al. 2015). Almost all these diseases correlate with excessive telomere shortening and consequent loss of telomere protection. These syndromes often shared similar characteristics: loss of immune function due to the loss of bone morrow stem cell reserves, specific cancer types, pulmonary fibrosis, gastrointestinal disorders,

neuropsychiatric condictions, diabetes, myocardiacal infarction, hair graying and skin pigmentation (Walne A.J. and Dokal B.J 2009). In addition, similarly to Terc deficient mice that show telomere shortening in successive generations, telomere syndromes show genetic anticipation of mutation in succeeding generations of a family pedigree.
Importantly, telomere maintenance plays a crucial role in tumor formation and progression. To bypass the end replication problem, cancer cell maintain telomere length by different mechanisms that in 90% of tumors correspond to telomerase reactivation (for more details see par. 1.4). Interestingly, mutations in Pot1 gene correlate with telomeric protection defects and cause a specific glioma type (Walsh K.M. et al. 2013).
Altogether this demonstrates how telomeres are important players at the interface between cancer and aging.

1.2 DNA damage control at telomeres

1.2.1 DNA damage response in mammalian cells

During their lifespan, eukaryotic cells are continuously exposed to intrinsic and extrinsic sources of DNA damage, a threat to genome integrity. To counteract this problem cells developed the DNA damage response pathways (DDR). DNA damage factors can be divided into three groups: sensors, transducers, and effectors depending on their function and the phase of the DDR they take part (Zhou B.B. and Elledge S.J. 2000).
The two most important transducers of DNA damage response belong to phosphatidylinositol 3-kinase-like-protein kinase family (PIKKs) and are represented by ATM (Ataxia telangiectasia mutated) and ATR (ATM and Rad3-related protein) kinases (Lempiainen H. and Halazonetis T.D. 2009; Lovejoy C.A. and Cortez D. 2009). ATM protein was identified in the human genetic disorder ataxia-telangiectasia that causes hypersensitivity to radiation and a defective response to a specific DNA lesion (Metcalfe J.A. et al. 1996; Pandita T.K. 2002). In contrast to ATM, ATR is essential for the cells, its deletion leads to early embryonic lethality in mouse and cell lethality in human cells (Brown E.J. and Baltimore D. 2000, 2003; de Klein A. et al. 2000; Cortez D. et al. 2001). This underlines that ATM and ATR are essential to signal DNA lesions and to induce a DNA damage response that finally activates DNA repair pathways. Importantly, ATM and ATR have a well-established role in signaling DNA damage at critically short or

dysfunctional telomeres thus ensuring telomere stability (Karlseder J. et al. 1999; d'Adda di Fagagna F. et al. 2003; de Lange T. 2009; Mcnees C.J. et al. 2010; Takai K.K. et al. 2011). Interestingly, very recent works demonstrated additional roles of ATM and ATR at telomeres. In fact, ATM and ATR have been demonstrated to recruits telomerase to telomeres and ATM in addition, is required for telomere elongation *in vivo* (Tong A.S. et al. 2015; Lee S.S et al. 2015). These findings add further relevance to the crucial role performed by ATM and ATR at telomeres and explain the long-standing observation of short telomeres in the ATM-deficient cells derived from ataxia telangiectasia (AT) patients (Metcalfe J.A. et al. 1996; Smilenov L.B. et al. 1997).

In mammalian cells, the main sensor of ATM pathway is the MRN complex composed by Mre11-Rad50-Nbs1 that recruits and activates ATM (Figure 1.5). ATM is activated not only by double-stranded DNA breaks (DSBs), but also by dsDNA ends with short single stranded DNA (ssDNA) that resembles "uncapped telomere" (Shiotani B. and Zou L. 2009; Celli G.B. and de Lange T. 2005). After activation of ATM, the subsequent events are: the phosphorylation of the histone variant γH2AX at the site of DNA damage by ATM (Meier A. et al. 2007; Savic V. et al. 2009), the spreading of γH2AX along the chromatin through the interaction with MDC1 (Stewart G.S. et al. 2003; Lee M.S. et al. 2005; Stucki M. et al. 2005; Lou Z. et al. 2006), accumulation of DNA-damage mediator 53BP1 and consequent activation of CHK2 downstream kinase (Shiloh Y. 2003; Lavin M.F. 2008).

ATR is activated in response to different types of DNA damage, including DSBs, base adducts, crosslinks and replication stress. However a single DNA structure is responsible for ATR activation and this structure contains single-stranded DNA (ssDNA) (Zhou B.B. and Elledge S.J. 2000; Jazayeri A. et al. 2006; Cimprich K.A. et al. 2008). The current model for ATR activation proposes that ATR is recruited at the site of DNA damage, or replication stress, and interacts with its cofactor ATRIP (ATR-Interacting Protein) that binds directly to RPA-coated ssDNA (Figure 1.5) (Zou L. et al. 2003; Ball H.L. et al 2005; Cortez D. et al. 2001). Importantly, activation of ATR requires the recruitment of ATR activators: the checkpoint clamp Rad9-Hus1-Rad1 (9-1-1 complex) that needs the Rad17-Rfc2-5 clamp to be loaded at stalled replication forks, TOBP1 and claspin (Cimprich K.A. et al. 2008). All these factors allow full activation of ATR. Recent data suggest that autophosphorylation of ATR is also important for its kinase activity (Liu S. et al. 2011). To

coordinates cell cycle arrest or fork restart ATR phosphorylates chromatin bound or soluble substrates. Among these, there are: γH2AX, the RPA2 subunit of RPA, subunits of ORC complex, DNA polymerase ε, and the CHK1 downstream kinase (Ward I.M. et al. 2001; Carty M.P et al. 1994; Robison J.G. et al. 2004; Matsuoka S. et al. 2007; Liu Q. et al. 2000). Claspin and TOPBP1 are necessary to induce CHK1 phosphorylation (Lee J. et al. 2003). TOPBP1 is a multi-functional protein that plays a role in both DNA synthesis and checkpoint activation and its interaction with MDC1 is important for CHK1 phosphorylation (Wang J. et al. 2011).

The cell cycle checkpoint kinases CHK2 and CHK1 are the main downstream kinases of ATM and ATR, respectively. These two kinases act to reduce cyclin-dependent kinase (CDK) activity by various mechanisms, some of which are mediated by activation of the p53 transcription factor or by inhibition of the phosphatases CDC25 (Bartek J. and Lukas J. 2007; Riley T. et al. 2008; Kastan M. B. and Bartek J. 2004). p53 and the CDC25 phosphatase represent the bottom elements (effectors) of DNA damage response signaling cascade that interface these pathways with the core of the cell-cycle progression machinery in order to induce a transient arrest, apoptosis, or senescence.

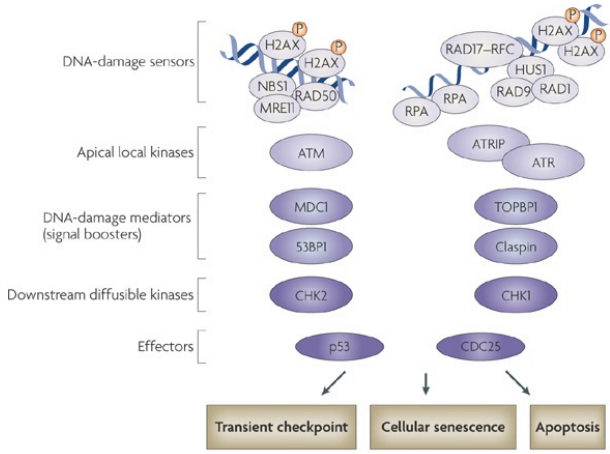

Figure 1.5. DNA damage response. The DDR is activated by DSBs and/or by the single-stranded DNA coated by RPA. DSBs are sensed by the MRE11–RAD50–NBS1 (MRN) complex that recruits the protein kinase ATM. ATM undergoes autophosphorylation and phosphorylates the histone H2A variant H2AX at the site of DNA damage. γH2AX is recognized by MDC1. MDC1 recruitment to γH2AX fuels the additional accumulation of MRN (to which MDC1 binds), which leads to amplified local ATM activity and the spreading of H2AX along the chromatin from the DSB. Exposure of modified histone residues further boosts the accumulation of the DNA-damage mediator 53BP1 at the sites of DNA damage, in addition to the ability of 53BP1 to bind to MDC1 directly. Phosphorylation and activation of the protein kinase CHK2 by ATM is dependent on MDC1 and 53BP1. RPA-coated single-stranded DNA triggers the recruitment of the heterodimeric complex ATR /ATRIP. ATR activity is boosted by additional ATR targets, such as the RAD9–HUS1–RAD1 (9–1–1) and RAD17–RFC complexes. In addition, ATR activity is stimulated by TOPBP1 and claspin, which is necessary for CHK1 phosphorylation. Both CHK1 and CHK2 are responsible for DDR signalling in distant nuclear regions from the DNA-damage site. Finally, p53 and the CDC25 phosphatases are the bottom elements of the DDR signalling cascade that interface this pathway with the core of the cell-cycle progression machinery. DDR-mediated arrest can be transient, and if DNA damage is effectively removed cells resume normal proliferation. However, if DNA damage is particularly severe, cells may undergo apoptosis or enter a protracted DDR-induced cell-cycle arrest that is termed cellular senescence (taken from D'adda di Fagagna F. 2008).

1.2.2 Repression of DNA damage response at telomeres

Shelterin allows t-loop formation that prevents telomeres from being recognized as double-stranded breaks by DNA damage signalling (Griffith J.D. et al. 1999). Dysfunctional telomeres could arise through natural or experimentally induced attrition of telomeric DNA or by inhibition or depletion of shelterin components. Uncapped chromosome ends are recognized as DSBs by the DDR pathways leading to the accumulation of DNA damage sensors such as 53BP1, MDC1 or γH2AX at telomeres. The association of these DDR factors with dysfunctional telomeres forms structures called telomere dysfunction induced DNA damage foci (TIFs) that can be visualized in immunofluorescence stainings (Figure 1.6, left panel) (Takai H. et al. 2003; d'Adda di Fagagna F. et al. 2003; Dimitrova N. and de Lange T. 2006). Loss of function experiments have shown the specific contribution of the different shelterin components in eliciting ATM/ATR activation at telomere. In particular, TRF2 has a major role in preventing ATM activation, while POT1/TPP1 and TRF1 are most involved in ATR signaling inhibition.

Deletion of TRF2 in mouse cells or its inhibition with a dominant negative allele in human cells, results in a DDR mediated by ATM (Celli G.B. and de Lange T. 2005; Karlseder J. et al. 1999) (Figure. 1.6, right panel). Recent data support a two-step mechanism for TRF2-mediated end protection (Okamoto K. et al. 2013). The initial step requires the dimerization domain of TRF2 that inhibits ATM activation. Next, TRF2 independently modulates the propagation of DNA damage signaling downstream of ATM activation, inhibiting the E3 ubiquitin ligase RNF168 at telomeres and consequently, preventing 53BP1 localization and chromosome fusions (Okamoto K. et al. 2013).

To prevent ATR activation TPP1/POT1a bind single-stranded telomeric DNA excluding RPA binding at telomeres (Figure. 1.6, right panel)(Takai K.K. et al. 2011). In addition, TIN2 is necessary for preventing ATR activation by TPP1/POT1a stabilization on the single stranded telomeric DNA.

Conditional TRF1-deleted mouse embryonic fibroblasts (MEFs) show the activation of DNA damage response showed by abundant telomere γH2AX foci and ATM/ATR activation at chromosome ends (Martìnez P. et al. 2009; Sfeir A. et al. 2009). In addition, recent evidences introduced also a role of TRF1 in mediating replication stress-induced ATR signaling by a mechanism that involves TIN2-dependent recruitment of the TPP1/POT1 heterodimers to exclude RPA from the lagging strand template (Zimmermann

M. et al. 2014). Together these data demonstrate that Shelterin suppresses DNA damage response at telomeres.

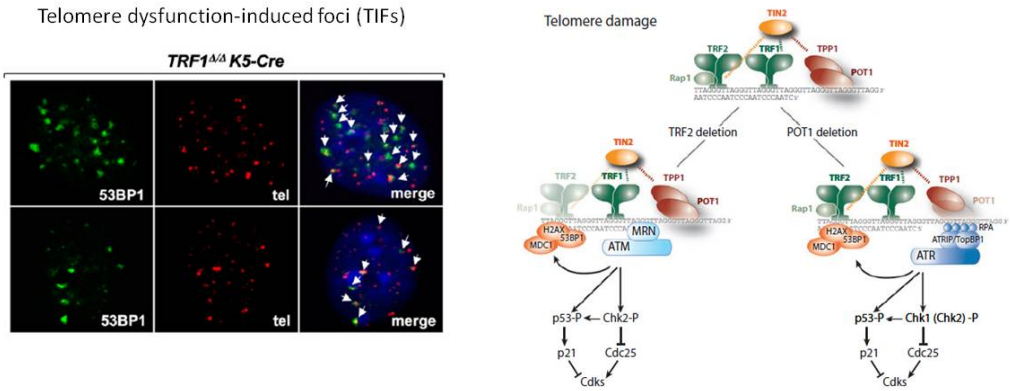

Figure 1.6. DNA damage response at telomere. Representative images of TIFs in TRF1-deleted mouse embryonic fibroblasts. Co-localization of 53BP1 and telomeric probe indicate an activation of DNA damage response at telomere (left panel) (taken from Martinez P. et al. 2009). Representative model of telomere damage response regulated by Shelterin complex. TRF2 deletion induces the activation of ATM pathway due to the unprotected dsDNA at chromosome end; in contrast POT1 deletion leads to RPA recruitment at 3'-overhang triggering the activation of ATR pathway (right panel) (taken from Palm W. and de Lange L. 2008).

1.3 Telomeric DNA damage repair

In addition to block DNA damage signaling, mammalian telomeres have to protect chromosome ends by the threat of DNA repair pathways: the non-homologous end joining (NHEJ) and the homology-directed repair (HDR) (Doksani Y. and de Lange T. 2014). NHEJ is the predominant repair mechanism in mammalian cells and it acts quickly by sealing the breaks and inducing chromosome fusions with the consequent formation of microdeletions. In contrast, HDR is a complex high-fidelity repair mechanism based on homologous recombination that can lead to changes in telomere length.

1.3.1 Repression of NHEJ

Dysfunctional telomeres are threatened by classical NHEJ repair pathway dependent on the activity of Ku70/80 and DNA ligase IV (Smogorzewska A. et al. 2002; Celli G.B. and de Lange T. 2005; Celli G.B. et al. 2006). NHEJ processing of dysfunctional telomeres results in chromosome fusions (the telomeres of both chromatids are fused to telomeres of other chromosomes), chromatid fusions (a single chromatid fused to another) or sister chromatid fusions (Konishi A. and de Lange T. 2008; Smogorzewska A. et al. 2002; Dimitrova N. and de Lange T. 2009; Hsiao S.J. and Smith S. 2009). Among shelterin

components, TRF2 has a crucial role in the repression of NHEJ: firstly through a mechanism that involves T-loop formation, but also through its recently discovered Inhibitor of DNA Damage Response domain (iDDR domain) (Okamoto K. et al. 2013). This domain interacts with both the MRN complex and the BRCC36 de-ubiquitinating enzyme, inhibiting the loading of 53BP1 at the sites of DNA damage. In addition to TRF2, POT1 and TPP1 have also a role in suppressing NHEJ. This was demonstrated in knockdown experiments for human POT1 or in POT1 knockout mouse cells that result in chromosome end-to-end fusions. In addition, telomere fusions have been observed in cells depleted of TPP1, presumably due to its role in POT1 recruitment and TRF2 stabilization at telomeres (Hockemeyer D. et al. 2007; O'Connor M.S. et al. 2006).

1.3.2 Homology-directed repair reactions at telomeres

In mammalian cells, homologous recombination (HR) represents an accurate mechanism to repair DNA double-strand breaks (DSBs). The presence of tandem repeats and single strand overhangs represents a considerable threat to telomere stability. Three types of HR have been observed at telomeres: i) T-loop homologous recombination, ii) Telomeric Sister Chromatid Exchange (T-SCEs) and iii) Recombination with interstitial sites (Figure 1.7) (Palm W. and de Lange T. 2008).

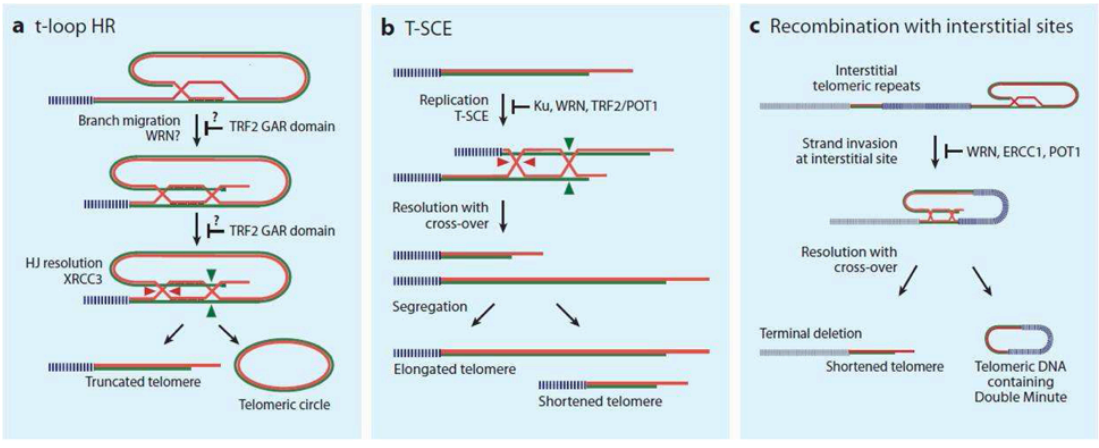

Figure 1.7. Homologous recombination repair at dysfunctional telomeres. a) Excision of the telomeric loop through t-loop HR. b) recombination between sister telomeres. c) recombination between a telomere and chromosome internal telomere-related sequences (taken from Palm W. and de Lange T. 2008).

1.3.2.1 T-loop homologous recombination

The T-loop structure of mammalian telomeres results from the telomeric single stranded 3′ overhang invasion into telomeric double-stranded DNA that generates the so-called D-loop. This strongly resembles an early step of homologous recombination (HR). TRF2 is the main component required for T-loop formation (Doksani Y. et al. 2013). In fact, TRF2 is able to induce topological changes in telomeres (Amiard S. et al. 2007; Poulet A. et al. 2009), but it can also bind Holliday junctions (HJ) with its amino-terminal domain *in vitro* stabilizing strand-invasion process (Fouche N. et al. 2006; Poulet A. et al. 2009). T-loop homologous recombination has been observed in cells overexpressing a TRF2 mutant lacking the amino-terminal domain (Wang R.C. et al. 2004). These cells show telomere shortening and accumulation of circular telomeric DNA (T-circles) formed by the resolution of Holliday Junctions generated by branch migration at the strand invasion point of the t-loop. This mechanism is dependent on XRCC3 resolvase and WRN DNA helicase that is responsible for branch migration in "t-loop HR" (Liu Y. et al. 2004; Li B. et al. 2008; Nora G.J. et al. 2010).

1.3.2.2 Telomeric sister chromatid exchange (T-SCE)

After replication, telomeres of duplicated sister chromatids can recombine. This type of recombination comprises the exchange of sister chromatid telomeric sequences, thus named: Telomeric Sister Chromatid Exchange (T-SCE). T-SCE can be visualized in metaphase chromosomes by Chromosome Orientation Fluorescent in Situ Hybridization (CO-FISH) (Palm W. and de Lange T. 2008). CO-FISH is a strand-specific FISH that involved selective removal of newly replicated strands from DNA of metaphase chromosomes resulting in single-stranded target DNA. The use of two different single stranded telomeric probes (a G-rich probe and a C-rich probe) guarantees a strand-specific hybridization that discriminates between telomeres produced by leading- versus lagging-strand synthesis (for details see Results Figure 3.2.8, Material and Methods par. 2.15) (Bailey S.M. et al. 2004). A merged signal of the two probes at the same chromosome end indicates that T-SCE occurred.

T-SCE can cause an unequal exchange of telomeres and can result that daughter cells inherit shortened telomeres. This leads to a shorter replicative life span in telomerase

negative cells (Doksani Y. and de Lange T. 2014). For this reason, T-SCE frequency has to be stringently controlled. The Ku70/80 heterodimer has been demonstrated to act as crucial repressor of HR at telomeres (Celli G.B. et al. 2006; Wang Y. et al. 2009). In addition, components of the shelterin complex repress the exchanges between sister telomeres. The highest frequency of T-SCE has been observed in cells lacking both TRF2 and Ku70 (15-20% of the chromosome ends) (Celli G.B et al. 2006). Single deletion of TRF2 or Ku70 is not sufficient to induce T-SCE, suggesting that the two proteins have a redundant role in suppressing recombination. Increased T-SCE frequency has also been observed in other settings: in Ku 70/80-deficient mouse cells that also lack Rap1 or both Pot1a and Pot1b (Palm W. et al. 2009; Sfeir A. et al. 2010). How Rap1 or POT1 repress HR has not yet been explained. Rap1/Ku70 double-knockout cells don't show DNA damage signaling at telomeres and undergo HR (Sfeir A. et al. 2010). In addition, the helicase WRN or RTEL1 can repress T-SCEs. In fact, mouse cells with severely shortened telomeres due to telomerase deficiency show high levels of T-SCEs in the absence of WRN. In a similar way, RTEL1 deficient mouse cells or human cells with mutated RTEL show high levels of T-SCEs (Laud P.R. et al. 2005; Sarek G. et al. 2015). Altogether these data indicate a major role of shelterin components and DNA helicases in suppressing T-SCE. This suggests that an unprotected state of telomeres or the accumulation of secondary DNA structures at telomeres favour telomeric recombination.
In addition, increased T-SCE has also been observed in mouse cells that lack telomeric heterochromatin components such as the Suv39h1 and Suv39h2 histon methyltransferases (HTMases), DNA methyl transferases (DNMTases) or retinoblastoma family proteins (Garcia-Cao M. et al. 2004; Gonzalo S. et al. 2005; Gonzalo S. et al. 2006). This demonstrate a role of the repressive chromatin status in preventing recombination at telomeres.

1.3.2.3 Homologous recombination with interstitial sites

The third HDR pathway involves recombination between chromosome internal stretches of TTAGGG repeats with chromosome terminal TTAGGG repeats. This can lead to terminal deletions of all sequence located distal to the interstitial TTAGGG repeats, producing an extrachromosomal element called Double-Minute chromosomes (TDMs).

Such elements includes telomeric sequences and the intrachromosomal telomeric repeats and their size is variable depending on the location of the interstitial sequences (Zhu X.D. et al. 2003; Laud P.R. et al. 2005). In human and mouse cells, this mechanism is not frequent due to the low content of chromosome internal telomeric DNA repeats (Palm W. and De lange T. 2008). However, TDMs have been observed in immortalized mouse embryo fibroblast lacking of the subunit ERCC1, an endonuclease (ERCC1/XRF) recruited to telomere by TRF2 (Zhu X.D. et al. 2003). In addition WRN counteracts TDM formation in presence of short telomere (Laud P.R. et al. 2005). Finally, reduction of POT1a and POT1b in immortalized mouse cells correlates with increased frequency of TDMs (He H. et al. 2006; Wu L. et al. 2006).

1.4 Telomere maintenance mechanisms

As previously reported, eukaryotic genome packaging into discrete linear chromosomes poses the important "end replication problem". It means that in the absence of any counterbalancing lengthening mechanism, progressive telomere shortening during cell proliferation eventually results in telomere dysfunction and a DNA damage response (DDR) at chromosome ends. This phase, in which tumor suppressor genes like p53 and pRb arrest cellular proliferation, is called replicative senescence or mortality stage 1 (M1) (Figure 1.8) (Chatziantonou V.O. 2001). In the case of a loss of p53 or Rb tumor suppressor pathways, cell division is still permitted causing further telomere shortening resulting in an excess of genomic instability and a massive cell death. This phenomenon is called crisis or mortality stage 2 (M2) (Figure 1.8) (Shay J.W. and Wright W.E. 2005).

The bypass of senescence or crisis and acquisition of unlimited replicative potential is a hallmark of tumorigenesis. This step requires the re-activation of Telomere Maintenance Mechanisms (TMMs) that are blocked in primary cells. Telomeres are important in both senescence (M1) and crisis (M2) as hTERT induction either before M1 or after M1 results in cell immortalization (Shay J.W. and Wright W.E. 2005).

In line with this, 90% of all human cancers achieve an indefinite proliferative potential through the upregulation of telomerase activity that is therefore a prime target for anticancer therapies (Shay J.W. and Bacchetti S. 1997). Of the remaining 10% of tumors,

most counteract telomere attrition using a non-telomerase mechanism referred to as Alternative Lengthening of Telomeres (ALT) (Bryan T.M. et al. 1997).

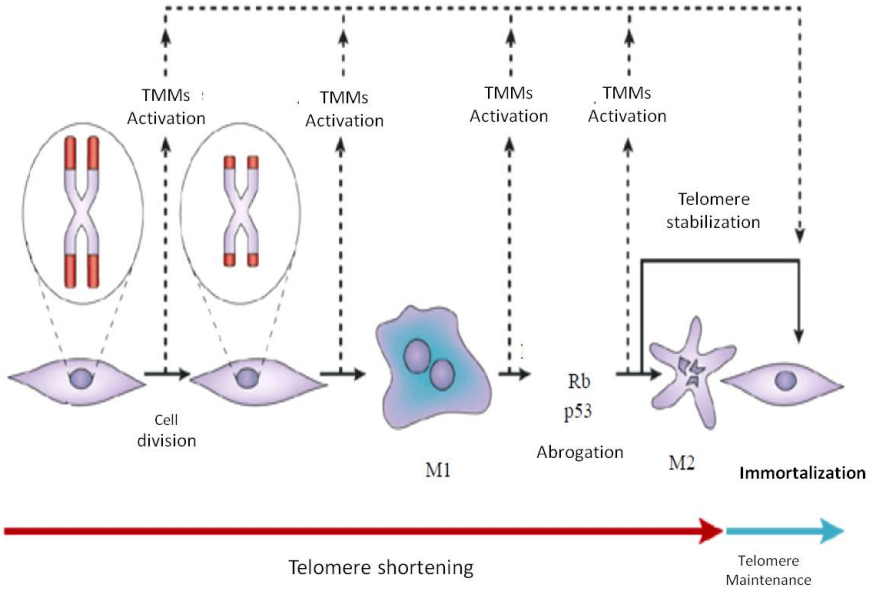

Figure 1.8. Cell fate in response to telomere shortening. Somatic cells can divide for a limited number of cell divisions. When cells reach Hayflick limit, they enter into cell cycle arrest (senescence), called M1 phase. The cells can bypass M1 phase by the abrogation of Rb and p53. Thus, telomeres get shorter finally leading to cell death, called M2 phase. Telomerase re-activation or induction of ALT mechanism in M2 phase lead to telomere maintenance with consequent cell immortalization (modified from Shay J.W. and Wright W.E. 2005).

1.4.1 Mechanisms of reactivation of telomerase activity

Initial studies of TERT expression and telomerase activity demonstrated a strong suppression of hTERT in somatic tissue. Conversely, high telomerase activity in germ cells and cancer cells associated with high expression of TERT consistently with the high proliferative potential of these cells (Kim N.W. et al. 1994).

The activation of telomerase as a mechanism to ensure unlimited cell proliferation is a hallmark for almost all human cancer (Shay J.W. et al. 1997). Several mechanisms have been reported to activate telomerase in cancer. Different oncogenes such as Myc and Wnt transcriptionally activate telomerase (Wu K.J. et. al. 1999; Hoffmeyer K. et al. 2012; Greider C.W. 2012). Alternatively, hTERT expression can be activated by epigenetic alterations or mechanisms involving alternative splicing (Kyo S. and Inoue M. 2002). Moreover, mutations increasing transcriptional activity of TERT promoter have been described in melanomas (Huang F.W. et al. 2013; Horn S. et al. 2013).

Even though telomerase activation can occur early in tumor development, telomerase activity is not necessary for cancer initiation but more importantly it can stimulate tumor progression by allowing telomere maintenance above a critically short length (Hackett J.A. and Greider C.W. 2002). In line with this, lack of telomerase activity at the early stage of tumor formation results in increased telomeric instability and it could favour carcinogenesis. Subsequently, activation of telomerase may be fundamental to allow cancer growth and progression (Begus-Nahrmann Y. et al. 2012; Ding Z. et al. 2012). Given the crucial role of telomerase in sustaining cancer growth, telomerase inhibitors were considered a powerful potential cancer therapy. However, antitelomerase therapy can activate alternative lengthening of telomeres (ALT) to maintain telomere length (Hu J. et al. 2012).

1.4.2 Alternative lengthening of telomeres

1.4.2.1 Mechanism of ALT

Differently from RNA-template dependent DNA synthesis by telomerase, ALT requires DNA templates (Dunham M.A. et al. 2000). This proposed model is supported by the observation that a DNA tag inserted into one telomere was copied to other non-homologous telomeres and was also duplicated in its original location in human cells that use ALT mechanism to maintain telomere length (defined as ALT cells) (Dunham M.A. et al. 2000; Muntoni A. et al. 2009; Neumann A.A. et al. 2013). This suggested that ALT depends on homologous recombination (HR) pathway. A putative four steps model is described in Figure 1.9 (left panel) (Pickett H.A. and Reddel R.R. 2015). The single-stranded G-overhang at the telomere terminus can invade homologous DNA forming an HR intermediate structure (step 1). Strand invasion step is followed by the template-directed synthesis of telomeric DNA that could be operated by polymerase δ or ζ, given their role in HR (step2) (Sharma S. et al. 2012; Maloisel L. et al. 2008). The third step consists in the processing of HR intermediate products that must occur before chromosome segregation. A fourth step of filling in of the complementary strand has been hypothesized, but is still unknown whether it occurs. The DNA template for new telomeric DNA synthesis by ALT may be a sister chromatid (Figure 1.9a) or telomeres could copy themselves looping out or looping back on themselves (Figure 1.9b-c). Recent

evidences also identified a long-range movement driven by a homology-directed searching mechanism that allows telomere clustering, providing distant copy templates for ALT activity (Figure 1.9d) (Cho N.W. et al. 2014).

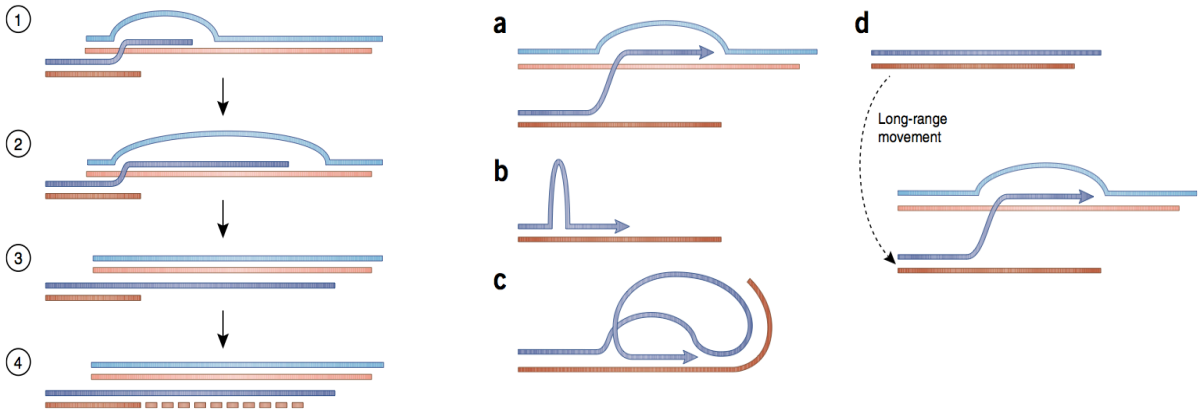

Figure 1.9. ALT mechanism. Putative four steps model of ALT mechanism (left panel). Different possible DNA copy templates in ALT (right panel)(taken from Pickett H.A. and Reddel R.R. 2015).

1.4.2.2 Phenotypic characteristics of ALT cells

In addition to canonical telomeric features, ALT cells show peculiar characteristics (Cesare A.J. and Reddel R.R. 2010). If there are activity assay for telomerase (TRAP assay), a rapid and efficient ALT activity assay is unavailable and the presence of ALT mechanism in cells or tumors is inferred from phenotypic features considered as markers of ALT cells. First of all, human ALT cells have abundant extrachromosomal telomeric DNA that includes circular forms such as double stranded telomeric circles (t-circles) and partially single-stranded circles (C-circles or G-circles), but also linear double-stranded DNA and very high molecular weight structure (t-complex DNA) (Nabetani A. and Ishikawa F. 2009; Henson J.D. et al. 2009). In ALT cells, telomeric DNA and associated binding proteins are found in a subset of promyelocytic leukaemia nuclear bodies (PML bodies) that are defined as ALT-associated PML bodies (APBs) (Yeager T.R. et al. 1999). Additional HR proteins including RAD51, RAD52, RPA, NBS1, SLX4, BLM, MRN, BRCA1, BRIT1 are enriched in APBs and are required for telomere maintenance in ALT cells. Thus it is attractive to speculate that ALT activity may occur in these nuclear bodies (Cesare A.J. and Reddel R.R. 2010). Other features of ALT cells include highly heterogeneous telomere lengths ranging from very short to extremely long (Bryan T.M. et al. 1995), rapid changes

in telomere length (Murnane J.P. et al. 1994; Perrem K. et al. 2001) and an increased level of recombination at telomeres (Londono-Vallejo J.A. et al. 2004).

1.4.2.3 Altered telomeric nucleoprotein structure in ALT cells

Distal end of human telomeres are usually composed by canonical TTAGGG repeats, while the proximal regions contain many variants of telomeric repeats (Baird D.M. et al. 1995; Baird D.M. et al. 2000). ALT telomeres have been found to contain an increased frequency of variant telomeric repeats. This could be explained as the result of ALT activity that, by stochastically amplifing canonical and variant repeats, has produced the spread of variant repeats throughout the telomeres (Conomos D. et al. 2012; Lee M. et al. 2014). These altered telomere sequences in ALT cells have two main consequences: loss of shelterin binding sites and the creation of new protein-binding sites. Decreased shelterin binding at telomere of ALT cells explains the elevated frequency of DNA damage response (DDR) and increased recombination frequency in these cells (Cesare A.J. et al. 2009). On the other hand, the TCAGGG variant creates a high-affinity binding site for the nuclear receptors COUP-TF2 and TR4 which recruit NuRD-ZNF827 nucleosome-remodeling and histone deacetylation complex, thus inducing a series of ALT-promoting effects (Conomos D. et al. 2014). This complex, in fact, facilitates telomere-telomere thethering and also the recruitment of HR proteins such as BRIT1 and BRCA1.

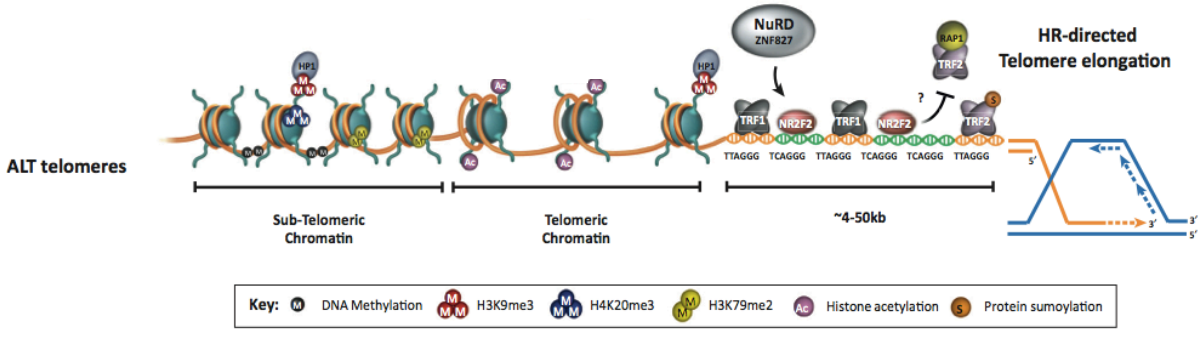

Figure 1.10. ALT telomeres nucleoprotein structure. ALT telomeres contain an increased frequency of variant repeats such as TCAGGG that provide the binding sites for nuclear receptors as NR2F2 and the nucleosome remodeling and histone deacetylation complex NuRD-ZNF827. In addition, ALT telomeres and subtelomeres display reduced heterochromatic marks H3K9me3 and H4K20me3 and elevated levels of histone acetylation. The more open chromatin configuration of ALT telomeres may promote homologous recombination directed telomere elongation. These features of ALT telomeres may lead to displacement of shelterin component TRF2 and perhaps its binding partner, RAP1 (modified from O'Sullivan R.J. and Almouzni G. 2014).

1.4.2.4 ALT positive tumors

Due to the lack of a practical ALT assay to screen a large number of tumors, the distribution of ALT is not known for many common cancer types. However, ALT tends to be most prevalent in tumors of mesenchymal origin. ALT is active in 50% of osteosarcomas, 30% of soft tissue tumors, 25% of glioblastoma multiforme (GBM) and 10% of neuroblastomas (Henson J.D. and Reddel R.R. 2010). Increasing evidence demonstrates a strong correlation between ALT activity in various cancer types and loss of ATP-dependent helicase ATRX or its binding partner, the H3.3 histone chaperone DAXX (Heaphy C.M. et al. 2011; Lovejoy C.A. et al. 2012; Lee J.C. et al. 2015). ATRX-DAXX complex has been demonstrated to bind telomeric repeats and G-quadruplex structures (Law M.J. et al. 2010) facilitating replication throughout aberrant secondary structure (Clynes D. et al. 2015). The complex is also involved in deposition of H3.3 at telomeres in mouse embryonic stem cells (Wong L.H. et al. 2010) and in telomere cohesion (Ritchie K. et al. 2008). Ectopic expression of ATRX in ALT cells suppresses ALT activity (Napier C.E. et al. 2015; Clynes D. et al. 2015). However to date it is not clear how DAXX/ATRX mediate ALT repression (Pickett H.A. and Reddel R.R. 2015).
For all these reasons ATRX mutation or absence of ATRX protein may serve as a useful biomarker for ALT in tumors. In parallel, abnormal ATRX expression has been found also in 86% of ALT cell lines (Lovejoy C.A. et al. 2012).

1.5 The epigenetic regulation of mammalian telomeres

1.5.1 Telomeric heterochromatin in telomere homeostasis

1.5.1.1 Telomeric chromatin structure

Telomeric chromatin shares several characteristics with pericentromeric heterochromatin, such as the ability to silence nearby genes. This phenomenon known as *"telomere position effect"* or TPE was first described in *D. melanogaster* but it is conserved also in yeast and in mammals (Levis R. et al. 1985; Gottschling D.E. 1990). Remarkably, treatment with the histone deacetylase inhibitor Trichostatin A (TSA) releases gene silencing, providing the first evidence that the chromatin status modulates the repressive

environment at mammalian telomeres (Baur J.A. et al. 2001; Koering C.E. et al. 2002). Differently to yeast, that only show nucleosomes in subtelomeric regions, vertebrate telomeres and subtelomeres have a classic nucleosomal organization with a slightly altered spacing (Makarov V. L. et al. 1993; Tommerup H. et al. 1994). Vertebrate telomeric chromatin is under-acetylated and shows characteristic features of other repetitive heterochromatic elements (Figure 1.11) (Benetti R. et al. 2007; Michishita E. et al. 2008). These include enrichment for H3K9me3 histone mark mediated by "suppressor of variegation" Suv39h1 and Suv39h2 Histone Methyl Transferases (HMTases) (Garcia-Cao M. et al. 2004; Peters A.H.F.M et al. 2001; Peters A.H.F.M. et al. 2003). Importantly, H3K9me3 allows the recruitment of HP1 to telomeres that in turn interacts with Suv4-20h1 and Suv4-20h2 HMTases for the establishment of telomeric H4K20me3 (Lachner M. et al. 2001; Schotta G. et al. 2004). Moreover, retinoblastoma family proteins (Rb1, Rbl1, Rbl2) have been found to interact with Suv4-20h HMTases to direct H4K20me3 to telomeric repeats (Garcia-Cao M. et al. 2002; Gonzalo S. and Blasco M.A. 2005). An additional histone methyl transferase Dot1L has been demonstrated to define telomeric heterochromatin mediating H3K79me2 thus enhancing the establishment of H4K20me3 (Jones B. et al. 2008). Together this suggests that Suv39h HTMases and Dot1L mediate a first preparation of chromatin substrate for a further chromatin compaction mediated by HP1 and Suv4-20h HMTases (Schoeftner S. and Blasco M.A. 2010). How telomeric chromatin under-acetylation is maintained remains to be well defined. It has only been reported that the histone deacetylase SIRT6 deacetylates H3K9 at telomeric chromatin (Michishita E. et al. 2008).

Telomeric histone code extends to repetitive and gene-poor subtelomeric regions (Benetti R. et al. 2008; Schoeftner S. and Blasco M.A. 2010). Differently from telomeric repeats that lack CpG sequences, mouse and human subtelomeric sequences are heavily methylated by the DNA methyltransferases DNMT1, DNMT3a, DNMT3b (Figure 1.11) (Gonzalo S. et al. 2006). Although telomeres and subtelomeres carry repressive chromatin marks, transcriptional activity has been detected at vertebrate telomeres. In particular, DNA methylation sensitive subtelomeric promoters drive the expression of Telomeric repeat-containing RNA (TERRA) by RNA polymerase II towards chromosome ends (Figure 1.11) (Azzalin C.M. et al. 2007; Schoeftner S. and Blasco M.A. 2008). Recent works have introduced additional players in telomeric chromatin formation. The histone 3/lysine 4 (H3/K4) HMT and transcriptional regulator MLL (Mixed-Lineage Leukemia) has been

demonstrated to associate with telomeres, to contribute to their H3/K4 methylation and regulate telomeric transcription at uncapped telomeres (Caslini C. et al. 2009). In addition, very recent evidences have shown that H3.3 histone variant is loaded by ATRX at telomeres and is targeted for K9 trimethylation promoting heterochromatin formation and telomeric transcriptional silencing (Wong L.H. et al. 2010; Udugama M. et al. 2015).

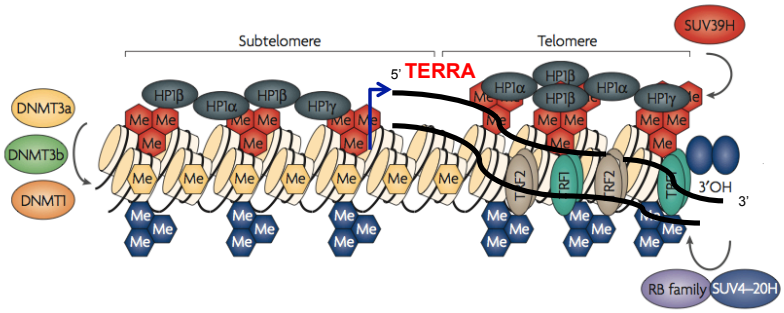

Figure 1.11. Assembly of mammalian telomeric and subtelomeric heterochromatin. Both telomeric and subtelomeric chromatin regions are enriched in trimetylated H3K9 and H4K20 and HP1 proteins. Subtelomeric chromatin is subjected to DNA methylation by DNMT1, DNMT3a, DNMT3b enzymes. Subtelomeric promoters drive the expression of Telomeric repeat-containing RNA (TERRA) (modified from Blasco M.A. 2007).

Loss of function mouse models have revealed that abrogation of master epigenetic regulators, such as histone methyltransferases, DNA methyltransferases and retinoblastoma family proteins correlates with loss of telomere length control (Blasco M.A. 2007). In particular, mouse cells that lack the Suv39h1 and Suv39h2 HTMases show decreased levels of H3K9 trimethylation and HP1 at telomeres in correlation with aberrant telomere elongation (Garcia-Cao M. et al. 2004). Similar effects have been observed in cells lacking all three members of the retinoblastoma family that show decreased levels of H4K20 thrimethylation at telomeres (Gonzalo S. et al. 2005; Garcia-Cao M. et al. 2004). Similarly, a decrease in DNA methylation, both globally and specifically at subtelomeric sequences, correlates with telomere elongation (Gonzalo S. et al. 2006). Consistent with abnormal telomere elongation, cells lacking DNMTs, Suv39h HMTs or retinoblastoma proteins show a global decrease of DNA methylation and increased homologous recombination at telomeres (Gonzalo S. et al. 2006; Gonzalo S. et al. 2005). In line with this, H3.3 deficient mouse embryonic stem cells display reduced levels of H3K9me3, H4K20me3 ant ATRX at telomeres. This correlates with increased telomeric transcription and with increased recombination and DNA damage at telomeres after induction of nucleosome disruption or replication stress (Udugama M. et al. 2015).

Altogether these data suggest that a compromised heterochromatic state at telomeres releases homologous recombination at chromosome ends resulting in abnormal telomere elongation.

1.5.1.2 Telomere shortening affects chromatin status

Progressive telomere shortening in telomerase-deficient mice induces epigenetic changes of subtelomeric and telomeric chromatin. Remarkably, short telomeres show a more "open" chromatin status defined by decreased levels of H3K9me3 and H4K20me3, decreased binding of HP1 and increased acetylation of histone H3 and H4 (Figure 1.12) (Benetti R. et al. 2007). This lower chromatin compaction allows an increased accessibility of telomeres to telomere-elongating mechanisms (telomerase or homologous recombination) (Blasco M.A. 2007). This could explain why ALT is activated by telomere shortening in a telomerase-negative context (Chang S. et al. 2003; Niida H. et al. 2000). In addition, telomerase has been shown to act only on the shortest telomeres in mammals, suggesting that telomeric chromatin structure may regulate the accessibility of telomerase to chromosome ends (Samper E. et al. 2001; Hemann M.T. et al. 2001). Altogether this suggests that the number of telomeric repeats controls the epigenetic status of heterochromatin (Blasco M.A. 2007; Benetti R. et al. 2007).

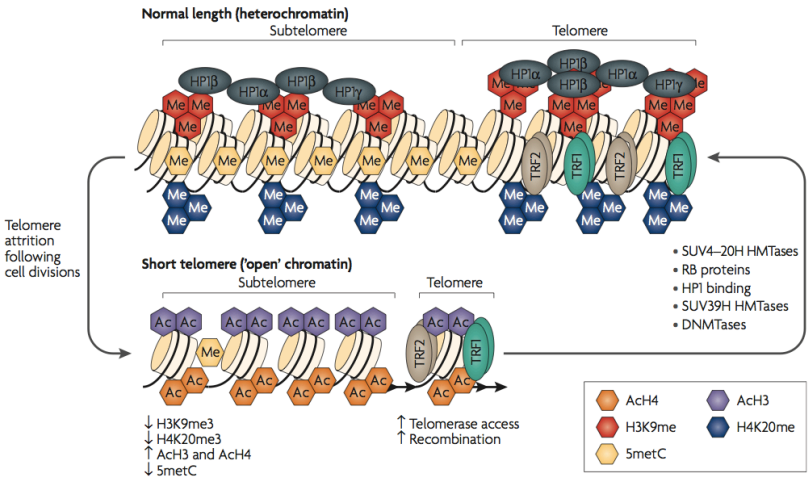

Figure 1.12. **Epigenetic modifications in the control of telomere length**. Normal-length telomeres have a compacted and "closed" chromatin conformation. As telomeres shorten during cell divisions, they show decreased heterochromatic marks concomitant with increased histone acetylation. This more "open" state favours telomere elongation mechanisms (telomerase or recombination) to increase telomere length. Once telomeres are sufficiently elongated they were assembled into heterochromatin (taken from Blasco M.A. 2007).

1.5.1.3 Epigenetic regulation of telomeres and human cancer

Global DNA hypomethylation and in particular hypomethylation of repetitive elements in the genome (subtelomeric and pericentric regions) are common feature of human cancer (Fraga M.F. et al. 2005). Importantly, global DNA hypomethylation and loss of H4K20me3 can be the consequence of abrogation of the Retinoblastoma family proteins, a frequent event in cancer (Gonzalo S. et al. 2005).

The activation of telomere maintenance mechanisms is crucial for the unlimited proliferative potential characteristic of cancer cells. Chromatin structure at telomeres is important to control telomere length homeostasis. In fact, abrogation of master epigenetic regulators, such as histone methyltransferases and DNA methyltransferases correlates with loss of telomere length control and aberrant recombination-dependent telomere elongation (Garcia-Cao M. et al. 2004; Gonzalo S. et al. 2005; Gonzalo S. et al. 2006; Blasco M.A. 2007). Interestingly, a negative correlation between subtelomeric DNA repeats hypometylation and telomere recombination (T-SCE) have been demonstrated in a large panel of human cancer cells (Vera E. et al. 2008). In line with this, a significant positive correlation has been found between recombination frequency at telomeres and mean telomere length in the same analysis. This suggests that subtelomeric hypomethylation-induced telomere elongation is mediated by ALT mechanisms. In addition, treatment with DNA demethylating agent 5-aza-deoxycitidine significantly increases T-SCE frequency in human cancer cell lines, thus indicating that epigenetic drugs can impact on telomere length homeostasis in human cancer cells (Vera E. et al. 2008). Together these findings suggest that telomere length in human cancer cells is influenced by the epigenetic status of chromatin.

1.5.2 Telomeric repeat-containing RNA: TERRA

1.5.2.1 TERRA biogenesis

Due to their repressive chromatin status and low gene density, chromosome ends were considered to be transcriptionally silent for a very long time. This long-standing dogma was overturned by the discovery that telomeric repeats are transcribed into a long non-coding RNA, called TERRA (telomeric repeat-containing RNA)(Azzalin C.M et al. 2007;

Schoeftner S. and Blasco M.A. 2008). The C-rich telomeric strand acts as template for TERRA transcription that starts at promoters located in subtelomeres (Figure 1.13) (Nergadze S.G. et al. 2009). Therefore, individual TERRA molecules consist of subtelomeric-derived sequences followed by a variable number of G-rich telomeric repeats (5′-UUAGGG-3′ in vertebrates) (Azzalin C.M et al. 2007; Schoeftner S. and Blasco M.A. 2008). TERRA molecules are transcribed by RNA polymerase II (RNAPII), as first shown in mammalian cells using RNAPII inhibitors (Figure 1.13) (Schoeftner S. and Blasco M.A. 2008). Human TERRA promoters have been identified in approximately 50% human subtelomeres and comprise CpG dinucleotide-rich tandem repeats of 39 and 37 base pair that locate at variable distance from telomeric repeats, immediately up-stream of TERRA transcription start-sites (Nergadze S.G. et al. 2009). Recently, a second class of TERRA promoters has been identified. They are located 5-10 kb away from telomeric repeats of 10 distinct human telomeres (Porro A. et al. 2014). The existence of different types of promoters supports the observation that TERRA transcripts are very heterogeneous for length (from 100bp to 9kb). Human TERRA 5′ ends display 7-methyl-guanosine cap structures and around 10% of TERRA molecules are polyadenylated at the 3′end (Azzalin C.M et al. 2007; Porro A. et al. 2010). Polyadenylation is a crucial determinant for TERRA localization: polyA- TERRA preferencially associates with telomeric chromatin, while polyA+ TERRA molecules localize to the nucleoplasm (Figure 1.13) (Porro A. et al. 2010). Interestingly, TERRA transcribed from a single telomere can associate with several chromosome ends in mouse. This means that TERRA can act not only *in cis* but also *in trans* in mouse (de Silanes I.L. et al. 2014). Association of TERRA with telomeres is negatively regulated by members of the nonsense-mediated RNA decay (NMD) such as the RNA/DNA helicase and ATPase UPF1 and the RNA endonuclease SMG6 (Figure 1.13) (Azzalin C.M. et al. 2007).

Many aspects of TERRA biogenesis and functions still remain to be investigated. TERRA has already been connected with various pathways of telomere regulation: telomeric chromatin formation, telomere replication, the DNA damage response at telomeres and telomere length regulation.

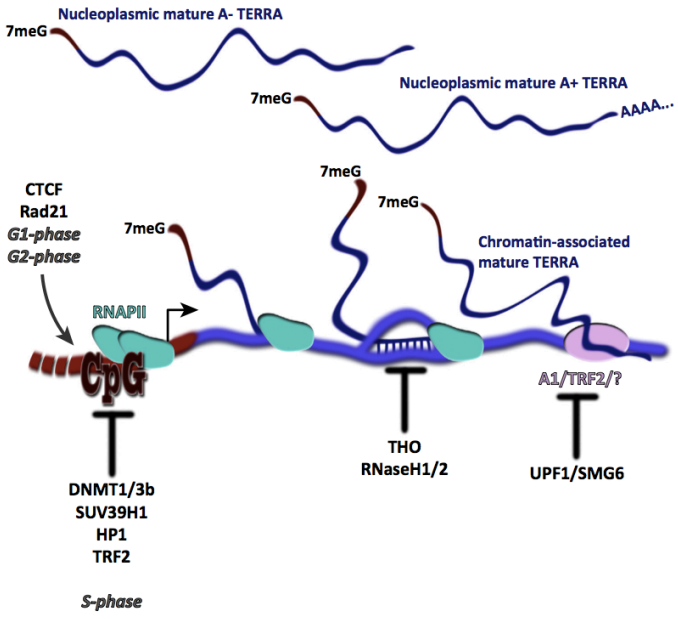

Figure 1.13. Regulation and biogenesis of TERRA. Human TERRA is expressed during G1 and G2 phases of the cell cycle but is repressed during S-phase. CTCF and Rad21 promote human TERRA transcription whereas DNMT1 and 3b, SUV39H1, HP1 and TRF2 repress TERRA. THO complex components associate human telomeres. THO and RNase H repress TERRA-dependent R-loops. hnRNPA1 (A1), TRF2, or other unknown factors may promote TERRA association with human telomeres. TERRA association with human telomeres is negatively regulated by the NMD components UPF1 and SMG6. In human cells, polyadenylated TERRA is not chromatin-associated whereas poly(A)$^-$ TERRA is bound to telomeric chromatin (taken from Azzalin C.M. and Ligner J. 2014).

1.5.2.2 TERRA and telomeric heterochromatin

TERRA transcripts associate with chromosome ends through the interaction with core components of telomeric structure. TERRA interacts with TRF1 and TRF2 shelterin components through TRF2 amino-terminal GAR domain and the carboxy-terminal myb domain (Deng Z. et al. 2009). In addition, TERRA interacts with telomeric heterochromatin components such as Suv39h1 and H3K9me3, HP1, subunits of the origin recognition complex (ORC) and MORF4L2, a member of the NuA2 histone acetyltransferase complex, thereby contributing to heterochromatin formation at chromosome ends (Deng Z. et al. 2009; de Silanes I.L. et al. 2010; Scheibe M. et al. 2013; Porro A. et al. 2014). Alterations of the heterochromatic status of telomeres directly impact on TERRA expression. Indeed, DNA methyl-transferase enzymes DNMT1 and DNMT3b repress TERRA transcription through CpG methylation (Figure 1.13) (Nergadze S.G. et al. 2009). In addition, Suv39h1 H3K9 histone methyltransferase and the H3K9me3-binding protein HP1α negatively regulate TERRA expression (Figure 1.13) (Arnoult N. et al. 2012). On the contrary, the chromatin organizing factor CTCF and the cohesin Rad21 (radiation-sensitive 21) act as positive regulators of TERRA transcription in a particular subset of

TERRA promoters which comprise a third repetitive element of 61bp tandem repeats bound by CTCF- Rad21 (Figure 1.13) (Deng Z. et al. 2012). Based on the finding that TERRA interacts with several components of telomeric heterochromatin, a role of TERRA in the control of chromatin status at telomeres has been suggested. In particular, TERRA has been demonstrated to stabilize the interaction between TRF2 GAR domain and the origin recognition complex (ORC1), thus promoting heterochromatin formation and transcriptional silencing at telomere (Sasaki T. and Gilbert D.M. 2007; Deng Z. et al. 2009). In line with this, a negative feedback loop has been proposed for TERRA transcription regulation in which longer TERRA molecules repress their own transcription upon telomere elongation by increasing trimethylation of H3K9 through recruitment of more histone methyltransferases and/or histone deacetylases (Arnoult N. et al. 2012).

1.5.2.3 TERRA and telomere replication

TERRA levels are regulated during cell cycle. In human cells, TERRA levels are higher in G1, decreases in S-phase and start increasing again in G2 (Porro A. et al. 2010). During the cell cycle, single-stranded telomeric DNA is bound by POT1/TPP1, but in S-phase ss-DNA may be bound by RPA to allow semiconservative DNA replication. After telomere replication, RPA needs to be removed from telomeric ssDNA to prevent persistent DNA damage activation. TERRA has been demonstrated to orchestrate the switch between RPA and POT1 at telomeres after replication. In particular, TERRA directly interacts *in vitro* with hnRNPA1 that can displace RPA from telomeric ssDNA (de Silanes L.I et al. 2014; Flynn R.L. et al 2011). An additional role of TERRA in assisting DNA replication is mediated by its interaction with the origin replication complex (ORC) that has a major role in pre-replication complex assembly in addition to heterochromatin formation (Deng Z. et al. 2009).

1.5.2.4 TERRA and DNA damage response

Emerging evidences suggested a correlation between TERRA expression levels and activation of DNA damage response (DDR) at telomeres. Partial depletion of TERRA expressed from chromosome 18 in mouse cells leads to telomere dysfunction-induced foci

(TIFs), suggesting a protective role of TERRA at telomeres (de Silanes L.I et al. 2014). In addition, TRF2 depletion that activates ATM and cause telomere fusions by NHEJ results in TERRA up-regulation at all transcribed telomeres (Denchi E.L. and de Lange T. 2007; Porro A. et al. 2014). Importantly, TERRA up-regulation seems to be an early event upon TRF2-depletion, occurring in parallel or even upstream of ATM activation (Porro A. et al. 2014). Interestingly, Porro and colleagues demonstrated that critical telomere shortening or telomere uncapping induced by loss of TRF2 causes TERRA up-regulation and TERRA dependent recruitment of the lysine-specific demethylase 1 (LSD1) to telomeres. LSD1, in turn, interacts with MRE11, a subunit of the MRE11/RAD50/NBS1 (MRN) complex required for the processing of 3' telomeric G-overhangs to promote chromosome fusions by NHEJ (Deng Y. et al. 2009; Porro A. et al. 2014). In addition to this role in chromosome ends processing at uncapped telomeres, TERRA transcripts have been demonstrated to induce chromatin structure changes in TRF2-depleted mouse cells (Porro A. et al. 2014). In these cells up-regulated TERRA associates with SUV39H1 H3K9 histone methyltransferase, which promotes accumulation of H3K9me3 at damaged telomeres and end-to-end fusions (Porro A. et al. 2014). Interestingly, accumulation of H3K9me3 may also serve for the recruitment of Tip60/KAT5 acetyltransferase, required for ATM activation (Porro A. et al. 2014). Together these data indicate that TERRA up-regulation induced by dysfunctional telomeres is important to mediate DNA repair and DNA damage activation at uncapped telomeres.

1.5.2.5 TERRA and telomere length regulation

1.5.2.5.1 Telomerase-dependent telomere elongation

TERRA is transcribed from telomeric C-rich strand, consequently its sequence is complementary to the RNA subunit of telomerase (hTR). This led to the hypothesis that TERRA may act as negative regulator of telomerase interacting with TERC. Experiments *in vitro* demonstrated that human TERRA is a potent *in vitro* inhibitor of telomerase by directly basepairing to telomerase RNA template, but also interacting with the catalytic subunit hTERT (Schoeftner S. and Blasco M.A 2008; Redon S. et al. 2010). However, TERRA binding proteins may prevent TERRA-telomerase interaction *in vivo* (de Silanes I.L.

et al. 2010; Redon S. et al. 2013). In line with this, *in vitro* experiments demonstrated that when hnRNPA1 binds TERRA, TERRA-mediated telomerase inhibition is alleviated (Redon S. et al. 2013). However, any evidence of the impact of TERRA on telomerase activity *in vivo* has been demonstrated to date. In addition, diverse evidences are in conflict with this hypothesis. Overexpression of TERRA due to the lack of DNA methyltransferases DNMT1 and DNMT3b in human cells does not impact on telomere elongation by telomerase (Farnung B.O. et al 2012). In line with this, expression of telomerase in fibroblast of ICF syndrome patients that show high levels of TERRA correlates with telomere elongation (Yehezkel S. et al. 2013).

As reported in par 1.5.1.1, a compromised heterochromatic state at telomeres can releases homologous recombination at chromosome ends resulting in abnormal telomere elongation. Given the role of TERRA in the control of heterochromatin at telomeres, should not be surprisingly that in the last few years elevated TERRA levels have been linked with homologous recombination-dependent telomere elongation.

1.5.2.5.2 Telomerase-independent telomere elongation (ALT)

Very recent evidences suggest that TERRA is intimately connected with telomere maintenance by ALT. For its high GC content and for the presence of transcriptional activity, telomeric DNA repeats are proposed to be prone to form secondary structures (G-quartets) and RNA-DNA hybrids. In fact, endogenous TERRA transcripts can base-pair with their template DNA strand and form RNA:DNA hybrid structures, known as R-loops (Figure 1.13, 1.14) (Balk B. et al. 2013; Pfeiffer V. et al. 2013; Arora R. et al. 2014; Yu T. Y. et al. 2014). In these structures, nascent RNA transcript anneals with DNA template strand, displacing the non-template strand that remains unpaired (Aguilera A. and Garcia-Muse T. 2012). R-loops structures are prone to mutations, recombination, replication forks stalling and chromosome rearrangements (Aguilera A. and Garcia-Muse T. 2012; Bermejo R. et al. 2012). Therefore, cells tightly regulate R-loops formation through the activities of different enzymes such as: RNase H1 and H2, which degrade the RNA part of the DNA-RNA hybrid (Aguilera A. and Garcia-Muse T. 2012), helicases, which unwind DNA-RNA hybrid structures (Paeschke K. et al. 2013) and factors involved in RNA biogenesis such as the THO/TREX protein complex (Figure 1.13, 1.14) (Huertas P. and Aguilera A. 2003).

Interestingly, accumulation of telomeric R-loop structures fosters homologous recombination-mediated telomere elongation as firstly demonstrated in yeast (Balk B. et al. 2013). In a recent work, Arora and colleagues reported the presence of telomeric R-loops in ALT positive human cancer cells (Arora R. et al. 2014). They demonstrated that RNase H1 localizes at telomeres in ALT cells but not in telomerase-positive cells and that RNase H1 overexpression decreases telomeric recombination rate and induces telomere shortening in ALT cells. TERRA expression is induced in ALT cells and TERRA molecules have been found into the ALT-associated PML bodies (APBs) (Arora R. et al. 2014). These recent results suggest a crucial role of TERRA in the maintenance of ALT telomeres. Interestingly, impairment of ATRX, the helicase frequently mutated in ALT tumors, induces accumulation of TERRA at telomeres in G2-M (Flynn R.L. et al. 2015). ATRX is reported to resolve G4 secondary structures thanks to its helicase activity (Udugama M. et al. 2015; Clynes D. et al. 2015). Whether ATRX has a role in resolving telomeric R-loops in ALT cells remain to be investigated. One hypothesis is that ATRX unwinding G4 secondary structures on the displaced strand of telomeric R-loop might favour TERRA displacement and re-annealing of telomeric DNA (Rippe K. and Luke B. 2015).

Together this suggests that ALT telomeres represent specific genomic loci that take advantage of R-loops to promote recombination and sustain telomere maintenance by ALT. In this scenario, regulation of TERRA association with telomere acquires a strong relevance in the context of ALT tumors.

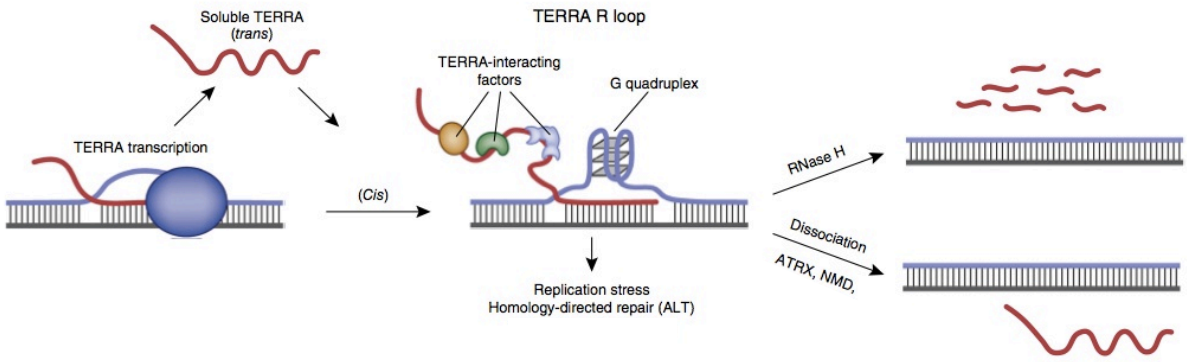

Figure 1.14 Formation and removal of telomeric R-loops. TERRA transcripts can base-pair with their template DNA strand and form RNA:DNA hybrid structures *in cis*. R-loop structure may be stabilized by a G-quadruplex forming at the displaced G-rich DNA strand. Both RNA-DNA hybrids and G-quadruplexes induce replication stress, thereby promoting HDR. The RNA-DNA hybrids can be resolved by RNase H–mediated degradation of TERRA or by factors which favor TERRA displacement such as protein components involved in nonsense-mediated RNA decay (NMD). ATRX helicase could drive displacement of TERRA from the R loop by resolving G-quadruplexes and/or act as an RNA-DNA helicase (modified from Rippe K. and Luke B. 2015).

1.5.2.6 TERRA related diseases

From the reported findings, it is getting clear that TERRA participates in the control of various aspects of telomere homeostasis. For this reason, transcriptional regulation of TERRA and its association with telomeres needs to be tightly controlled. TERRA disregulation has been recently linked to disease. ICF syndrome (immunodeficiency, centromeric instability, facial anomalies) is a rare autosomal recessive immune disorder caused by mutations in the DNA methyltransferase 3b (DNMT3b) gene. In ICF individuals, several repetitive sequences are hypomethylated, satellite 2 regions are decondensed and this correlate with chromosomal instability (Yehezkel S. et al. 2008). As expected, ICF primary fibroblasts also show hypo-methylated TERRA subtelomeric promoters and consequent increase of TERRA levels. In addition, ICF cells display abnormally short and/or unprotected telomeres and increased telomere repeats loss (signal-free ends) (Yehezkel S. et al. 2008). This suggests a functional link between increased TERRA levels and telomeric repeats loss in ICF patients. The hypothesis to test is that increased TERRA transcription might promote replicative stress and excess of telomeric R-loops in these patients.

1.6 Telomeres and genomic instability

1.6.1 Replication stress and genomic instability

DNA replication represents a central cellular process that duplicates and propagates the genome with its intrinsic epigenetic information. During S-phase, replisomes can encounter physiologically or environmentally created barriers that may interfere with DNA replication and hamper its progression. This phenomenon is called replication stress and is characterized by the slowdown of DNA synthesis and/or the stalling of replication fork. Replication stress leading to DNA mutations, breakages and consequent chromosomal fragility and rearrangements represent the primary cause of genomic instability (Gailard H. et al. 2015). Replication fork progression may encounter different types of obstacles: DNA damage, protein barriers, heterochromatin, secondary DNA structures or transcribed genes (Figure 1.15). In fact at transcribed loci, in addition to the

torsional stress generated in the DNA by concomitant replication and transcription, another cause of replicative stress is the co-transcriptional formation of R-loops (Helmirich A. et al. 2011). DNA damage that causes replication stress can be spontaneous or induced by DNA damage agents (UV, cisplatin, camptothecin) or by inhibitors of DNA polymerases activity (hydroxyurea (HU), aphidicolin) (Recolin B. et al. 2014). The presence of each of these barriers results in a replication pause that could be transient or could induce replication fork collapse with consequent exposition of ssDNA stretches or DSBs that triggers the S phase checkpoint (Bartek J. et al. 2004). ATR is activated by ssDNA stretches bound by replication protein A (RPA) while ATM responds to DSBs (For more details see par. 1.2.1). In particular activated ATR phosphorylates CHK1 in order to induce cell cycle arrest and to promote replication fork stabilization and restart. In addition, ATR also activates dormant origins of replication in the vicinity of stalled forks in order to complete replication of the impared regions while inhibiting late firing origins to guarantee avaibility of limiting replication factors such as RPA (Toledo L.I. et al. 2013). In support of the importance of RPA in the induction of S phase checkpoint activation, mutations in Rpa1 result in defective repair of DSBs, chromosomal instability and cancer in mouse (Wang Y. et al. 2005).

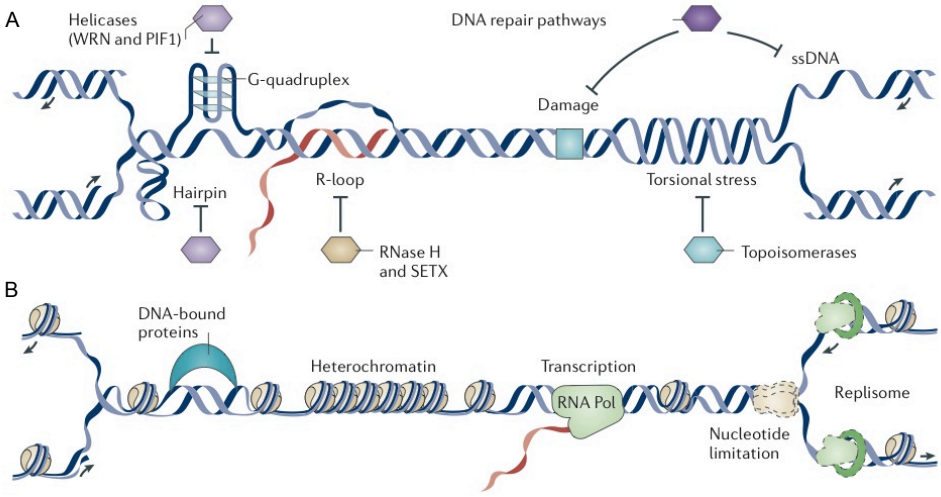

Figure 1.15. Impared replication fork progression. **A**. Several DNA secondary structures can impair fork progression: hairpins, G-quadruplexes, R-loops, altered DNA topology, single-stranded DNA (ssDNA) or double-strand breaks (DSBs). Key factors involved in resolving or removing specific obstacles are shown: DNA helicases such as Werner syndrome helicase (WRN) and PIF1, topoisomerases that remove DNA supercoils alleviating torsional stress; RNA-DNA helicase senataxin (SETX) or ribonuclease RNase H, which remove the R-loops; DNA repair pathways that repair DNA lesions, gaps or breaks. **B**. Other factors and conditions can also impair replication fork progression, such as DNA-bound proteins, heterochromatin, transcribed genes, shortage of replication factors (such as nucleotides and replication protein A (RPA))(modified from Gailard H. et al. 2015).

Replication fork restart after stalling requires specific enzymatic activities performed by different groups of proteins. Among these, we find the human RecQ-helicases: Werner syndrome helicase (WRN), Bloom syndrome helicase (BLM), which are mutated in human syndromes characterized by premature aging and cancer predisposition (Mohaghegh P. and Hickson I.D. 2001). WRN and BLM are able to revert fork-like substrates *in vitro* and are required for the rescue of replication fork block (Pichierri P. et al. 2001; Davies S.L. 2007; Machwe A. et al. 2011). At stalled replication forks, endonucleases complexes such as MUS81-EME1 and SLX-SLX4 activate cleavage of the fork generating DSBs (Hanada K. et al. 2007; Schwartz E.K and Heyer W.D. 2011). Importantly MUS81 and SLX4 deficiencies have been linked with cancer predisposition (Pamidi A. et al. 2007; Hodskinson M.R. et al. 2014). Two other groups of proteins have been reported to be important to stabilize and protect stalled replication forks from endonuclease degradation: Fanconi Anemia (FANC) proteins and the breast cancer susceptibility factors: BRCA1 and BRCA2 (Schlacher K. et al. 2011; Schlacher K. et al. 2012; Lossaint G. et al. 2013). Importantly, under persistent replication stress stalled replication forks can collapse producing DNA breaks that are preferentially repaired by error-free homologous recombination-directed repair. BRCA proteins show an important role in promoting HR repair at collapsed forks. In particular, BRCA1 prevents error-prone NHEJ repair removing 53BP1 at the site of breakage and promotes DNA resection of the DSBs (Bunting S.F. et al. 2010). Differently, BRCA2 associates with RAD51 promoting replacement of RPA with RAD51 on ssDNA (Thorslund T. et al. 2010). In addition, to complete HR-mediated repair BLM helicase is required to process HR intermediates (Wechsler T. et al. 2011).

From these findings it appears that a strong correlation exists between mutations/loss of factors involved in replication stress prevention and predisposition to cancer. Interestingly, genomic instability induced by replication stress has been proposed to be an early event in tumorigenesis. An early step in tumor formation might involve alterated function of several genes that control replication stress and genome integrity (Gailard H. et al. 2015).

1.6.2 R-loops: modulators of genome structure and stability

Short RNA-DNA hybrids normally form during DNA replication (Okazaki fragments) and transcription processes (at the active sites of RNA polymerase). They adopt an intermediate conformation between B form of dsDNA and the A form of dsRNA and are more stable than dsDNA (Roberts R.W. and Crothers D.M. 1992). In addition, longer tracts of RNA-DNA hybrids can be formed in the cells, when the nascent RNA molecule hybridizes with its antisense/DNA template, thus inducing the displacement of sense ssDNA. These structures formed by the RNA-DNA hybrid and the displaced ssDNA are known as R-loops. RNA-DNA hybrids are prone to form in genomic regions with negative supercoiling, high G-content and with the presence of nicks or G-quadruplexes in the displaced ssDNA (Duquette M.L. et al. 2004; Roy D. and Lieber M.R. 2009; Roy D. et al. 2010). For their strong capability to modulate genome structure, R-loops represent a great source of genomic instability (Santos-Pereira J.M. and Aguilera A. 2015). In fact R-loops can induce DNA damage by diverse mechanisms. The stretch of exposed ssDNA is more unstable than dsDNA and for this reason more susceptible to transcription associated mutagenesis (TAM), recombination (TAR) and DSBs (Muers M. 2011; Wimberly H et al. 2013). Various DNA and RNA modification enzymes such as activation induced cytidine deaminase (AID) and members of APOBEC deaminases can generate abasic sites that can induce base substitutions or nicks in ssDNA regions that are then processed in DBSs during replication (Nabel C.S. et al. 2014; Skourti-Stathaki K. et al. 2014). In addition, very recent evidences demonstrated the involvement of nucleotide excision repair (NER) endonucleases in processing R-loops into DBSs (Sollier J. et al. 2014). Importantly, the RNA-DNA hybrids can be a great barrier to replication fork progression thus causing chromosomal fragility and genome rearrangements (for more details see par. 1.6.1) (Gan W. et al. 2011; Aguilera A. and Garcia-Muse T. 2012). For all of these reasons, cells have developed diverse activities to limit the accumulation of R-loop. R-loop formation is prevented by topoisomerase 1(TOP1) that resolves the negative supercoiling formed behind RNA pol II during transcription and by specific RNA-binding proteins involved in RNA biogenesis (THO complex and splicing factor SRSF1) or in RNA surveillance such as exoribonucleases exosome component 3 and 10 (EXOSC3 and EXOSC10) (Tuduri S. et al. 2009; Gomez-Gonzalez B. et al. 2011; Santos-Pereira J. M. and Aguilera A. 2015). In addition, R-loops are removed either by degradation of RNA mediated by RNase H

enzymes or unwound by DNA-RNA helicases such as senataxin (SETX) that also have a role in transcription termination (Wahba L. et al. 2011; Skourti-Stathaki K. et al. 2014). Importantly, dysfunction in factors related to R-loop metabolism and stabilization of stalled replication forks induced by R-loops have been linked with various human neurodegenerative disorders and may be responsible of genomic instability in cancer (table 2).

Gene	Disease	Cause
SETX	Ataxia-ocular apraxia type 2 (AOA2) and amyotrophic lateral sclerosis type 4 (ALS4)	Mutations in the RNA–DNA helicase *SETX*
FXN	Friedreich ataxia (FRDA)	Expansion of GAA repeats in *FXN* gene promotes R-loop formation, H3K9me2 and decreased *FXN* expression
FMR1	Fragile X syndrome (FXS) and fragile X-associated tremor/ataxia syndrome (FXTAS)	Expansion of CGG repeats in *FMR1* gene promotes R-loop formation, H3K9me2 and decreased *FMR1* expression
C9orf72	Amyotrophic lateral sclerosis (ALS) and frontotemporal dementia (FTD)	Expansion of GGGGCC repeats causes R-loop formation and accumulation of aborted transcripts
BRCA1	Cancer	Genome instability caused by R-loop accumulation in BRCA1-deficient cells
BRCA2	Cancer and Fanconi anaemia (FA)	Genome instability caused by R-loop accumulation in BRCA2-deficient cells
FIP1L1	Cancer	Genome instability caused by R-loop accumulation in FIP1L1-deficient cells inferred by the yeast mutant *fip1Δ*
BRE1	Cancer	Genome instability caused by R-loop accumulation in BRE1-deficient cells
SRSF1	Cancer	Deregulation of cancer-associated genes due to *SRSF1* overexpression
ORF57	Kaposi sarcoma-associated herpesvirus (KSHV)	Sequestration of human TREX complex by ORF57 causes R-loop formation and DNA damage

C9orf72, chromosome 9 open reading frame 72; FIP1L1, factor interacting with PAPOLA and CPSF1; *FMR1*, fragile X mental retardation 1; *FXN*, frataxin; H3K9me2, histone H3 lysine 9 dimethylation; *SETX*, senataxin; *SRSF1*, serine/arginine-rich splicing factor 1.

Table 2. Genes related to R-loop metabolism that can cause human disease if dysfunctional (from Santos-Pereira J. M. and Aguilera A. 2015)

Recent evidences in yeast revealed that R-loops are also formed *in trans*. It means that an RNA transcribed at one locus forms an RNA-DNA hybrid with a homologous DNA sequence at a different locus (Wahba L. et al. 2013). This implicates that the nascent RNA invades a double stranded DNA, a process promoted by the homologous recombination-directed repair factors Rad51 and Rad52 (Figure 1.16). In this manner, an RNA transcript could form hybrids with its transcriptional locus, but also with other loci with similar sequences across the genome. Therefore, R-loop formation *in trans* strongly enhances the impact that these structures can have on genome structure and function (Costantino L. and Koshland D. 2015).

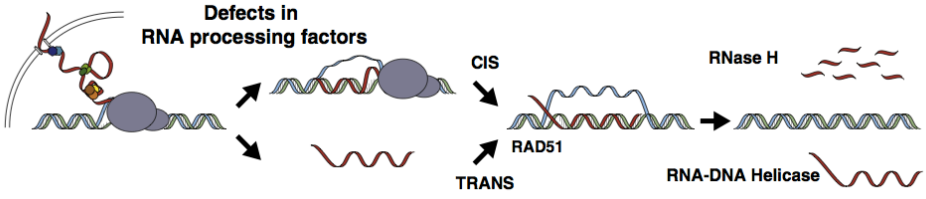

Figure 1.16. **R-loop can form *in cis* or *in trans* as a consequence of defects in RNA processing factors**. Formation *in trans* required RAD51 that mediated strand invasion of dsDNA in a different locus from that of transcription. R-loops dissolution is mediated by RNase H enzymes or RNA-DNA helicases (from Costantino L. and Koshland D. 2015).

1.6.3 Genomic regions prone to replicative stress and chromosome fragility

Human genome DNA is structured in the canonical B-form that can be properly replicated by DNA polymerases (Cea V. et al. 2015). However, a particular base content in certain DNA sequences can render defined genomic regions susceptible to replication stress and consequent fragility. Key exemples are G-rich sequences that fold into G-quadruplexes, "Common fragile sites" (CFSs) and "Early replicating fragile sites" (ERFs). G-rich sequences can form a quadruplex stabilized by Hoogsteen hydrogen bonds, known as G-quadruplex structure (Figure 1.17, left panel) (Sen D. and Gilbert W. 1988). G-quadruplexes (G4) are more stable than a classic B-form DNA and are reported to block the progress of DNA replication and the transcription bubble (Maizels N. and Gray L.T. 2013). Various DNA helicases such as RecQ helicases BLM and WRN and the Fanconi Anemia protein FANCJ are involved in the resolution of G4 structures (Brosh R.M. Jr et al. 2001; Wu Y. et al. 2008; Johnson J.E. et al. 2010).

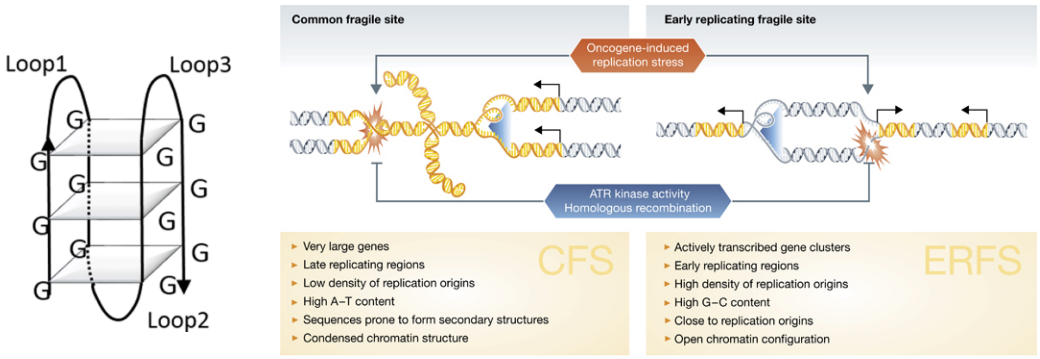

Figure 1.17. **DNA sequences prone to replication stress and fragility.** G-quadruplex structure (left panel) (taken from Cea V. et al. 2015). Summary of principal characteristics of CFSs and ERFs (righ panel) (taken from Mortusewicz O. et al. 2013).

Common fragile sites (CFSs) are large genomic regions that can span hundreds to thousands of kilobases and have a high content in AT-rich sequences. CFSs are sequences that initiate replication late in S phase or are slow in replication (Figure 1.17, right panel). CFSs have a high flexibility and under replication stress conditions are prone to fold into secondary structures. These structures can create a barrier to replication fork progression leading to fork stalling and DNA breaks in these sites. Interestingly, R-loops have been found at Common fragile sites (CFSs) where collisions between replication and transcription machineries occur. In line with this, RNase H overexpression rescues

genomic instability associated with these CFSs (Helmrich A. et al. 2011).

Early replicating fragile sites (ERFSs) are regions that undergo fork collapse under replication stress but they have been localized in proximity of early firing origins of replication. Nussenzweig and colleagues observed that ERFSs are GC-rich, possess repetitive elements such as LINEs and SINEs and are associated with highly transcriptional active genes (Figure 1.17, right panel) (Barlow J.H. et al. 2013). Although ERFSs and CFSs show different sequence features, they both need ATR kinase activity and homologous recombination to prevent fork collapse and mediate fork restart and repair (Mortusewicz O. et al. 2013). However, CFSs are the most relevant in cancer. Importantly, recent data have shown that the majority of recurrent cancer specific translocation breakpoints maps to CFSs (Burrow A.A. et al. 2009). In addition, CFSs are the preferential target sequence of oncogene-induced replication stress in pre-malignant lesions (Tsantoulis P.K. et al. 2008). In support of the relevance of CFSs in cancer, there is also the observation that oncogene amplified regions and tumor suppressor genes often overlap with CFSs (Hellman A. et al. 2002; Blumrich A. et al. 2011; Ohta M. et al. 1996). Recent data also identified ERFSs that frequently coincides with breakpoints of most B cell lymphoma rearrengements (Barlow J.H. et al. 2013). Together this closely links replication stress and chromosome fragility with cancer formation.

1.6.4 Telomere fragility

Telomeres represent a hallmark model for chromosome fragility: they are repetitive elements with heterochromatic structure, they are transcribed and in addition their G-rich sequence can form secondary structures (G-quadruplex) (Blasco M.A. and Martinez P. 2015). For these reasons, telomeres resemble fragile sites (Sfeir A. et al. 2009). Telomere fragility can be visualized by telomeric DNA FISH. Fragile telomeres appear as multimeric signals at chromosome ends of metaphase chromosomes. Shelterin and additional telomere accessory factors are required to ensure the progression of replication fork and to prevent telomere fragility (Blasco M.A. and Martinez P. 2015). The telomere repeat binding factor TRF1 has a central role in suppressing telomere fragility. In fact, deletion of TRF1 results in mutitelomeric signals (MTSs), ATR activation, end-to-end fusions, increased frequency of sister telomere associations but also the formation of ultrafine

anaphase bridges (UFBs) (Figure 1.18) (Martinez P. et al. 2009; Sfeir A. et al. 2009; d'Alcontres M.S. et al. 2014). A very recent work demonstrated that TRF1 abrogation in liver under chronic replicative stress correlates with increased ploidy of hepathocytes caused by endoreduplication (Beier F. et al. 2015). In addition, TRF1 interacts with the helicase BLM to specifically suppress lagging strand telomere fragility (Figure 1.18) (Zimmermann M. et al. 2014). In fact, combined depletion of TRF1 and BLM increases the number of MTSs specifically at lagging strand telomere, the G-rich strand prone to form G4 structure that BLM is able to unwind. Also Topoisomerase IIα (TopoIIα) has been demonstrated to bind telomeres in a TRF1-dependent manner to resolve DNA replication intermediates. TopoIIα depletion correlates with telomere fragility at both telomeric strands and formation of ultrafine anaphase bridges (d'Alcontres M.S. et al. 2014).

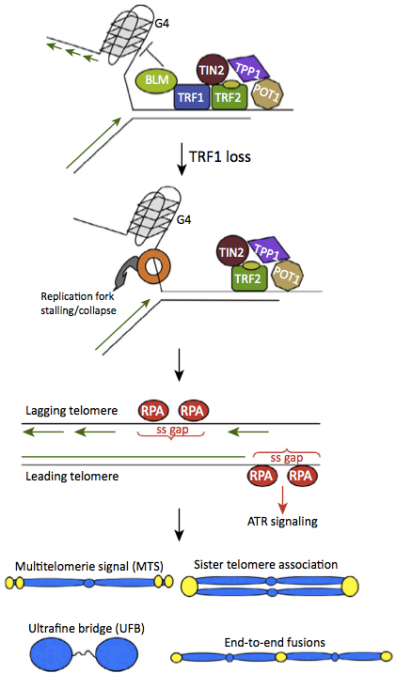

Figure 1.18. Model for TRF1 role in telomere replication. TRF1 recruits BLM helicase to resolve G quadruplexes in the G strand, preventing lagging strand fragility. TRF1 loss results in telomere fragility, ATR activation, end-to-end fusions, sister telomere associations, and increased frequency of ultrafine bridges. The current model proposes that deletion of TRF1 results in single-strand (ss) gaps at sites of fork stalling that are coated by Replication Protein A (RPA) to further induce ATR signaling (from Martinez P. and Blasco M.A 2015).

Conditional deletion of mouse Trf2 results in a strong damage response at telomeres that leads to chromosome end to end fusion by the non-homologous end-joining pathway, loss of the 3'overhang without affecting telomere replication (Celli G.B. and de lange T. 2005;

Sfeir A. et al. 2009). However, TRF2 allows telomeric association of various helicases or endonucleases such as Werner (WRN), Flap endonuclease 1 (FEN1) and Regulator of telomere length (RTEL) to prevent replication fork stalling, but also to ensure correct formation and disassembly of T-loop and to assist telomeric recombination processes (Figure 1.19) (Blasco M.A. and Martinez P. 2015). In particular, TRF2 physically interacts with WRN helicase that resolves G-quadruplexes on the lagging strand telomere and prevents lagging strand telomere loss (Crabbe L. et al. 2004). In addition, WRN has been recently reported to facilitate telomeric recombination processes such as T-loop formation/resolution, telomeric sister chromatid exchange and break-induced replication (BIR). Importantly the strand exchange activity of WRN on telomeric DNA is enhanced by interaction with TRF2 (Edwards D.N. et al. 2014). FEN1 is an endonuclease that participates in Okazaki fragment processing during lagging strand synthesis and it has been demonstrated to localize to telomeres through the interaction with TRF2 (Liu Y. et al. 2004). In line with this, FEN1 was shown to prevent lagging strand telomere fragility and loss (Saharia A. et al. 2008; Saharia A. et al. 2010). In addition, FEN1 interacts with both RecQ helicases, WRN and BLM (Sharma S. et al. 2005). Finally, RTEL associates to telomeres though the interaction with TRF2 to carry out two important functions. RTEL facilitates T-loop unwinding and prevents G-quadruplex formation during telomere replication (Vannier J.B. et al. 2012; Uringa E.J. et al. 2012; Sarek G. et al 2015). In fact, in addition to telomere fragility, loss of RTEL causes telomere length heterogeneity and accumulation of telomeric circles indicating a role in T-loop disassembly *in vivo* (Vannier J.B. et al. 2012). Interestingly, the role of RTEL in telomere fragility suppression is dependent on its interaction with the replication clamp protein PCNA, a processivity factor for DNA polymerases (Vannier J.B. et al. 2012; Vannier J.B. et al. 2013).

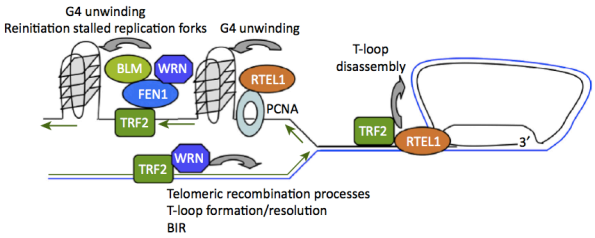

Figure 1.19. TRF2 allows the recruitment to telomeres of various factors required for telomere replication and recombination processes. WRN helicase associates with telomeres in a TRF2-dependent manner during S phase and has been proposed to resolve G-quadruplexes and to facilitate telomeric recombination processes. FEN1 localizes to telomeres through interactions with TRF2. FEN1 also binds BLM and WRN helicases and has been proposed to prevent telomere fragility by facilitating G-quadruplex unwinding and reinitiating stalled replication forks during lagging telomere synthesis. Finally, TRF2 interacts with RTEL1 to disassemble telomeric (T) loops during S phase. RTEL1 also facilitates G-quadruplex unwinding at telomeres interacting with PCNA, thus preventing telomere fragility (taken from Martinez P and Blasco M.A 2015).

Together these findings demonstrate that telomeres have evolved complex mechanisms that involve shelterin and telomere-associated proteins to prevent telomeric fragility, a source of telomeric DNA damage and instability.

1.6.5 Replication stress triggers recombination at ALT telomeres

Telomeres in ALT cells show a different structure compared to the hallmarks of telomerase positive cells. ALT telomeres reach high telomere length, contain increased frequency of variant telomeric repeats sequences and are characterized by a reduced abundance of shelterin proteins. This renders telomeres potentially even more difficult to replicate. In this scenario, high levels of replication stress may be considered a feature of ALT (O'Sullivan R.J. and Almouzni G. 2014). In fact, restart of stalled replication forks could potentially trigger ALT activity. In line with this, deletion of RTEL in mouse cells, which have long telomeres, cause formation of extra chromosomal telomeric repeats (ECTR). Importantly ECTR formation was blocked using drugs that completely stall the replication fork (Vannier J.B. et al. 2012). This means that stalled replication forks spontaneously can form intermediate structures recognized by homologous recombination machinery. In addition to this, ALT cells and tumors often lack the activity of ATRX/DAXX complex implicated in G quadruplex resolution structures and heterochromatin formation at telomeres (Figure 1.20A). Interestingly, ATRX deficiency has been linked with stalling of replication forks and consequent replicative stress (Leung J.W.C et al. 2013). In ALT tumors and cells, G-quadruplexes structures could accumulate and block DNA replication

fork progression (Figure 1.20B). Consequent stalled/collapsed replication forks could provide a reservoir of DNA intermediates to homologous recombination machinery to perform ALT activity. In line with increased replication stress, a high proportion of telomeres in ALT cells are associated with activated DNA damage response. This renders ALT telomeres hypersensitive to ATR inhibitors (Flynn R.L et al. 2015).

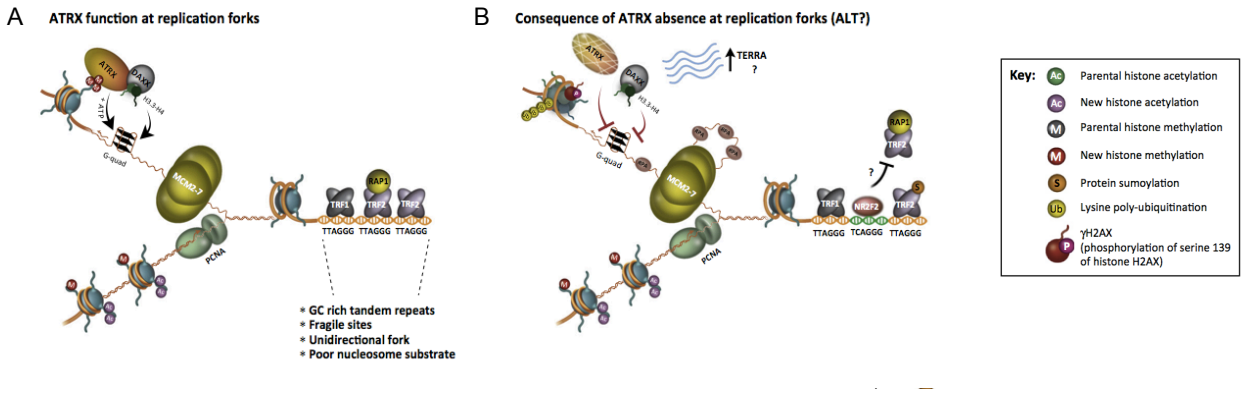

Figure 1.20. Chromatin assembly mechanisms at mammalian telomeres. A. ATRX function at replication fork. G-quadruplexes form at telomeres and ATRX binds to chromatin via H3K9me3 to catalyze the ATP dependent unwinding of these structures. This enables DAXX mediated incorporation of histone H3.3–H4 dimers and faithful chromatin assembly at tandem repeats. **B**. In the absence of ATRX, G-quadruplexes remain unresolved and impede deposition of histone H3.3–H4 by the histone chaperone, DAXX. This may lead to prolonged replicative stress as illustrated by the accumulation of replication protein A (RPA) on ssDNA. At ALT telomeres, changes in the telomeric sequence may displace shelterin proteins (TRF2). This could augment replicative difficulties at ALT telomeres. Changes in chromatin might alter transcription of telomeric non- coding RNA (TERRA) (taken from O'Sullivan R.J. and Almouzni G. 2014).

Aim of the thesis

Telomeric repeats are organized into heterochromatin structures specifically defined by the interplay of epigenetic regulators (HMTases, DNMTases, HDACs), chromatin remodeling factors and the long non-coding RNA, TERRA. Together these players characterize and regulate the epigenetic status of telomeres.

Changes in chromatin structure and TERRA abundance at telomeres have been linked with loss of telomere length control, activation of DNA damage response and genomic instability.

My PhD thesis aimed:

- to define the impact of the histone H3K9 specific methyltransferase Suv39h1 on telomere homeostasis and carcinogenesis using a transgenic mouse model (**project 1**);

- to obtain new insights into the molecular function of TERRA in telomere regulation by identifying novel proteins with binding specificity for TERRA UUAGGG RNA repeats (**project 2**).

2. Material and Methods

2.1 Cell lines and culture

Feeder independent mouse ES cells were cultured on 0.2% gelatin-coated plates in mESC self-renewal medium (Dulbecco's modified Eagle's medium (DMEM) supplemented with 15% knockout serum replacement (Gibco), 1% non-essential amino acids (Gibco), 1mM sodium pyruvate (Invitrogen), 1% L-glutamine (Invitrogen), 0.1 mM β-mercaptoethanol and 1000U/ml mouse Leukemia Inhibitory Factor (LIF). pMEFs were cultured in DMEM, high glucose; 10% fetal bovine serum; L-glutamine and Pen/Strep (all Invitrogen). Human cancer cell lines used were obtained from ATCC and have not been cultured for longer than 6 months. Human lung adenocarcinoma cell line H1299 was grown in Roswell Park Memorial Institute (RPMI) medium (Lonza) supplemented with 10% fetal bovine serum, L-glutamine, Pen/strep (Life Technologies). Osteosarcoma cells (U2-OS) were cultured in low glucose Dulbecco's modified Eagle's (DMEM) medium (Lonza) with 10% fetal bovine serum, L-glutamine and Pen/Strep (Life Technologies).

2.2 Transgenic animal model

Trangenic animals were generated using the CMV-loxP-Stop-loxP-Suv39h1-pA cassette excised from the vector using PvuII/SalI, purified and injected into the pronuclei of fertilized oocytes obtained from C57BL/6 x CBA F1 mice at the CNIO transgenics unit and founder mice were established. Founder animals were backcrossed for 3 generations to a pure C57BL/6 background to obtain the Suv39h1 transgenic line studied here. Suv39h1Stop transgenic animals were crossed with homozygous CMV-Cre recombinase transgenic animals (Zinyk D.L. et al. 1998) to give rise to Suv39h1ΔStop-CMV-Cre mice (in this study: Suv39h1ΔStop) and heterozygous CMV-Cre (in this study "control" mice) offsprings. Mice were generated and maintained at the CNIO under specific-pathogen-free conditions in accordance with the recommendations of the Federation of European Laboratory Animal Science Associations. All efforts were made to minimize suffering.

2.3 siRNAs and vectors transient transfection

Cells were seeded (number cells of varies depending on the cell line) and the day after were transfected. For siRNAs transfection RNAi-MAX Lipofectamine (Invitrogen) was used at a final concentration of 30-60nM according to the manufacturer's suggestions. 72 hours post-transfection experiments were perfomed. Transfected siRNAs used are listed below:
ON-TARGETplus non-targeting siRNA#1 (Dharmacon)
ON-TARGETplus smartpool TRF1 siRNAs (Dharmacon) Human
ON-TARGETplus smartpool NONO siRNAs (Dharmacon) Human
ON-TARGETplus smartpool SFPQ siRNAs (Dharmacon) Human
RNAse H1 siRNA (eurofins): 5' ACAAACCAAAGAGCGGAAAUUCAUG(dTdT) 3'

A variable amount of specific vectors was transfected using Lipofectamine 2000 (Invitrogen) according to the manufacturer's suggestions. Vectors used for transient transfections: pCDNA, pCDNA-HA-Suv39h1, pCDNA 3.1-mCherry, pLHCX-mCherry-RNase H1.

2.4 Generation of p54nrb and PSF stable cell lines

H1299 and U2-OS p54nrb stable cell lines have been generated with retroviral transduction of pLPC and pLPC-NFLAG p54nrb vectors. Infected cells have been selected using puromicine (1ug/ml). Differently, H1299 and U2-OS PSF stable cell lines have been generated through single transfection of linearized pLPC (control) or combined transfection of linearized pLPC and pCMVmyc-PSF vectors. Transfected cells have been selected using puromicine (1ug/ml).

2.5 Retroviral transduction of human cells

HEK 293GP (Gag and Pol) were used as packaging cell line. The solution DNA-$CaCl_2$ (2,5 M $CaCl_2$ sterilized by filtration) for a 10cm dish was prepared adding sequentially: H_2O up to 450 ul, 50ul $CaCl_2$ and 5-10 ug of specific plasmid DNA. In a different tube 500ul of 2X HBS (Table 1) were added and the DNA solution was transferred drop by drop to the 2X HBS. The solution was mixed introducing air bubbles and incubated for 20-30 minutes

to allow efficient formation of DNA-$CaPO_4$ precipitates. Then, the solution was added dropwise to the cells previously covered with 10 ml of fresh medium and incubated at 37 C°. The day after the medium was changed and the cells were incubated for 48 hours. Subsequently, the supernatant containing the virus was collected, filtered and added in a tube with 1ml of serum (FBS) and 8ug/ml of polybrene. This solution was used to infect U2-OS and H1299 cells. The day after, medium was changed. After 24 hours the specific antibiotic to select transfected cells was added.

2X Hepes-buffer saline (HBS)	**For 50ml/ stock solution**
50mM Hepes pH7	10ml (250 mM)
280 mM NaCl	5 ml (2,8 M)
1.5 mM Na_2HPO_4	0,5 ml (150 mM)
	To 50 ml with H_2O

2.6 TERRA-pull down

Cells were resuspendend in Buffer A (10 mM HEPES pH 7.9, 1.5 mM $MgCl_2$, 10 mM KCl, 0.5 mM DTT, 1x PMSF, and complete proteinase inhibitor (Roche)) incubated on ice for 10 minutes and homogenized in the presence of 0.05% NP-40 using a Dounce homogenizer pestle. Obtained nuclei were pelleted and resuspended in Buffer C* (20 mM HEPES pH 7.9, 25% (v/v) glycerol, 1.5 mM $MgCl_2$, 0.2 mM EDTA, 0.5 mM PMSF, 0.5 mM DTT, 1x PMSF, complete proteinase inhibitor (Roche)). NaCl was added to reach a final concentration of 400mM. Extracts were incubated on ice for 20 minutes and sonicated. Samples were centrifuged to obtain the supernatant containing nuclear proteins. NaCl concentration was diluted with Buffer C diluent (20 mM HEPES pH 7.9, 1.5 mM $MgCl_2$, 0.2 mM EDTA, 0.5 mM DTT, PMSF, complete protease inhibitor (Roche)) to reach a final concentration of 150mM NaCl. Extracts were precleared using strepatviding agarose beads (Invitrogen). Beads were removed by centrifugation and nuclear extracts were supplied with RNase Inhibitor (RNase OUT, Invitrogen), yeast tRNA (Invitrogen, final concentration 100ng/ml), Heparin (Sigma, final concentration 5ug/ml), RNA oligos biotin-r[UUAGGG]$_6$ or biotin-r[EGFP] (both MWG eurofins) and agarose-streptavidin beads (Invitrogen). Sample were incubated for 1hr at 4ºC. Beads were washed in Binding Buffer (20 mM HEPES pH 7.9, 20% glycerol, 0.2 mM EDTA, 150 mM NaCl, 0.05% NP-40, 1mM

PMSF, 0,5 mM DTT, complete protease inhibitor cocktail, RNase OUT (Invitrogen)) and bound proteins were eluted using 2x Laemli sample buffer. Eluted proteins were separated on a one dimensional SDS-PAGE and subjected to silver staining (Invitrogen). Specific biotin-r[UUAGGG]$_6$ binding proteins were cut out from the gel and identified by mass spectrometry.
Biotin-EGFP: 5′ AAGGACGACGGCAACUACAAGACCCGCGCCGAGGUGAAGU 3′
Biotin-TERRA: 5′ UUAGGGUUAGGGUUAGGGUUAGGGUUAGGGUUAGGG 3′

2.7 Immunoprecipitation

Cell lysates were prepared with ice-cold lysis buffer containing 50 mM Tris-HCl, pH 8, 150 mM NaCl, 5mM EDTA, 1mM DTT, 1mM PMSF, 1 mM beta-glycerophosphate, 1mM Na_3VO_4, 5 mM Na_2F, and protease inhibitor cocktail (Sigma) plus 5% glycerol and 1% NP-40. After centrifugation and preclearing, lysates were incubated at 4 °C with specific antibodies or rabbit IgG as negative control (check 2.23 antibodies table). After 2 hours, protein-A agarose-beads (Santa Cruz) were added to each IP and incubated overnight. The resin was then washed and bound proteins were eluted in sample buffer 2X and subjected to SDS-PAGE followed by western blotting.

2.8 Western Blotting

Lysis buffers used for protein extract preparation were supplied with complete protease and phosphatases inhibitors (Roche). Whole-cell lysates were prepared using a modified RIPA buffer (20 mmol/L Tris-HCl (pH 7.5) 350 mmol/L NaCl, 1 mmol/L Na_2EDTA, 1 mmol/L EGTA, 1% NP-40, 1% sodium deoxycholate, 2.5 mmol/L sodium pyrophosphate, 1 mmol/L b-glycerophosphate, 1mmol/L Na_3VO_4, 1 mg/mL leupeptin). After sonication and centrifugation, supernatants were recovered and subjected to western blot. For the preparation of nuclear extracts, cells were resuspended in Buffer 1 [20 mmol/LHepes-KOH (pH 7.9), 10 mmol/L KCl, 1.5 mmol/L MgCl2, 1 mmol/L EDTA, 1 mmol/L EGTA, 0.2% NP40] and incubated for 10 minutes on ice. Nuclei were centrifuged and lysed in Buffer 2 (20mmol/L Hepes-KOH (pH 7.9), 350 mmol/L NaCl, 1.5 mmol/L $MgCl_2$, 10 mmol/L KCl, 10% glycerol, 1 mmol/L dithiothreitol). Then they were sonicated and

centrifuged. Supernatants were recovered as nuclear extracts. Protein extracts were separated on SDS-polyacrylamide gels. After transfer, membranes were incubated with primary antibodies (check 2.23 antibodies table). Then the membranes were incubated with secondary antibodies bound to the HRP enzyme (horseradish peroxidase-conjugated antibody) (GE Healthcare) and the levels of proteins expression were detected by chemiluminescence using the ECL system (GE Healthcare) with subsequent exposure on autoradiography film (GE Healthcare).

2.9 ChIP assay and telomere dot-blots

Cells were fixed adding formaldehyde directly to culture medium to a final concentration of 1% and incubated for 15 min at room temperature on a shaking platform. Cross-linking was then stopped by the addition of glycine to a final concentration of 0.125 M. Cross-linked cells were washed twice with cold PBS, collected and lysed for 10 minutes at 4 °C in 1% SDS, 50 mM Tris-HCl (pH 8.0) and 10 mM EDTA containing protease inhibitors. Lysates were sonicated to obtain chromatin fragments >1 kb and centrifuged for 15 min in a microcentrifuge at room temperature. Chromatin was diluted 1:10 with 1.1% Triton X-100, 0.01% SDS, 1.2 mM EDTA, 167 mM NaCl and 16.7 mM Tris-HCl (pH 8.0) containing protease inhibitors and precleared with Protein A or Protein G agarose beads (Santa Cruz). Chromatin fragments were incubated with 3,5µg of specific antibodies (check 2.23 antibodies table) or rabbit/mouse IgG as negative control at 4°C overnight on a rotating platform. Protein A or Protein G agarose beads were then added and the incubation continued for 1 h. Immunoprecipitated pellets were washed with 0.1% SDS, 1% Triton X-100, 2 mM EDTA, 20 mM Tris-HCl (pH 8.0) and 150 mM NaCl (one wash); 0.1% SDS, 1% Triton X-100, 2 mM EDTA, 20 mM Tris-HCl (pH 8.0) and 500 mM NaCl (one wash); 0.25 M LiCl, 1% NP-40, 1% sodium deoxycholate, 1 mM EDTA and 10 mM Tris-HCl, pH 8.0 (one wash); and 10 mM Tris-HCl (pH 8.0) and 1 mM EDTA (two washes). Chromatin was eluted from the beads twice by incubation with 250 µl of 1% SDS/ 50mM NaHCO3 for 15 min at room temperature with rotation. After adding 20 µl of 5 M NaCl, cross-links were reversed by incubation for 4 h at 65 °C. Samples were supplemented with 20 µl of 1 M Tris-HCl (pH 6.5), 10 µl of 0.5 M EDTA, 20 µg of RNase A and 40 µg of proteinase K and were incubated for 1 h at 45°C. DNA was recovered by

phenol-chloroform extraction and ethanol precipitation and then, spotted into a dot-blot with a Hybond N+ membrane which was hybridized with a telomeric probe obtained from a plasmid containing 1.6 kb of TTAGGG repeats. We quantified the signal using ImageQuant software. For total DNA samples, aliquots corresponding to a 1:10 dilution of the amount of lysate used in the immunoprecipitations were processed along with the rest of the samples during the crosslink reversal step. We calculated the amount of telomeric or major satellite DNA immunoprecipitated in each ChIP based on the signal relative to the corresponding total telomeric or major satellite DNA signal, respectively. In all cases, we represented the ChIP values as a percentage of the total input telomeric DNA.

2.10 Immunofluorescence

Cells were washed with 1x PBS and, fixed in 4% paraformaldehyde (PFA) for 15 minutes. Subsequently cells were washed with 1x PBS and treated with citrate buffer [0.1% (w/v), 0.05% Triton X-100] for 10 minutes at room temperature. Cells were blocked for 45 minutes in 3% BSA (1XPBS, 0.1% Tween-20) and incubated with primary antibodies (check 2.23 antibodies table) diluted in blocking solution for 2h at room temperature in a wet chamber. Cells were washed three times in 0.3% (w/v) BSA (1xPBS)/0.1% Tween-20 for 5 minutes and incubated with Alexa-fluor secondary antibodies (Invitrogen) diluted 1:500 in washing solution for 1h in a wet chamber. After the incubation three washes were performed in 1x PBS with 0.1% Tween-20 for 5 minutes. In particular, in the second wash was added the 20 DAPI (Vector Laboratories) to stain the nuclei. The slides were mounted with Vectashield. In particular for S9.6 immunofluorescence, cells were fixed in ice-cold methanol for 10 minutes and permealized with acetone on ice for 1 minutes. All washing and antibody solutions were performed in 4xSSC instead of 1X PBS.
Images were captured using confocal (Nikon Eclipse C1Si on TE-2000U) or classic immunofluorescence (Leica DM4000B) microscope. For classic immunofluorescence analysis, the number of co-localizations per focal plane was counted. For confocal microscopy analysis, number of co-localizations was counted on the image resulting from the sum of three Z-stacks. Quantitative immunofluorescence analysis were performed using ImageJ. The Student t test was used to calculate the statistical significance.

2.11 Immunohistochemistry

Skin samples were fixed in 10% buffered formalin, embedded in paraffin wax and sectioned at 4 μm. After de-paraffination, sections were processed with 10 mM sodium citrate (pH 6.0) for 20 min at 95°C. After blocking in 5% goat serum cells were incubate with respective primary and secondary antibodies (check 2.22 antibodies table). Primary antibody was incubated for 1 hour at room temperature. Secondary Cy3-goat anti-rabbit antibody (1:400; Jackson Immuno Research Laboratories, Inc.) for 60 min at room temperature; slides were mounted in Vectashield. Quantitative image analysis of mouse tail skin sections was performed by confocal microscopy (H3K9me3) using a TCS-SP2-A-OBS-UV Leica microscope with Metamorph software (version 6.3r6) platform followed by picture analysis as previously described (Blanco R. et al. 2007).

2.12 RNA-FISH

Cells were washed with 1XPBS and than permeabilized in three steps of 30 seconds each in cytobuffer (100mM NaCl, 300mM Sucrose, 3mM $MgCl_2$, 10mM Pipes pH6.8), cytobuffer/0,5%Triton-X, cytobuffer. Cells were then fixed for 10 min at room temperature in ice-cold 4% PFA in PBS. Cells were then dehydrated in ice-cold 70% ethanol twice for 2 minutes, ice-cold 90% ethanol for 1 minute, ice-cold 100% ethanol for 1 minute. Dried slides were incubated with 7 μl of TERRA probe overnight in a humid chamber (2XSSC, 50% formamide) at 37°C. Slides were washed once in 2XSSC for 3 minutes at room temperature, three times in 2XSSC for 5 minutes at 37°C and once in 2XSSC (supplied with DAPI) for 5 minutes at room temperature. Then, slides were transfered in 4XSSC and mounted in Vectashield. TERRA probe was obtained from a plasmid containing 1.6 kb of TTAGGG repeats and labeled with FISH Tag DNA kit (Invitrogen). Images were captured with Leica DM4000B microscope. At a chosen exposure time, the number of foci per nucleus was counted. The Student t test was used to calculate the statistical significance.

2.13 Immunofluorescence and RNA-FISH

Cell were permeabilized with cytobuffer as described in RNA-FISH and fixed for 10 min at room temperature in 4% PFA in PBS. After 5 min at room temperature in 0.1% sodium citrate/0.1% Triton X-100, cells were blocked for 1h at room temperature in PBS containing 3% (w/v) BSA, 0.1% Tween-20. Primary antibodies (check 2.23 antibodies table) were incubated for 1 h at room temperature. Cells were washed three times in 0.3% (w/v) BSA (1xPBS)/0.1% Tween-20 for 5 minutes and incubated with Alexa-fluor secondary antibodies (Invitrogen) diluted 1:500 in washing solution for 1h in a wet chamber. After the washing step for the secondary cells were fixed at room temperature for 2 minutes with 4% PFA and dehydrated in ice-cold ethanol. At this point RNA-FISH was performed as described in par. 2.12. Images were captured with Leica DM4000B microscope. The number of co-localizations per focal plane was counted. The Student t test was used to calculate the statistical significance.

2.14 Telomere length analyses on metaphase spreads

For telomere Q-FISH on metaphase spreads exponentially growing primary mouse embryonic fibroblasts (pMEFs) were incubated with 0.1 μg/mL colcemide (GIBCO) for 5 h at 37°C. Cells were collected and centrifuged at 900 rpm for 5 minutes. Pellet was resuspended in 1 ml of medium and 9 ml of hypotonic solution (0.03M Na-Citrate) previously heated at 37°C were added under constant vortexing. Then, cells were incubated for 25 minutes at 37°C and centrifuged for 5 minutes at 900 rpm. The hypotonic solution was removed leaving only 1 ml and then 2 ml of fix solution (Methanol: acetic acid 3:1) were added drop by drop under constant vortexing. Subsequently, other 9 ml of fix solution were added. Fixation step has been repeated twice. Then metaphase spreads were prepared: 200ul of each sample were dropped from a distance of 1 meter on the slide previously washed with methanol and treated with 45% acetic acid. The slides were dried overnight in the dark at room temperature (RT). The day after, cells were hydrated for 15 minutes with 1X PBS and then fixed with 4% formaldehyde for 2 minutes. After three washes with 1X PBS, the slides were incubated with pepsin solution (200mg of pepsin, 168ul of HCl, 200 ml of H2O) for 10 minutes at 37°C in the bath. Fixing and washing steps were repeated and then the slides were

dehydrated with three successive washes, respectively, in 70%, 90%, and 100% ethanol for 5 minutes each and left to dry for 20 minutes. PNA telomere probe $(TTAGGG)_4$ was prepared by resuspending 5 ng of lyophilised probe in 200µl of water and then incubated at 37 ° C for 5 min, 70 ° C for 3 min, and again at 37 ° C for 5 min. PNA-telomere probe solution (Table 1) was added to each slide and denaturated at 80 ° C for exactly 3 minutes. After 2h of incubation in the dark in a humid chamber, slides were washed twice with FISH solution (Table 2) for 15 minutes at RT. Further 3 washes of 5 minutes with 1XTBS/0,01% Tween-20 at RT were performed, followed by a wash in 1X TBS with DAPI for 5 minutes. Slides were then dehydrated with 3 washes, respectively in 70%, 90%, 100% of ethanol and mounted in Vectashield. Images were captured in a linear acquisition mode using a COHU CCD camera on a Leica DMRB microscope. The Wilcoxon–Mann– Whitney rank sum test was used for statistical comparisons of the mean telomere length.

Table 1: probe solution

Stock	**to 250 ul (10 slides)**	**Final concetration**
1M Tris pH 7.2	2.5 ul	10mM
Buffer MgCl pH 7.0 (25 mM MgCl, 9 mM citric acid, 82 mM Na_2HPO_4)	21.4 ul	
Deionized Formamide	175.0 ul	70%
probe 25ug/ml	5.0 ul	0.5 ug/ml
BM 10% (blocking reagent)	12.5 ul	0.25%
H_2O	33.6 ul	

Table 2: FISH solution

Stock	**To 400 ml**	**Final concentration**
Formamide	280 ml	70%
1M Tris pH 7.2	4ml	10mM
BSA 10%	4ml	0.1%
H_2O	112	

2.15 Chromosome Orientation FISH (CO-FISH)

Confluent cells were subcultured in the presence of 5′-bromo-2′-deoxyuridine (BrdU; Sigma) at a final concentration of 10μM and then were allowed to replicate their DNA once at 37 °C overnight. During the final 2-3 h, colcemid was added. For H1299 we used a colcemid concentration of 1μg/ml for 2 h at 37°C while for U2-OS we used a concentration of 0.2μg/ml for 3 h at 37°C. Cells were then recovered and metaphases prepared as described in par. 2.13. The slides were dried overnight in the dark at room temperature (RT). Slides were rehydrated in 1× PBS for 10 min at room temperature, incubated with 0.5 mg/ml RNaseA (in PBS, DNase free) for 10 min at 37°C and stained with 0.5 μg/ml Hoechst 33258 in 2× saline sodium citrate solution (SSC) for 15 min at room temperature in the dark. Subsequently, slides were placed in a shallow plastic tray, covered with 2× SSC and exposed to 365 nm ultraviolet light at room temperature for 25 min. The BrdU-substituted DNA strands were digested with at least 3 U/μl of Exonuclease III at room temperature for 10 min. Slides were washed in 1× PBS and then fixed with 4% formaldehyde for 2 minutes. After three washes with 1X PBS, the slides were incubated with pepsin solution (200mg of pepsin, 168ul of HCl, 200 ml of H2O) for 10 minutes at 37°C in the bath. Fixing and washing steps were repeated and then the slides were dehydrated with three successive washes, respectively, in 70%, 90%, and 100% ethanol for 5 minutes each and left to dry for 20 minutes. Cy3 $(TTAGGG)_7$ probe solution (see par. 2.14, Table 1) was added to each slide. The slides were not subjected to DNA denaturation. After 2h of incubation in the dark in a humid chamber, slides were washed twice with FISH solution (see par. 2.14, Table 2) for 15 minutes at RT. Further 3 washes of 5 minutes with 1XTBS/0,01% Tween-20 at RT were performed, followed by a wash in 1X TBS for 5 minutes. Then the slides were dehydrated with three successive washes, respectively, in 70%, 90%, and 100% ethanol for 5 minutes each and left to dry for 20 minutes. $(CCCTAA)_7$ probe labeled with Rhodamine Green (see par. 2.14 Table 1) was added to each slide. The slides were not subjected to DNA denaturation. After 2h of incubation in the dark in a humid chamber, slides were washed twice with FISH solution (see par. 2.14 Table 2) for 15 minutes at RT. Further 3 washes of 5 minutes with 1XTBS/0,01% Tween-20 at RT were performed, followed by a wash in 1X TBS with DAPI for 5 minutes. Slides were then dehydrated with 3 washes, respectively in 70%, 90%,

100% of ethanol and mounted in Vectashield. Metaphase spreads were captured with Leica DM4000B microscope.

2.16 Telomeric DNA FISH

Cells were washed in 1X PBS and fixed with 4% formaldehyde for 2 minutes at RT. After three washes for 5 minutes with 1X PBS in agitation, the slides were incubated in pepsin solution, previously heated, for 10 minutes at 37 ° C in the bath. The fixing and washing steps were repeated a second time and then the slides were dehydrated with three successive washes, respectively, in 70%, 90%, and 100% ethanol for 5 minutes each and left to dry for 20 minutes. Then 15 ul of PNA-telomere probe were added to each slide and cover with a coverslip, so the slides were denaturated at 80 ° C for 3 minutes exactly. The slides were then incubated for 2 h at RT in the dark in a humid chamber. To remove the coverslip two washes were performed of 15 minutes with FISH solution (Formamide 70%, Tris pH 7.2 10mM, BSA 0.1%, H2O) at RT, followed by 3 washes of 5 minutes in 1XTBS with 0,01% of Tween 20 at RT and one wash in 1X TBS with DAPI for 5 minutes. The slides were then dehydrated with 3 washes, respectively in 70%, 90%, 100% of ethanol, then mounted with Vectashield. Images were captured using Leica DM4000B microscope. Telomere signals intensity of interphase nuclei was analyzed using TFL-TELO software. The Student t test was used to calculate the statistical significance.

2.17 Immunofluorescence and telomere FISH

Immunofluorescence combined with telomeric DNA FISH was performed in U2-OS cells seeded on slides and H1299 blocked in metaphase using colcemid (1ug/ml for 3 hours) and spotted by cytospin centrifugation on slides. Cells were fixed for 20 minutes with 4% formaldehyde in PBS and permealized with PBS 0.1% Triton X-100 for 7 minutes at room temperature. Then, cells were washed two times with 1X PBS and were blocked with 3% (w/v) BSA 1XPBS for 20 minutes at 37°C. Subsequently, slides were incubated with primary antibodies (check 2.23 antibodies table) diluted in blocking solution at 4° C overnight. Cells were washed twice in 0.05% Triton X-100 1XPBS for 5 minutes and then incubated with secondary antibodies for 1 hour at room temperature. After

immunostaining, telomeric FISH was performed as described in par. 2.16 with minor modifications. Images were captured using Leica DM4000B microscope.

2.18 TERRA Northern Blot and qRT-PCR

To perform Northern blot analysis total RNA (10 μg) was loaded onto 1.2% formaldehyde agarose gels and separated by electrophoresis. RNA was then transferred to Nylon membranes and blots were incubated with ^{32}P-labelled telomeric probe obtained from a plasmid containing 1.6 kb of TTAGGG repeats.
For RT–PCR analysis, total RNA (1.5 μg) was reverse transcribed with random oligos (2pmol) and telomere-specific primers (2pmol) (TEL Rev: 5′ CCTAACCCTAACCCTAAC CCTAACCCTAA 3′) at 55 °C using SuperScript III reverse transcriptase (Invitrogen). For quantitative SYBR green reactions, different TERRA transcripts were analysed using the following chromosome specific primers:
Chr. 1q-21q Fw: 5′ TCTCGGTGCGCAGGATTCAGA 3′,
Chr. 1q-21q Rev: 5′ GTCACAGACCAGTTAGAATG 3′,
Chr. 2q-10q-13q Fw: 5′ GTCAGAGACCAGTTAGAACG 3′,
Chr. 2q-10q-13q Rev: 5′ GGTGCGCAGGATTCAGAGAG 3′.
TERRA transcripts levels were normalized to global histone H3 levels:
H3 Fw: 5′GTGAAGAAACCTCATCGTTACAGGCCTGGT3′,
H3 Rev: 5′CTGCAAAGCACCAATAGCTGCACTCTGGAA 3′.

2.19 Quantitative real-time PCR

Total RNA was prepared using QIAzol Lysis Reagent (Qiagen) and reverse transcribed with QuantiTect Reverse Transcription Kit (Qiagen) according to the manufacturer's instructions. Quantitative PCR was performed using the QuantiFast SYBR Green PCR Kit (Qiagen) and analyzed with the CFX96 Real-Time PCR Detection System (BIO-RAD. mRNA levels were normalized to actin. PCR primers used for quantitative Real-Time PCR (Schuler M. et al. 2003):
Bax FW: 5′ GGAGCAGCTTGGGAGCG 3′,
Bax REV: 5′ AAAAGGCCCCTGTCTTCA 3′,

Puma FW: 5′ ACCTCAACGCGCAGTAC 3′,
Puma REV: 5′ TGAGGGTCGGTGTCGAT 3′,
β-actin FW: 5′ CACACCCGCCACCAGTTC 3′,
β-actin REV: 5′ CCCATTCCCACCATCACACC 3′.

2.20 Colony formation assays using pMEFs

Low passage of pMEFs of control and Suv39h1ΔStop transgenic mice were infected with a recombinant, replication deficient retroviral vector expressing E1A and H-*ras* as previously described (Efeyan A. et al. 2009). Puromycin selection for 3 days was used to eliminate non-transduced cells. After 19 days colonies were stained with Giemsa and colony number and size was determined.

2.21 Isolation, culture and colony forming assays using primary mouse keratinocytes

Skin keratinocytes were isolated from the back skin of newborn mice. For colony forming assays 10^4 or $5x10^5$ keratinocytes were seeded on a mitomycin C treated J2-3T3 feeder layer and cultivated in CnT-O2 medium with supplement and antibiotics (CELLnTEC, Advanced Cell Systems AG) for 11 days. Subsequently cells were fixed with 18,5% formaldehyde and stained in with 1% Rhodamine B. Colony size and numbers were assessed.

2.22 Skin carcinogenesis

Age-matched (8- to 12-wk-old) mice of each genotype (37 control; 6 Suv39h1ΔStop) were shaved and treated with a single dose of DMBA (7,12-Dimethylbenz[α]anthracene; 0.1 µg/µL in acetone; Sigma). Mice were subsequently treated twice weekly with TPA (12-O-tetradecanoylphorbol-13-acetate; 12.5 µg in 200 µL of acetone each treatment; Sigma) for 15 wk. Papilloma formation and growth was followed in weekly examinations during additional 15 weeks.

2.23 Antibodies table

Antibodies	company	WB	IF	IP	Chip
Mouse anti–Actin	Sigma, A2228	✓			
Mouse anti-ATM (clone 5C2)	Santa Cruz, sc-23922	✓			
Mouse anti-pATM (S1981) clone 10H11.E12	Santa Cruz sc-23922	✓			
Rabbit anti-ATR	Cell Signalling, 2790	✓			
Rabbit anti-pATR (S428)	Cell Signalling, 2853	✓			
Rabbit anti-Bax	Cell signaling, 2772	✓			
Mouse anti-DNA-RNA Hybrid (S9.6)	Kerafast, ENH001		✓		
Mouse FUS/TSL (4H11)	Santa Cruz, sc-47711	✓			
Mouse anti- γH2AX (ser139) clone JBW301	Millipore, 06-70	✓	✓		
Rabbit anti-global histone H3	Abcam, ab1791	✓			
Rabbit anti-H3K9me3	Upstate, 07-442	✓	✓		
Rabbit anti-HP1β	Abcam, 10478		✓		
Mouse anti-HP1γ	Upstate, 05-690		✓		
Goat anti-Lamin A/C (clone N-18)	Santa Cruz, sc-6215	✓			
Rabbit anti-NONO	A300-582A,Bethyl lab	✓	✓	✓	✓
Mouse anti-p53 (DO-1)	Santa Cruz, sc-126	✓			
Mouse anti-p53 (PAb 240)	Abcam, ab26	✓			
Rabbit PML (H-238)	Santa Cruz, sc-5621		✓		
Rabbit anti-PSF/SFPQ	A301-321A, Bethyl lab	✓		✓	✓
Mouse anti-PSF (clone B92)	Sigma, P2860	✓	✓		
Rabbit Rad51 (H-92)	Sant Cruz, sc-8349		✓		
Rabbit anti-phospho RPA32(S33)	A300-246A, Bethyl Lab		✓		
Mouse anti-Suv39h1	Abcam, ab12405	✓			
Rabbit anti-topoisomerase II alpha	Abcam, ab 74715		✓		
Rabbit anti-TRF1(N-19)	Santa Cruz, sc-6165-R		✓		
Rabbit anti-mouse TRF1	produced in house				✓
Mouse anti-TRF2 (4A794)	Millipore, 05-521	✓	✓		✓

3. Results

3.1 Project 1: altered telomere homeostasis and resistance to skin carcinogenesis in Suv39h1 transgenic mice

3.1.1 Suv39h1 transgenic mice show increased levels of global H3K9me3

In order to define the impact of the HMTase Suv39h1 overexpression *in vivo,* a conditional transgenic mouse model has been generated. Suv39h1 cDNA was cloned downstream of a floxed transcriptional stop-cassette (pA) that blocks transgene-transcription driven from the upstream located CAGGS promoter (Figure 3.1.1A). This CMV-loxP-Stop-loxP-Suv39-pA cassette was used to generate a transgenic mouse line that was crossed with CMV-Cre transgenic mice (Zinyk D.L. et al. 1998) to obtain animals with excised of transcriptional stop-cassette (Suv39h1ΔStop/CMV-Cre; in this study: "Suv39h1ΔStop" mice) and heterozygous CMV-Cre mice (in this study: "control"). Deletion of the transcriptional stop cassette and Suv39h1 mRNA levels in primary mouse embryonic fibroblast (pMEFs) derived from Suv39h1StopΔ embryos have been verified by southern blot and q-RT PCR, respectively (data not shown, Petti E. et al. 2015). Transgenic mice were created at the Spanish National Cancer Center (CNIO), Maria Blasco Lab. Western blotting with specific anti-Suv39h1 antibody confirmed ectopic expression of Suv39h1 in nuclear extracts of pMEFs obtained from Suv39h1ΔStop embryos (Figure 3.1.1B). Whole cell extracts prepared from H1299 transiently transfected with a control vector (pcDNA) or HA-tagged Suv39h1 (HA-Suv39h1) have been included to confirm Suv39h1 antibody specificity. Suv39h1 protein levels are increased in Suv39h1StopΔ pMEFs. To control whether ectopically expressed Suv39h1 is enzymatically active, we measured global levels of tri-methylated histone 3 lysine-9 (H3K9me3) in Suv39h1ΔStop pMEFs by western blotting. As expected, Suv39h1ΔStop pMEFs show significantly increased levels of H3K9me3 compared to control pMEFs (Figure 3.1.1C-D). Together these results indicate that deletion of the floxed transcriptional stop-cassette results in Suv39h1 transgene expression and correlates with increased global levels of H3K9me3 in Suv39h1ΔStop pMEFs.

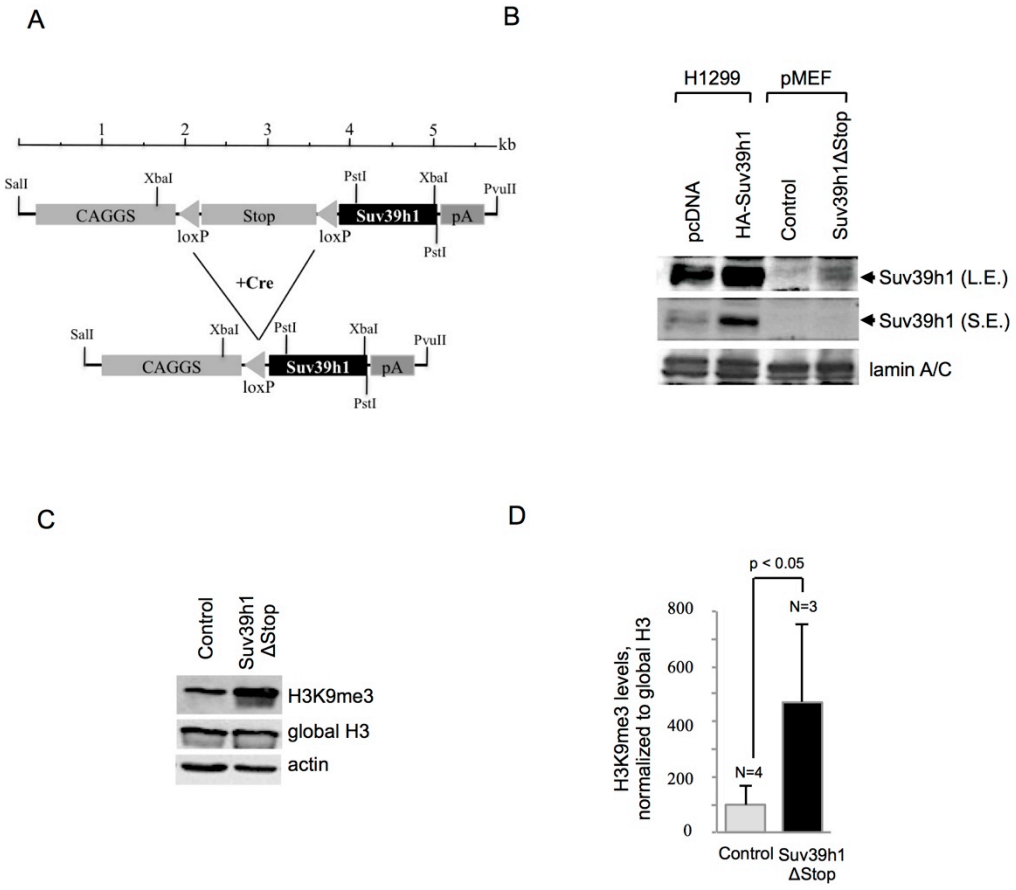

Figure 3.1.1. Suv39h1 transgenic mice. A. Schematic representation of the Suv39h1 transgenic vector. Restriction sites for transgene-cassette excision. **B**. Suv39h1 expression levels in pMEFs derived from control and Suv39h1ΔStop transgenic mice as determined by western blotting using nuclear extracts (pMEFs). Whole cell extracts prepared from H1299 transiently transfected with a control vector (pcDNA) or HA-tagged Suv39h1 (HA-Suv39h1) were loaded to verify specificity of the anti-Suv39h1 antibody. Weak Suv39h1 signals in Suv39h1ΔStop pMEFs are due to low antibody affinity in western blotting experiments. Arrows indicate the specific Suv39h1 band, L.E.: long exposure, S.E.: short exposure. **C**. Increased H3K9me3 expression levels in pMEFs obtained from control and Suv39h1ΔStop transgenic mice as determined by western blotting. Antibodies against global histone H3 were used to control for equal loading. Quantification of H3K9me3 levels shown in **D**. H3K9me3 levels were normalized to global histone H3 levels. N=number of different pMEF pool used for each genotype; standard deviations are indicated; a Student's t-test was used to calculate statistical significance.

3.1.2 Suv39h1 overexpression impacts on HP1β nuclear distribution and increases H3K9me3 levels *in vivo*

Given the role of Suv39h1 in heterochromatin formation, we whished to explore the impact of Suv39h1 overexpression on chromatin structure *in vivo*. Quantitative immunofluorescence for H3K9me3 demonstrated that Suv39h1 overexpression significantly increases H3K9me3 staining intensity in the nuclei and at chromocenters of Suv39h1ΔStop pMEFs compared to control cells, thus confirming the western blot results (Figure 3.1.2A-B). H3K9me3 serves as a high affinity binding site for the recruitment of HP1 proteins, which in turn interact with Suv4-20h1 and Suv4-20h2 HMTases to establish

constitutive heterochromatin at pericentric and telomeric repeats (Lachner M. et al. 2001; Garcia-Cao M. et al. 2004). In order to test whether increased H3K9me3 could impact on the structure of constitutive heterochromatin, immunostainings for HP1β and HP1γ were performed in control and Suv39h1ΔStop pMEFs. We found that Suv39h1 overexpression changes the nuclear distribution of HP1β from a concentrated staining at DAPI rich chromocenters to a more dispersed pattern (Figure 3.1.2C). Differently, HP1γ distribution appears to be not clearly affected by Suv39h1 overexpression (Figure 3.1.2D). Notably, quantitative immunofluoresce for HP1β and HP1γ demonstrated that HP1β and HP1γ levels remain unchanged in the nuclei of Suv39h1ΔStop pMEFs compared to control cells (Figure 3.1.2E-F). In line with previous studies, these results demonstrate that increased H3K9me3 levels in different chromatin sites can result in changed nuclear localization pattern of HP1β whithout changing total HP1β and HP1γ abundance (Melcher M. et al. 2000; Czitkovich S. et al. 2001).

In order to validate the impact of Suv39h1 on heterochromain formation *in vivo*, we used confocal microscopy to measure global H3K9me3 levels on tail sections prepared from adult Suv39h1ΔStop mice. In line with results in pMEFs, we found significantly increased H3K9me3 average levels in the nuclei of skin cells obtained from Suv39h1ΔStop transgenic mice (Figure 3.1.2G-H). We conclude that Suv39h1 overexpression increased global H3K9me3 level in pMEFs as in transgenic mice and impact on HP1β distribution without any effect on HP1β and HP1γ global levels.

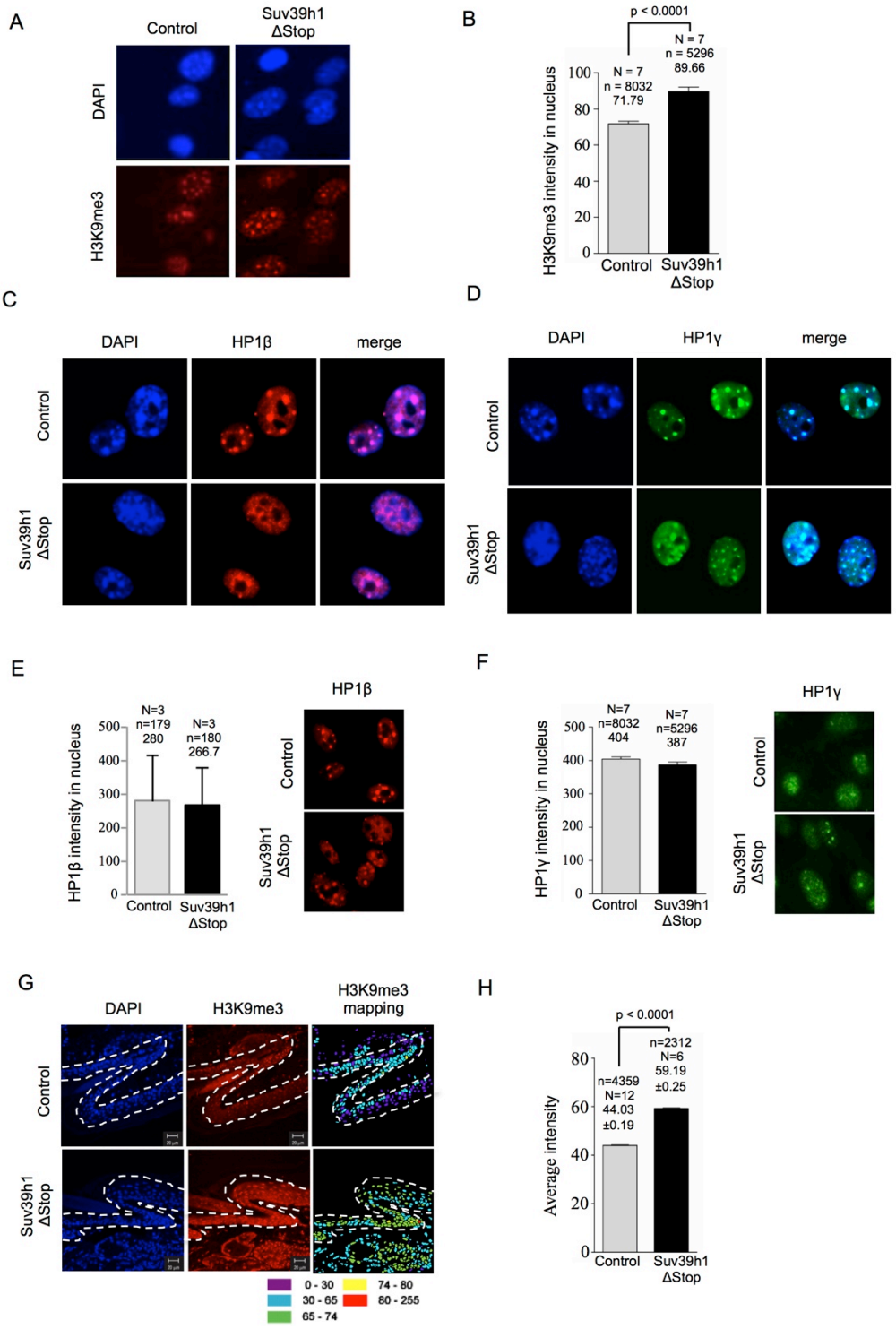

Figure 3.1.2. Suv39h1 overexpression increases H3K9me3 in transgenic pMEFs and animals.
A. Increased nuclear H3K9me3 levels in pMEFs obtained from control and Suv39h1ΔStop transgenic mice as determined by automated confocal microscopy. **B**. Quantification of confocal H3K9me3 immunofluorescence of samples shown in A. Suv39h1 overexpression results in a significant increase in H3K9me levels. **C**. Suv39h1 overexpression results in a re-distribution of HP1β in pMEFs, as determined by immunofluorescence staining. **D**. Suv39h1 does not impact on the localization of HP1γ, as determined by immunofluorescence staining. **E**. Suv39h1 overexpression does not impact on global HP1β levels in Suv39h1ΔStop pMEFs, as determined by classic quantitative immunofluorescence. Left panel: quantification; right panel, representative images. **F**. Suv39h1 overexpression does not impact on global HP1γ levels in Suv39h1ΔStop pMEFs, as determined by automated confocal quantitative immunofluorescence. Left panel: quantification; right panel, representative images. **G**. Immuno-histochemistry on adult skin tail sections using H3K9me3 specific antibodies. Suv39h1ΔStop mice display increased H3K9me3 levels as demonstrated by confocal microscopy and signal intensity mapping (see material and methods). H3K9me3 intensity ranges are indicated by a color code that is based on arbitrary fluorescence units. **H**. Quantification of average H3K9me3 intensity. Average H3K9me3 levels are significantly increased in tail skin sections of Suv39h1ΔStop mice. N=number of independently prepared pMEF cultures or mice tested; n= number of nuclei analyzed; arbitrary fluorescence intensity values are indicated; standard deviations are indicated; p-values indicate statistical significance.

3.1.3 Ectopic Suv39h1 expression drives telomere shortening in pMEFs

Abrogation of master epigenetic regulators, such as histone methyl-transferases and DNA methyltransferases has been linked with loss of telomere length control (Blasco M.A. 2007). In particular, Suv39h1 and Suv39h2 double knockout (Suv39hDN) pMEFs or cells that lack DNMTs or Suv4-20h1 and h2 show a loss of chromatin compaction at telomeres resulting in recombination dependent telomere elongation (Garcia-Cao M. et al. 2004; Gonzalo S. et al. 2006; Benetti R. et al. 2007). To investigate the impact of Suv39h1 overexpression on telomere chromatin structure and telomere length homeostasis, we performed telomeric chromatin immunoprecipitation experiments (ChIP) and telomere length analysis in Suv39h1ΔStop pMEFs and control pMEFs. In line with increased global H3K9me3 levels, telomeric ChIP revealed that ectopic Suv39h1 expression causes an approximately 50% increase in H3K9me3 at telomeric and major satellite repeats without affecting the abundance of HP1γ or H4K20me3 (Fig. 3.1.3A-D). In addition, Suv39h1 overexpression does not impact on the abundance of TRF1 shelterin component at telomeric TTAGGG repeats (Figure 3.1.3A,C). Quantitative telomeric DNA-FISH demonstrated that increased chromatin compaction at telomeres induced by Suv39h1 overexpression correlates with telomere shortening in Suv39h1ΔStop pMEFs compared to control pMEFs (Figure 3.1.3.E). Dividing telomere intensity signals into three different length categories: <30kb, 30-70kb, >70kb, we observed that Suv39h1ΔStop pMEFs display an increased number of short telomeres (< 30 kb) and reduced number of long telomeres (> 70 kb) compared to control cells (Figure 3.1.3F). This data is in line with telomere elongation in Suv39h1/h2 double knockout mice (Garcia-Cao M. et al. 2004). Together, this indicates that Suv39h1 HTMase acts as negative regulator of telomere length in mouse cells.

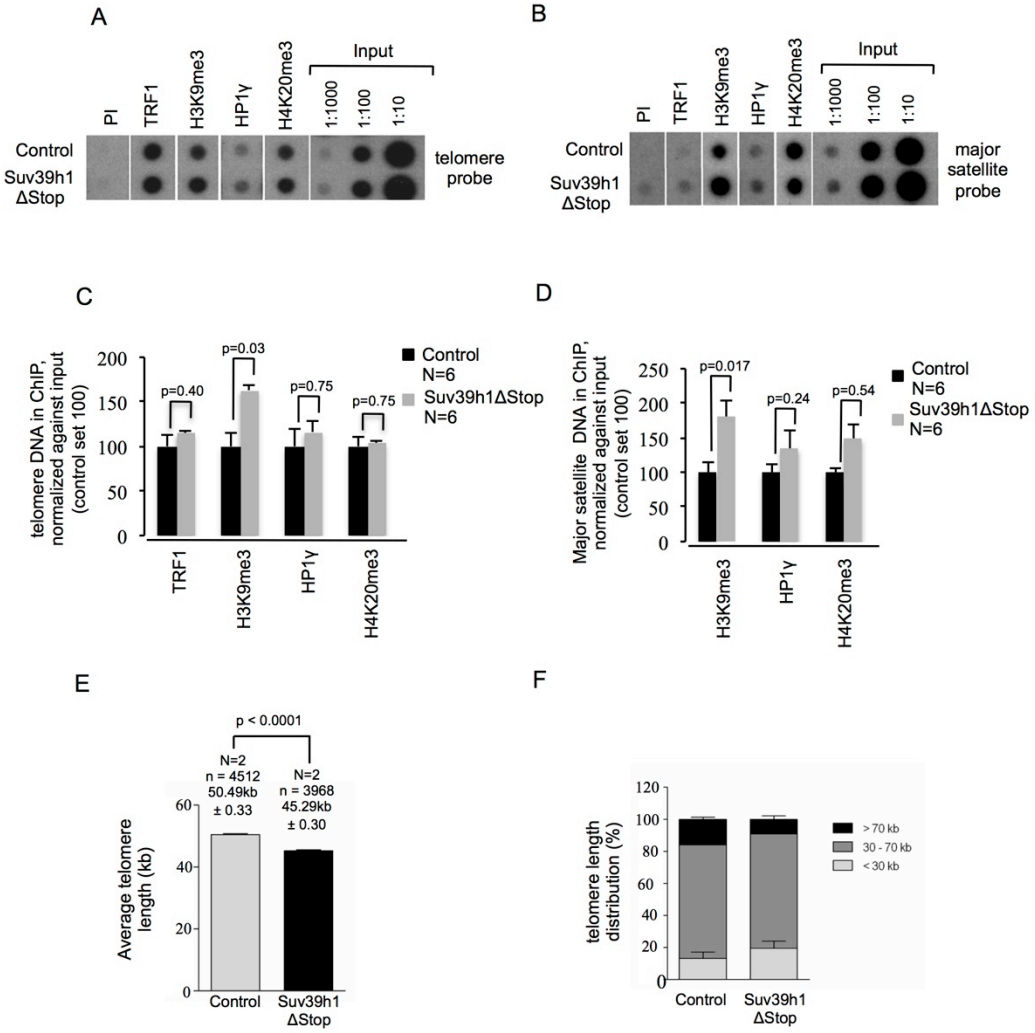

Figure 3.1.3. Compaction of telomeric chromatin and telomere shortening in Suv39h1ΔStop pMEFs. A. Suv39h1ΔStop pMEFs display augmented H3K9me3 levels at telomeric repeats, as determined by ChIP. Representative images are shown. **B**. Suv39h1ΔStop pMEFs display augmented H3K9me3 levels at pericentric major satellite repeats. Representative images are shown. **C**. Quantification of immunoprecipitated telomeric DNA using the indicated antibodies; signals were normalized to the input material. **D**. Quantification of immunoprecipitated major satellite repeats; signals were normalized to the input material. **E**. Quantitative telomere Q-FISH on metaphase chromosomes obtained from control and Suv39h1ΔStop pMEFs. Average telomere length is significantly shorter in Suv39h1ΔStop transgenic mice when compared to pMEFs with normal Suv39h1 expression. **G**. Telomere length distribution in Suv39h1ΔStop pMEFs and control pMEFs. Accumulation of short telomeres (<30kb) and reduction of long telomeres (>70kb) in Suv39h1ΔStop pMEFs. N, number of independently prepared pMEF cultures analyzed; standard deviations are indicated; n, number of telomeres analyzed; statistical significance is indicated by p-values

3.1.4 Suv39h1 overexpression increased resistence to oncogenic transformation

Several studies have introduced a role of Suv39h HTMases in the control of cell proliferation and mitotic progression (Melcher M. et al. 2000; Czitkovich S. et al. 2001). Suv39h1/2 double null mice show increased B cell lymphoma frequency and genomic instability suggesting a role for Suv39h1/2 in tumor suppression (Peters A.H.F.M. at al. 2001). In line with this, loss of Suv39h HTMases has been demonstrated to accelerate Ras

or myc driven tumorigenesis, caused by an impairment of oncogene induced senescence (Braig M. et al. 2005; Reimann M. et al. 2010). Moreover, Suv39h1 overexpression induces mitotic defects in human cancer cells and increases the immortalization of primary erythroblasts (Melcher M. et al. 2000; Czvitkovich S. et al. 2001).

However the effect of elevated Suv39h1 expression on tumor suppression has not yet been studied *in vivo*. To address this point, we tested the impact of Suv39h1 overexpression on pMEFs proliferation and oncogene-induced transformation. Primary fibroblasts derived from control and Suv39h1ΔStop embryos were transduced with retroviral expression vectors for E1A and H-*ras* and colony forming assays were performed. We found that transduced Suv39h1ΔStop pMEFs show a 50% reduction of colony forming potential compared to transduced control pMEFs (Figure 3.1.4.A-B). This result suggests that Suv39h1 antagonizes immortalization driven by the Ras and E1A pathways. In order to elucidate the mechanism that confers resistance of Suv39h1ΔStop pMEFs to oncogenic transformation, we analyzed the p53 tumor suppressor pathway. Importantly, we found a significant upregulation of p53 protein levels in Suv39h1ΔStop pMEFs (Figure 3.1.4C). In line with this, we also found transcriptional activation of pro-apoptotic genes: Puma and Bax (Figure 3.1.4D).

Together these data indicate that Suv39h1 overexpression increases tumor-surveillance by p53. Increased p53 activity improves resistance of primary MEFs to oncogenic transformation by E1A/H-*ras*. Importantly, loss of Suv39h1 was reported to result in impared oncogene induced senescence in N-Ras transgenic mice (Braig M. et al. 2005). Together, this underlines that increasing Suv39h1 activity improves tumor suppression.

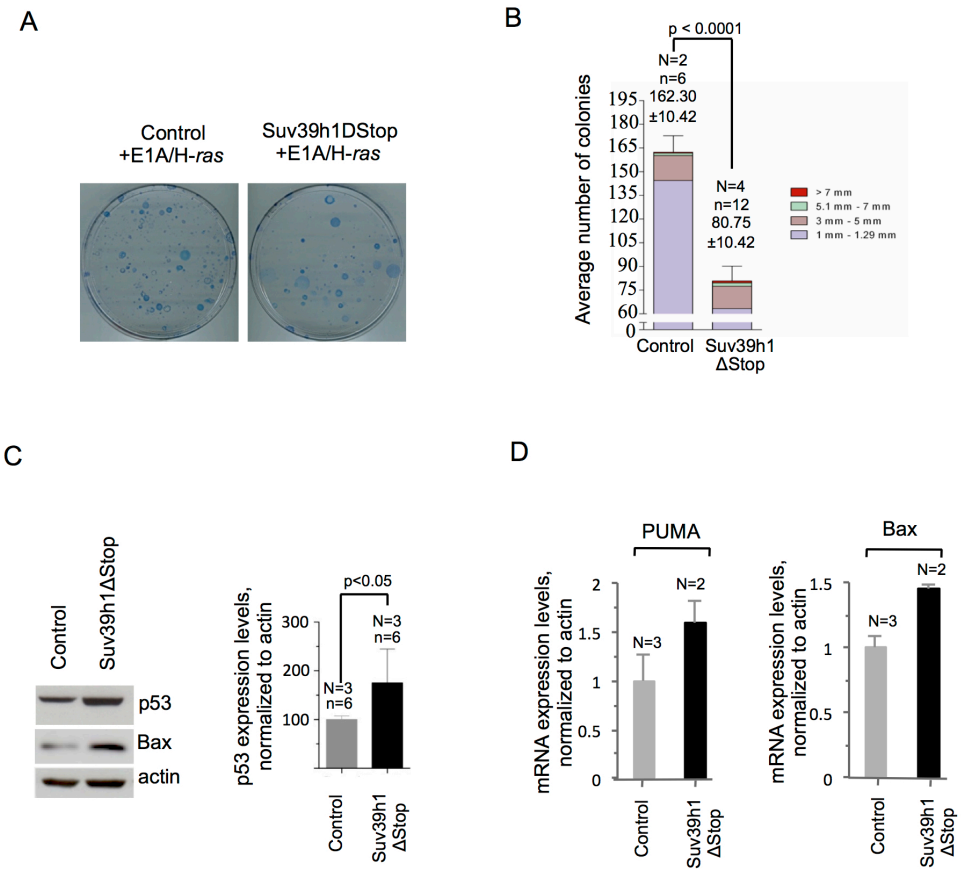

Figure 3.1.4. Suv39h1 overexpression limits immortalization of primary MEFs. A. Colony forming assay of control and Suv39h1ΔStop transgenic pMEFs after retroviral transduction of H-*ras* and E1A. Representative images are shown. **B**. Suv39h1 overexpression results in reduced immortalization as indicated by limited colony formation potential. Color code indicates diameter of formed colonies (mm). **C**. Left panel: western blotting indicates elevated p53 protein levels in Suv39h1ΔStop pMEFs. Actin was used as a loading control. Right panel: quantification of western blotting results. **D**. Quantitative real-time PCR of p53 target genes Bax and Puma. Actin was used to normalize expression levels. N, number of independently prepared cell cultures analyzed; n, number of total numbers of experiments or replicas analyzed; standard deviations are indicated; statistical significance is indicated by p-values.

3.1.5 Suv39h1 transgenic mice are resistant to skin carcinogenesis

We performed colony forming assay using primary keratinocytes prepared from the back skin of Suv39h1ΔStop and control animals to reproduce pMEFs data. In the absence of oncogenic stress, Suv39h1ΔStop keratinocytes showed a significant 25% reduction in colony forming potential compared to control cells (Figure 3.1.5A-B). *In vitro* experiment indicated that increased Suv39h1 improves resistance to oncogenic transformation. To explore the tumor suppressive role of Suv39h1 *in vivo*, we subjected wild-type or Suv39h1ΔStop mice to a skin carcinogenesis protocol. After initial treatment of the back skin of experimental mice with the DNA damaging agent DMBA (7,12-Dimethylbenz[α]anthracene), mice were treated with the mitogen TPA (12-O-tetradecanoylphorbol-13-acetate) for a period of 15 weeks (Figure 3.1.5C). This treatment

results in the accumulation of oncogenic H-*ras* mutations that finally induce skin papillomas (Balmain A. et al. 1984). To follow tumor formation, the number and dimensions of developed skin papillomas were measured for 30 weeks after DMBA treatment. As expected, control mice efficiently developed papillomas during the course of the experiment (Figure 3.1.5D). In contrast, Suv39h1ΔStop mice show a dramatically reduced frequency of papilloma formation, suggesting that Suv39h1 overexpression confers resistance to DMBA/TPA induced carcinogenesis (Figure 3.1.5D). These data indicate that ectopic Suv39h1 increases resistance to skin carcinogenesis *in vivo*.

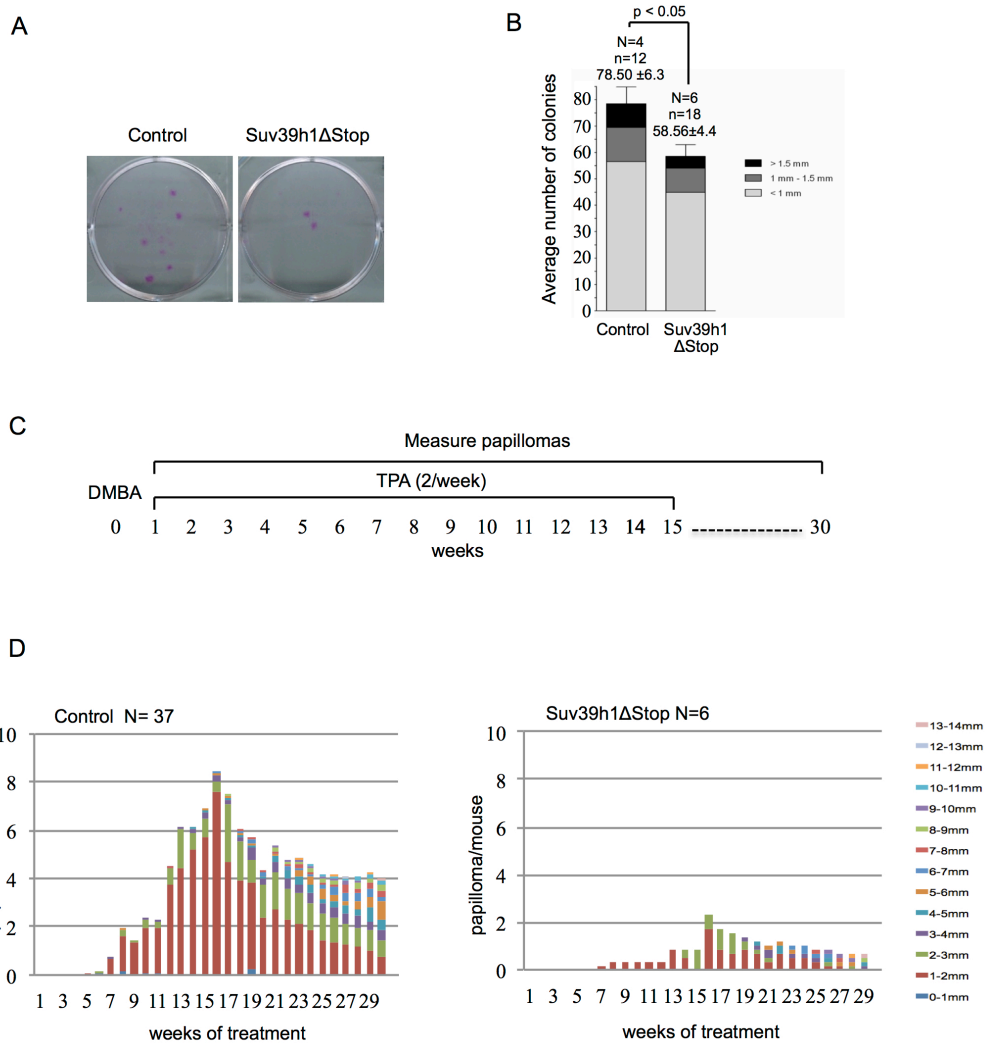

Figure 3.1.5. Suv39h1 overexpression confers resistence to skin carcinogenesis. A. Colony forming assays using primary mouse keratinocytes prepared from the back skin of control or Suv39h1ΔStop newborn mice. Representative images are shown. **B**. Suv39h1ΔStop keratinocytes display reduced colony forming potential. Color code indicates diameter of formed colonies (mm). **C**. Schematic representation of the DMBA/TPA skin carcinogenesis protocol. After an initial DMBA treatment, the back skin of experimental mice was treated twice per week with TPA for a total period of 15 weeks. Papilloma formation and size were monitored in weekly inspections. **D**. Papilloma formation in control and Suv39h1ΔStop mice during DMBA/TPA skin carcinogenesis. Papilloma formation is efficiently impaired in Suv39h1ΔStop mice. Color code indicates diameter of formed papillomas (mm).

Altogether, our results demonstrated that Suv39h1 HMTase is a negative regulator of telomere length and represents an interesting target modulating p53 tumor suppressor activity and improving resistance to oncogene induced transformation.

3.2 Project 2: identification of novel TERRA interactors that control mammalian telomeres

3.2.1 A RNA affinity assay to identify novel TERRA interacting proteins

To obtain new insights into the biological function of TERRA, an *in vitro* RNA pull-down experiment was performed to identify novel TERRA interacting proteins. Nuclear extracts prepared from mouse embryonic stem cells (mESCs) were incubated with biotinylated TERRA oligos containing $[UUAGGG]_6$ repeats (biotin-r-$[UUAGGG]_6$) or with biotinylated negative control RNA oligos consisting a 36 nucleotide sequence of the EGFP cDNA (biotin-r[EGFP]) (Figure 3.2.1A). After incubation, protein complexes bound to biotin-r$[UUAGGG]_6$ or biotin-r[EGFP] were recovered using streptavidine beads, extensively washed, eluted and subjected to gel-electrophoresis (Figure 3.2.1A). Silver staining revealed that biotin-r$[UUAGGG]_6$ and biotin-r[EGFP] are commonly bound by a series of proteins (Figure 3.2.1B). Importantly, biotin-r$[UUAGGG]_6$ eluate shows a specific enrichment of 13 proteins, that were subsequently identified by mass spectrometry (Proteomics unit, Istituto Regina Elena IRE/IFO) (Figure 3.2.1B, bands labeled with *). In line with previous studies, these include TERRA interacting proteins: Fused in Sarcoma/TranSlocated in Liposarcoma (FUS/TSL) (Takahama K. et al. 2013) and a series of heterogeneous nuclear ribonucleoproteins (hnRNPs) (de Silanes I. L. et al. 2010), confirming the specificity of our approach. In addition to already reported TERRA interactors, we found that polypyrimidine tract-binding protein-associated splicing factor (PSF/SFPQ) and the nuclear RNA-binding protein 54 kDa (p54nrb in human, NONO in mouse) interact with TERRA (Figure 3.2.1B). We also found an enrichment of DAZAP1 (DAZ associated protein 1), an RNA-binding protein involved in spermatogenesis that is not subject of this study (Hsu L.C.L. et al. 2008). Western blotting on eluates obtained from TERRA pull-down confirmed results from mass spectrometry analysis in mESCs

(Figure 3.2.1C) and human H1299 non-small cell lung carcinoma cells (Figure 3.2.1D). As expected actin was not detected in biotin-r[UUAGGG]$_6$ or biotin-r[EGFP] eluates (Figure 3.1C-D). We conclude that PSF and p54nrb are novel TERRA interacting proteins.

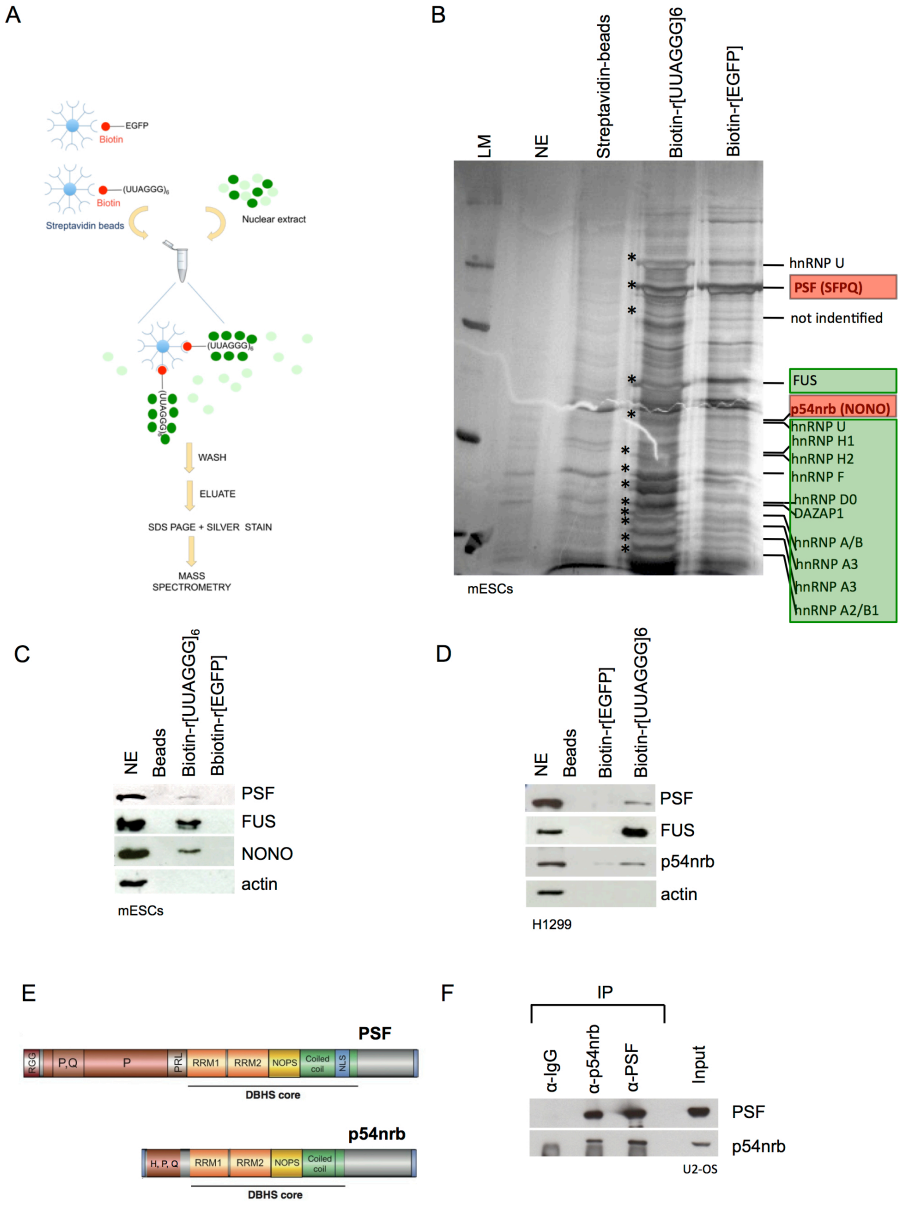

Figure 3.2.1. PTB-associated splicing factor (PSF) and nuclear RNA-binding protein 54 kDa (p54nrb) interact with TERRA. A. RNA pull-down strategy. Nuclear extracts prepared from mESCs were incubated with biotinylated r[UUAGGG]$_6$ or biotinylated r[EGFP] RNA oligonucleotides. Complexes were recovered using streptavidine beads, washed, eluted and subjected to SDS-PAGE followed by Silver staining and mass spectrometry analysis. **B**. Silver staining of SDS-PAGE gels after mono-dimensional electrophoresis of eluates obtained from RNA-pull down experiments using biotinylated r[UUAGGG]$_6$, biotinylated r[EGFP] RNA oligonucleotides or empty beads. A nuclear extract (NE) was loaded. Candidate TERRA interacting proteins were identified by mass spectrometry. Pull-down experiments identify PSF and p54nrb as novel TERRA interacting protein. **C-D**.Western blotting of TERRA pull down eluates using specific anti-p54nrb and anti-PSF antibodies confirms binding specificity of p54nrb and PSF for UUAGGG RNA repeats in mESCs (C) and H1299 cells (D). FUS western blotting confirms specificity of pull-down. Actin was used as a loading control. **E**. Domain structure of PSF and p54nrb. RGG, RGG box; P, proline-rich domain including subdomain (P,Q); H, P, Q histidine/proline/glutamine-rich region, ; PRL, PR linker; NLS, nuclear-localization sequence. RRM1, RNA recognition motif 1; RRM2, RNA recognition motif 2; NOPS, NONA/ParaSpeckle domain (modified from Yarosh A. et al. 2015). **F**. p54nrb and PSF form a complex as demonstrated by anti-p54nrb and anti-PSF immunoprecipitation experiments. Control Immunoglobulins (IgG) were used.

3.2.2 PSF and p54nrb are multifunctional regulators of RNA/DNA

PSF and p54nrb belong to the conserved family of Drosophila Behavior Human Splicing (DBHS) proteins, which also include PSPC1 (paraspeckle protein component 1) (Shav-Tal Y. and Zipori D. 2002; Bond C.S. and Fox A.H. 2009). Of notice, we did not detect PSPC1 in eluates from TERRA RNA pull down experiments. DHBS proteins share a core domain arrangement consisting of two RNA-recognition motifs (RRMs), a conserved sequence known as NONA/ParaSpeckle (NOPS) domain and a coiled-coiled domain (Figure 3.2.1E). The NOPS and RRM domains are important for the formation of homodimers and heterodimers among the DHBS proteins (Passon D.M. et al. 2012). Consequently, p54nrb and PSF often co-localize and co-purify together, as demonstrated by co-immunoprecipitation (Figure 3.2.1F). DHBS proteins localize in the nucleoplasm and nucleolar caps as well as in paraspeckles (Fox A.H. and Lamond A.I. 2010). Paraspeckles are subnuclear bodies formed by the association of the NEAT1 (nuclear-enriched abundant transcript 1) long non coding RNA (lncRNA) with DBHS proteins (Bond C.S. and Fox A.H. 2009; Chen L.L. and Carmichael G.G. 2009). A major function of Paraspekles consists in gene regulation by nuclear retention of mRNAs, mechanism involved in many cellular processes such as stress responses, viral infection and circadian rhythm maintenance (Fox A.H. and Lamond A.I. 2010).
Initial studies demonstrated a role for PSF and p54nrb in splicing or transcriptional regulation, respectively (Patton J.G. et al. 1991; Hallier M. et al. 1996; Basu A. et al. 1997). However, subsequent studies have linked PSF and p54nrb with a wide range of cellular activities such as RNA metabolism, transcriptional regulation and DNA repair.

3.2.2.1 PSF and p54nrb in RNA metabolism

The first function attributed to PSF was pre-mRNA splicing (Patton J.G. et al. 1991; Patton J.G. et al. 1993). *In vitro* studies provided evidence that PSF has a role in the early spliceosome formation. Subsequent proteomic and biochemical studies demonstrated a role of PSF in the second catalytic step of splicing (exon joining) of some pre-mRNA substrates, thus suggesting a role of PSF as alternative splicing regulator (Jurica M.S. and Moore M.J. 2003; Ajuh P. et al. 2000; Gozani O. et al. 1994; Fu X.D. and Ares M. Jr. et al. 2014). Accordingly, recent works demonstrated that PSF represses or promotes exon

inclusion in the final mRNA of some specific pre-mRNAs (Ray P. et al. 2011; Heyd F. and Lynch K.W. 2010; Kim K.K. et al. 2011; Cho S. et al. 2014). In addition to a direct regulation of the spliceosome, PSF may impact on splicing through its effect on transcription and 3′-end processing (Yarosh C.A. et al. 2015). In fact, PSF and p54nrb have been identified in a complex containing the U1A protein (distinct from the U1snRNP) important to couple splicing and polyadenylation at suboptimal polyadenylation sites (Liang S. and Luts C.S. 2006). Furthermore PSF/p54nrb recruits the exonuclease XRN2 to facilitate pre-mRNA 3′-end processing and transcription termination (Kaneko S. et al. 2007). In addition to splicing and 3′-end processing, the PSF/p54nrb complex is involved in permitting nuclear retention of selected mRNAs in paraspeckles. The signal for nuclear retention is established by ADAR (Adenosine De-Aminase RNA-specific), RNA-editing enzymes that catalyze the deamination of adenosines (A) to inosines (I) in the mRNAs to be retained. PSF/p54nrb complex has high affinity for hyperdited RNAs and retains these RNAs within paraspeckles, thus preventing their export to the cytoplasm (Zhang Z. and Carmichael G.G. 2001; Chen L.L. and Carmichael G.G. 2009). In conclusion, PSF/p54nrb complex is able to regulate gene expression impacting at least on three coupled steps of RNA processing: splicing, 3′-end processing and nuclear export. Interestingly, PSF and p54nrb are also implicated in DNA-mediated nuclear processes such as transcription and DNA repair.

3.2.2.2 PSF and p54nrb in transcriptional regulation

PSF and p54nrb have been demonstrated to act as transcriptional regulators. PSF/p54nrb stimulate transcription of ribosomal protein genes (RPL18) by binding a tandem sequence motif that functions as enhancer (Roepcke S. et al. 2011). In addition, PSF/p54nrb complex specifically binds to the RNA polymerase II (Pol II) C-terminal domain and enhance transcription by forming a bridge between Pol II transcription machinery and other splicing or polyadenylation factors (Emili A. et al. 2002). Interestingly, PSF has been demonstrated to act as negative regulator of transcription by imposing a repressive chromatin status to its target genes. For exemple, PSF is able to recruit histone deacetylases (HDACs) to DNA-bound nuclear hormone receptors or circadian rhythm-controlling factors, often through the interaction with the HDAC-associated protein SIN3A

(Mathur M. et al. 2001; Dong X. et al. 2007; Duong H.A. et al. 2011). PSF can also directly interact with DNA to repress transcription of neighboring genes, as has been observed for IL-8. Interestingly, during viral infection NEAT1 induction relocates PSF from the IL8 promoter to the paraspeckles, leading to transcriptional activation of IL8 (Imamura K. et al. 2014).

3.2.2.3 PSF and p54nrb in DNA repair

Recent studies have highlighted the role of PSF and p54nrb in DNA damage response and repair. In particular PSF has been demonstrated to be mainly involved in homology-directed repair (HDR), while p54nrb has functional relevance for non homologous end joining (NHEJ) (Yarosh C.A. et al. 2015). Evidences *in vitro* demonstrated that PSF alone binds to ssDNA and dsDNA to promote D-loop formation between ssDNA and dsDNA and shows DNA pairing activity of complementary ssDNAs (Akhmedov A.T. and Lopez B.S. 2000). In addition, PSF binds directly to DSBs through its N-terminal region (RGG domain and prolin-rich domain) (Ha K. et al. 2011; Morozumi Y. et al. 2009; Rajesh C. et al. 2011). The same region is also involved in the interaction with RAD51D, a member of RAD51 family that plays an integral role in preserving genomic stability by homologous recombination-directed repair (Rajesh C. et al 2011). Notably, PSF activates strand invasion and stimulates the repair activity of RAD51 complex, thus promoting HR (Akhmedov A.T. and Lopez B.S. 2000; Morozumi Y. et al. 2009). Consistent with this, deficiency of PSF leads to sister chromatid cohesion defects, chromosome instability and increased sensitivity to DNA damaging agents (Rajesh C. et al 2011).

A role of p54nrb in NHEJ is supported by the finding that p54nrb co-immunoprecipitates with proteins involved in DSBs repair along the NHEJ pathway (Salton M. et al. 2010). The role of p54nrb in DNA damage response is supported by a NONO knockout mouse model (Li S. et al. 2014). Murine embryonic fibroblast (MEFs) derived from wild-type and knockout of NONO, the mouse homolog of p54nrb, show the same growth rates and cell cycle distribution in absence of genotoxic stress but show increased sensitivity to radiation. Remarkably, NONO knockout correlates with increased level of the DHBS protein family member PSPC1, that replaces the role of NONO in interacting with PSF. Cells depleted for both NONO and PSPC1 become markedly radiosensitive and show

delayed DNA DSB repair (Li S. et al. 2014). Along these lines of evidence, a very recent work demonstrates a role of p54nrb in triggering the intra-S-phase checkpoint in response to UV-induced DNA damage. In particular, depletion of p54nrb in HeLa cells reduces the chromatin loading of TOBP1 and prevents full activation of ATR upon UV-induced DNA damage. Despite DNA damage, p54nrb-depleted cells continue to synthesize DNA and fail to block new origin firing (Alfano L. et al. 2015).
In conclusion, p54nrb and PSF are the example of how splicing and gene regulation factors can act as gatekeepers of genome integrity (Naro C. et al. 2015).

3.2.3 p54nrb-TERRA interaction is mediated by PSF

Given the interaction between p54nrb and PSF, we tested whether p54nrb or PSF is responsible for TERRA interaction. To address this point we performed RNA pull-down assays using p54nrb- or PSF-depleted H1299 cells. Western blotting analysis of pull-down eluates with specific antibodies for PSF and p54nrb was performed (Figure 3.2.2). As expected, biotin-r[UUAGGG]$_6$ oligos are specifically bound by PSF and p54nrb in control cells. Importantly, PSF conserves its ability to bind biotinylated TERRA oligos also when p54nrb is depleted. Differently, p54nrb interaction with biotinylated TERRA oligo is impared in PSF-depleted H1299 cells. As expected, Lamin A/C was not detected in biotin-r[UUAGGG]$_6$ or biotin-r[EGFP] eluates. This result suggests that the interaction of p54nrb with the TERRA non-coding RNA is mediated by PSF. This data will be still validated by telomere ChIP.

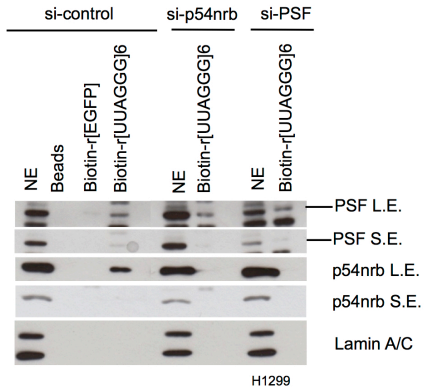

Figure 3.2.2. p54nrb-TERRA interaction is mediated by PSF. RNA pull down experiments were performed in H1299 cells transfected with the indicated siRNAs. Eluates obtained from RNA-pull down experiments using biotinylated r[UUAGGG]$_6$, biotinylated r[EGFP] RNA oligonucleotides or empty beads were subjected to western blotting with antibodies against p54nrb and PSF. Representative image of two independent experiments. A nuclear extract (NE) was loaded for each condition. Lamin A/C was used as a loading control. L.E., low exposure; S.E., short exposure.

TERRA transcripts have been demonstrated to directly interact with telomeric chromatin (Schoeftner S. and Blasco M.A. 2008; Azzalin C.M. et al. 2007). Our novel TERRA interacting proteins are integrated into various cellular processes linked to RNA metabolism and DNA integrity. To validate whether p54nrb and PSF are candidate telomere regulators, we wished to localize them at telomeres.

3.2.4 PSF and p54nrb localize to telomeres

PSF and p54nrb have been demonstrated to localize in the nucleoplasm and in paraspeckles (Fox A.H. and Lamond A.I. 2010). Using U2-OS osteosarcoma cells, PSF and p54nrb exhibit a nuclear punctuated pattern as shown by confocal microscopy (Figure 3.2.3A). Importantly, co-staining of p54nrb and PSF with the telomere binding proteins TRF2 or TRF1 revealed a telomeric localization of p54nrb and PSF. To obtain independent evidences for the enrichment of p54nrb and PSF at telomeres, we performed telomeric chromatin immunoprecipitation (ChIP) experiments using specific antibodies against p54nrb and PSF (Figure 3.2.3B). Mouse/rabbit immunoglobulins (IgG M, IgG R) and TRF2 antibody have been used as negative and positive control, respectively. DNA was purified from immunoprecipitated chromatin, transferred to a nitrocellulose membrane and subjected to Southern blotting using a labelled telomere probe. Importantly, p54nrb and PSF bind to telomeric chromatin, thus supporting data from confocal microscopy. As expected, TRF2 and the TERRA interactor FUS are enriched at telomeric repeats. To increase evidence of telomeric localization of p54nrb and PSF, we also performed anti-p54nrb co-immunoprecipitation experiment (Figure 3.2.3C). We found that p54nrb co-immunoprecipitates with PSF as well as with TRF2 telomere binding protein. Together these results provide evidence for the binding of p54nrb and PSF to telomeres.

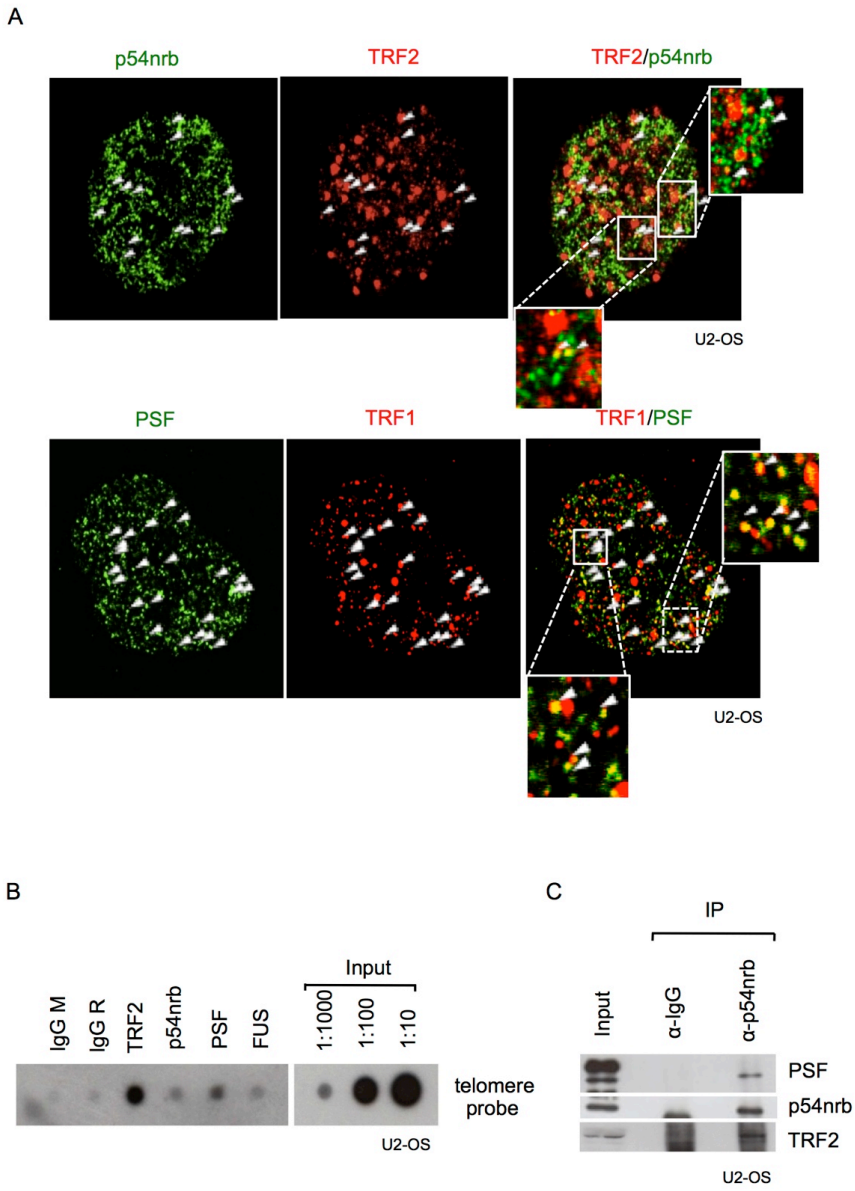

Figure 3.2.3. PSF and p54nrb localize to telomeres. A. p54nrb and PSF colocalize with TRF2 and TRF1, respectively, as show by representative images of confocal microscopy analysis. **B**. p54nrb and PSF interact with telomeric chromatin as determined by telomeric ChIP. Telomeric repeats binding of TRF2 and FUS was used as positive control. Control immunoglobulins mouse (IgG M) and rabbit (IgG R) were used. Serial dilutions of chromatin extract (input) prepared from U2-OS cells were loaded. Representative image of two independent experiments is shown. **C**. PSF/p54nrb complex interacts with TRF2 as shown by anti-p54nrb immunoprecipitation experiment. Control Immunoglobulins (IgG) were used.

3.2.5 PSF and p54nrb suppress TERRA accumulation at telomeres

Given the role of p54nrb and PSF RNA binding proteins as multifunctional regulators of RNA metabolism, we performed p54nrb and PSF loss of function experiments to address whether p54nrb and PSF impact on TERRA expression levels or TERRA abundance at telomeres. TERRA RNA-FISH experiments in U2-OS cells revealed that RNAi-mediated p54nrb and PSF depletion results in an increased number of focal TERRA signals per

nucleus (Figure 3.2.4A-C). Transfected cells were divided into five categories based on the number of TERRA foci (Figure 3.2.4B). At the chosen exposure time, the majority of control cells show 0-3 TERRA foci per nucleus. Conversely, most of p54nrb-depleted cells and PSF-depleted cells show a number of TERRA foci between 4 and 7 or 8 and 11, respectively (Figure 3.2.4B). Consistent with this, the fraction of cells with more than 3 TERRA foci per nucleus is significantly increased in cells depleted of p54nrb or PSF (Figure 3.2.4C). Remarkably, the observed accumulation of TERRA in nuclei of p54nrb- and PSF-depleted cells is not the result of increased total TERRA levels as demonstrated by northern blot and by quantitative real time PCR (qRT-PCR) using primers that amplify subtelomeric portions of TERRA transcripts arising from chromosomes 1, 21 or chromosomes 2, 10, 13 (Figure 3.2.4D-E). These results suggest that PSF and p54nrb have not impact on TERRA expression levels, but rather prevent TERRA accumulation at telomeres in U2-OS cells.

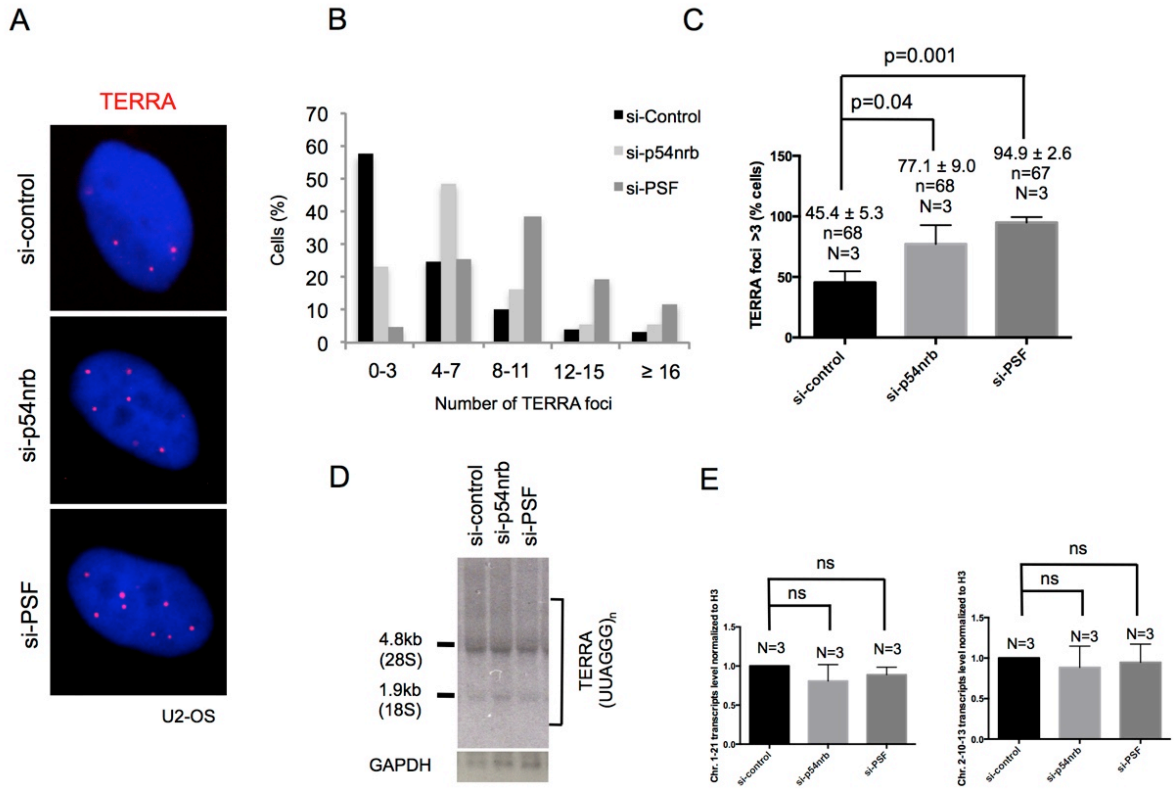

Figure 3.2.4. p54nrb and PSF regulate association of TERRA with telomeric chromatin. **A**. U2-OS cells were transfected with p54nrb or PSF specific siRNAs, and TERRA RNA-FISH experiments were performed to detect chromatin-associated TERRA. Representative images are shown. **B**. Classification of transfected cells according to the number of TERRA foci. **C**. Depletion of p54nrb or PSF significantly increases the percentage of cells with more than 3 TERRA foci per nucleus. **D**. Classical TERRA northern blotting of RNA extracts prepared from p54nrb or PSF siRNA transfected cells. Representative image of two independent experiments. p54nrb or PSF knock-down does not alter TERRA expression or TERRA size distribution. GAPDH probe was used as loading control. **E**. p54nrb or PSF knock-down does not alter TERRA transcription. Levels of TERRA transcripts arising from chromosomes 1, 21 or chromosomes 2, 10, 13 were quantified using qRT-pcr. TERRA expression levels were normalized against histone 3 (H3) levels. Means (bars) and SDs (error bars) are reported. N=number of independent experiments. n= number of analyzed nuclei. A student t-test was used to calculate statistical significance; p-values are shown.

3.2.6 Loss of PSF/p54nrb causes DNA damage at transcribed telomeres

Several studies have demonstrated that PSF and p54nrb are important to activate DNA damage response and to mediate DNA repair processes. In addition, alterations of TERRA abundance at telomeres has been linked to telomere dysfunction and DNA damage response at telomeres (de Silanes L.I. et al. 2014; Porro A. et al. 2014). To test whether TERRA accumulation induced by PSF and p54nrb depletion in U2-OS cells is linked to DNA damage response activation, we combined TERRA RNA-FISH with antibody staining for the DNA damage marker γH2AX (Figure 3.2.5A-B). Interestingly, we found that p54nrb- and PSF-depleted cells show an increased percentage of TERRA foci that co-localize with γH2AX compared to control cells (Figure 3.2.5B). Telomere damage was verified by anti-γH2AX immuno-telomere DNA FISH at metaphase chromosomes of H1299 cells depleted for p54nrb or PSF (Figure 3.2.5C-D). Together these experiments show that p54nrb and PSF suppress TERRA accumulation and prevent DNA damage response activation at telomeres. To check whether accumulation of dysfunctional telomeres in cells depleted for p54nrb and PSF fueled a global DNA damage response activation, we performed western blotting to analyze major markers of the DNA damage checkpoints (Figure 3.2.5E-F). Treatment with replication inhibitor hydroxyurea (HU) was used as positive control of DNA damage response activation. We found that depletion of p54nrb and PSF induces phosphorylation of the histone variant γH2AX and increases global p53 levels in U2-OS cells (Figure 3.2.5F). However, we didn't observe significant changes of γH2AX levels in H1299 cells (p53 null) (Figure 3.2.5 E). Interestingly, we found a slight induction of ATR in both H1299 and U2-OS cell lines depleted for PSF (Figure 3.2.5E-F). Remarkably, phosphorylated ATM appears to be not affected by p54nrb and PSF RNAi. In conclusion, western blot experiments show that depletion of p54nrb or PSF induces a modest global DNA damage response activation. This suggests that in normal conditions p54nrb and PSF prevent DNA damage activation in some specific genomic loci that include telomeres.

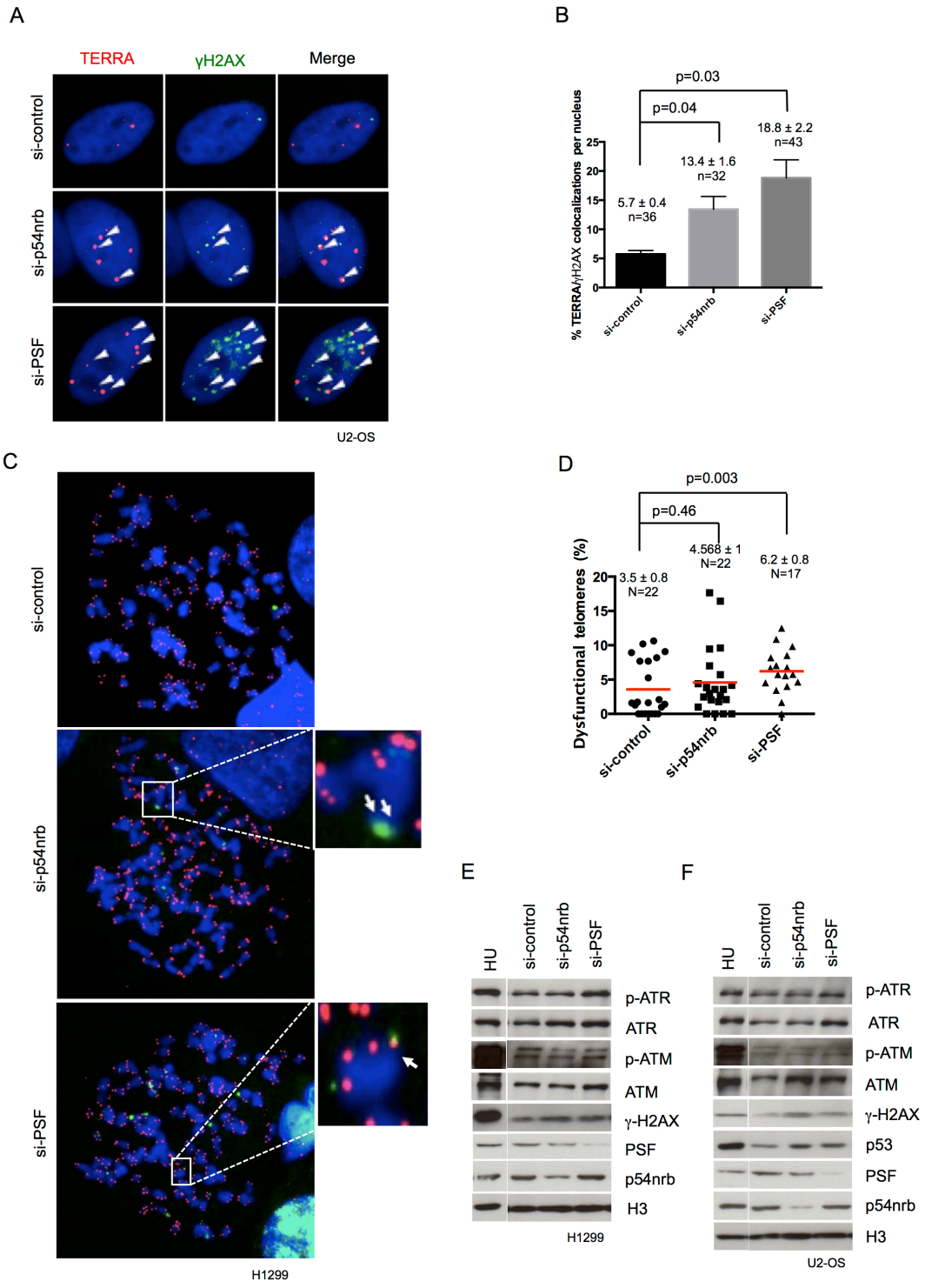

Figure 3.2.5. p54nrb and PSF prevent DNA damage activation at telomeres. **A**. U2-OS cells were transfected with p54nrb or PSF specific siRNAs and TERRA RNA-FISH combined with anti-γH2AX staining was performed. Representative images are shown. **B**. Depletion of p54nrb or PSF significantly increases the percentage of TERRA foci that colocalize with γH2AX per nucleus. n=number of analyzed nuclei. Means (bars) and SDs (error bars) are reported. A student t-test was used to calculate statistical significance; p-values are shown. **C.** H1299 cells were transfected with p54nrb or PSF specific siRNAs, blocked in metaphase using colcemide (1ug/ml, 2h) and then collected. Metaphase spreads were prepared by cytospin centrifugation. Staining with anti-γH2AX combined with telomeric DNA FISH was performed. Representative images are shown. **D**. Knock-down of p54nrb or PSF increased the percentage of dysfunctional telomeres. Each dot represents the percentage of dysfunctional telomeres (telomeres that co-localize with γH2AX) of one metaphase. Metaphases from three independent experiments were analyzed. At least 1000 chromosome ends were analyzed for each condition. Red bars indicate means. N= number of analyzed metaphases. p-values were computed using the Student's t-test. Nuclear extracts of H1299 (**E**) and U2-OS cells (**F**) depleted for p54nrb or PSF were analyzed by western blotting. Classical markers of DNA damage response activation were analyzed. Representative images are shown. Cells treated for 6 h with 5 mM hydroxyurea (HU) were used as controls for DNA damage response activation; histone 3 (H3) was used as loading control.

3.2.7 PSF and p54nrb prevent telomeric replicative stress

ATR responds to different types of DNA damage including DSBs and replication stress (Cimprich K.A. et al. 2008). In particular, ATR is activated by the presence of single-stranded DNA (ssDNA) coated by replication protein A (RPA), a situation that is often generated at stalled replication forks (Zhou B.B. and Elledge S.J. 2000; Jazayeri A. et al. 2006).

In order to explain the mechanism by which p54nrb and PSF depletion leads to dysfunctional telomeres, we hypothesized that aberrant accumulation of TERRA transcripts at telomeres induced by depletion of p54nrb or PSF might interfere with the progression of DNA replication machinery, thus inducing replication stress. To validate this hypothesis, we performed TERRA RNA-FISH combined with immunofluorescence for RPA32 phosphorylated at Serine 33 (RPA32pSer33), which can be used as a marker for replication stress (Figure 3.2.6A-B). Importantly, we found that the percentage of TERRA foci that co-localize with RPA32pSer33 strongly increases upon p54nrb and PSF silencing (Figure 3.2.6B). This suggests the existence of DNA replication stress at telomeres. To independently validate this result, we performed co-immunofluorescence experiments (co-IF) using TRF2 antibody combined with RPA32pSer33 (Figure 3.2.6C-D). As expected, HU treatment of U2-OS cells leads to a vast accumulation of RPA32pSer33 in foci dispersed across the entire nucleus (Figure 3.2.6C). In line with RNA-FISH data, we found that depletion of p54nrb and PSF correlates with increased RPA32pSer33 recruitment at telomere (Figure 3.2.6D). Together these results show that PSF and p54nrb prevent replication stress at telomeres.

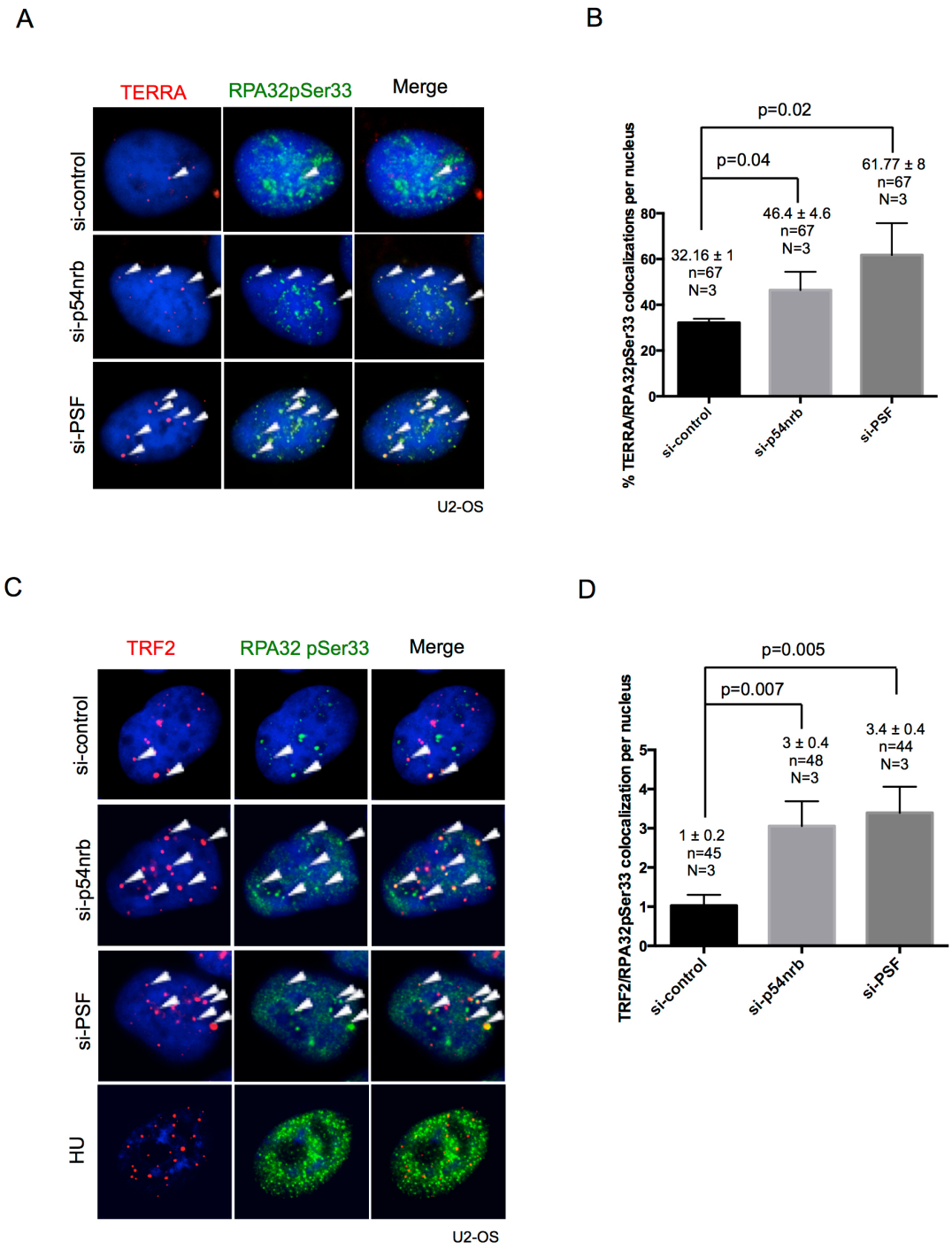

Figure 3.2.6. p54nrb and PSF prevents replicative stress at telomeres. A. U2-OS cells were transfected with p54nrb or PSF specific siRNAs and TERRA RNA-FISH combined with anti-RPA32pSer33 staining was performed. Representative images are shown. **B**. Depletion of p54nrb or PSF significantly increases the percentage of TERRA foci that colocalize with RPA32pSer33 per nucleus. **C**. Immunofluorescence with anti-TRF2 and anti-RPA32pSer33 antibodies was performed in U2-OS cells depleted for p54nrb or PSF. Representative images are shown. **D**. Depletion of p54nrb or PSF significantly increases the number of TRF2-RPA32pSer33 co-localizations per nucleus. Cells treated for 6 h with 5 mM hydroxyurea (HU) were used as controls for RPA32pSer33 activation. N=number of independent experiments; n=number of analyzed nuclei. Means (bars) and SDs (error bars) are reported. A student t-test was used to calculate statistical significance; p-values are shown.

3.2.8 PSF and p54nrb suppress formation of telomeric RNA:DNA hybrids

TERRA transcripts might interfere with proper DNA replication by prolonged base-pairing with their template DNA (the telomeric C-strand). Such telomeric RNA:DNA hybrids structures have been demonstrated in human cancer cells (Arora R. et al. 2014). In these structures, the non-template strand (G-strand) remains unpaired and exposed as ssDNA loop. TERRA base-pairing with its template (C-strand) is particularly favoured by the high content of G-C base pairs and by the propensity of G-rich telomeric strand to form secondary structures (G4-quadruplexes) (Figure 3.2.7C). To test whether p54nrb and PSF can mediate R-loops accumulation by RNA:DNA hybrids formation, we took advantage of an antibody that recognizes RNA:DNA hybrids sequence (S9.6) (Figure 3.2.7C). Anti-S9.6 immunofluorescence staining combined with TRF1 antibody allowed to detect increased numbers of telomeric RNA:DNA hybrids in U2-OS cells depleted for PSF compared to control cells (Figure 3.2.7A-B). This effect was reproduced by knockdown of RNaseH1 that eliminates stretches of RNA from RNA:DNA hybrids (Figure 3.2.7B). We also observed an increase of telomeric RNA:DNA hybrids in p54nrb-depleted cells. However this increase does not result statistically significant. Further experiments in conditions of p54nrb stable knockdown will address this point. Loss of telomere/hybrid co-localizations upon knockdown of TRF1 validates the specificity of co-localization events (Figure 3.2.7A).

To have further evidence of the role of PSF and p54nrb in suppressing RNA:DNA hybrid formation, we used over-expression of RNAseH1 to rescue RPA32pSer33 loading at telomeres in U2-OS cells depleted for both p54nrb and PSF (Figure 3.2.7D-E). Depletion of PSF/p54nrb increased the number of co-localizations between RPA32Ser33 and TRF2 shelterin component compared to control cells, indicative for R-loop formation (Figure 3.2.7E). Importantly, over-expression of mCherry-RH1 in U2-OS depleted for both PSF and p54nrb reduced the loading of RPA32pSer33 at telomeres (Figure 3.2.7E). This confirms that PSF and p54nrb suppress telomeric RNA:DNA hybrids formation that promote the generation of R-loops.

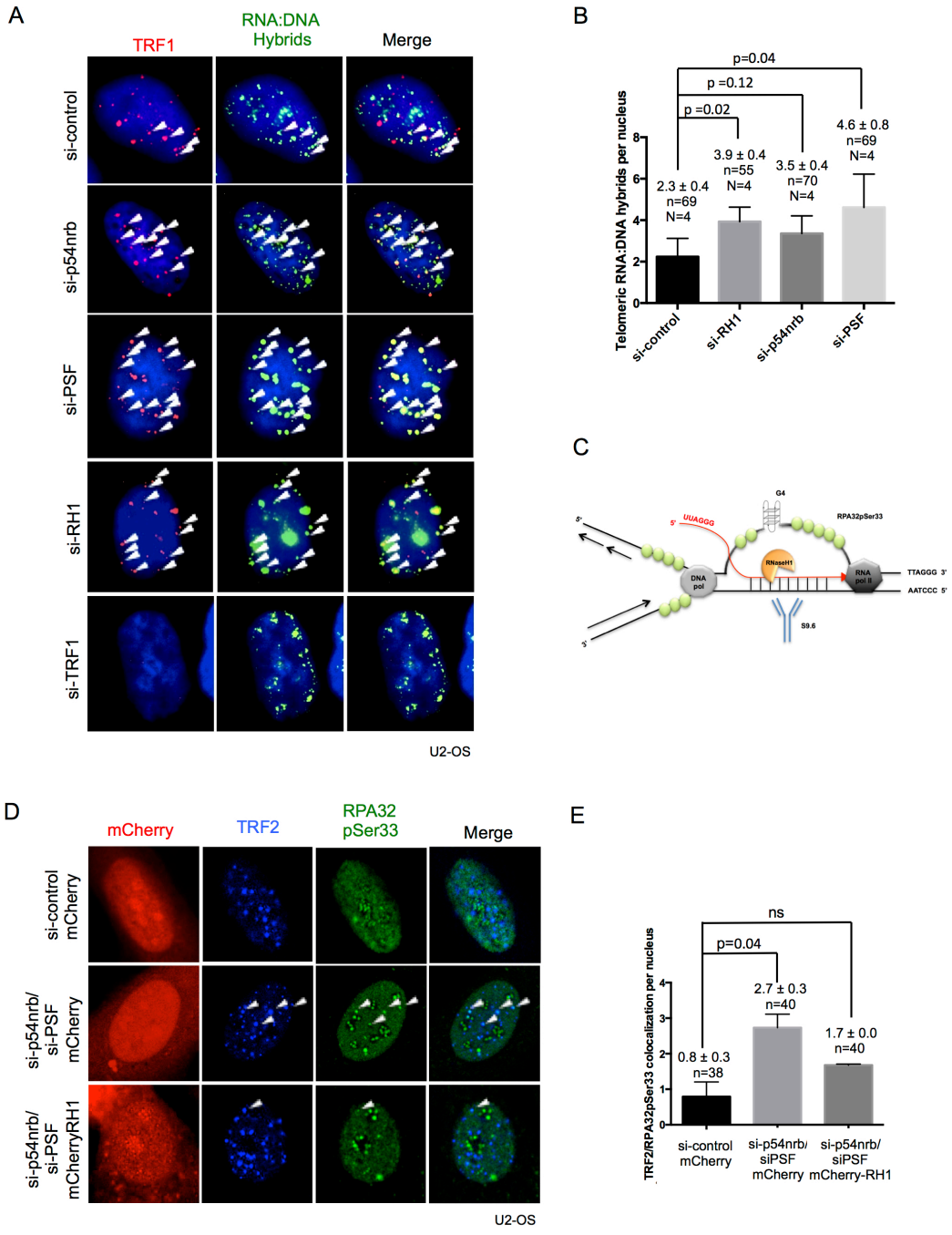

Figure 3.2.7. p54nrb and PSF suppress formation of telomeric RNA:DNA hybrids. A. U2-OS cells were transfected with p54nrb, PSF and RNase H1 specific siRNAs and immunofluoresce experiments with anti-TRF1 and anti-RNA:DNA hybrids (S9.6) antibodies were performed. TRF1 siRNA was used as control of TRF1 antibody specificity. Representative images are shown. **B**. Depletion of p54nrb or PSF increases the number of RNA:DNA hybrids that co-localize with TRF1. Similar effect is induced by knockdown of RNase H1 that eliminates stretches of RNA from RNA:DNA hybrids. N= number of independent experiments; n=number of analyzed nuclei. Means (bars) and SDs (error bars) are reported. A student t-test was used to calculate statistical significance; p-values are shown. **C**. Schematic model of the impact caused by loss of p54nrb and PSF at telomeres. TERRA transcript remains annealed with its template DNA (C-strand) forming an RNA:DNA hybrid structure. The non-template strand (G-strand) remains unpaired and exposed as ssDNA. These structures are named R-loops and are particularly favoured by G-rich telomeric strand formation of secondary structures (G4-quadruplexes). R-loops are demonstrated to be a barrier for DNA replication machinery progression, thus causing stalling of replication forks. This situation leads to the increase of free single stranded telomeric DNA bound by RPA32pSer33 produced at stalled replication fork, but also by the exposition of the G-strand telomere that remains unpaired. RNaseH1 digests the RNA part of the RNA:DNA hybrids, thus favouring the re-annealing of telomeric dsDNA. S9.6 antibody recognizes RNA:DNA hybrids structures. DNA pol, DNA polymerase; RNA pol II, RNA polymerase II. **D**. Ectopic expression of mCherry-RNase H1 in U2-OS cells depleted of both p54nrb and PSF decreases RPA32pSer33 loading at telomeres as shown by confocal microscopy analysis. Representative images are shown. **E**. mCherry-RNase H1 decreased the number of colocalization between TRF2 and RPA32pSer33; n=number of analyzed nuclei. Means (bars) and SDs (error bars) are reported. A student t-test was used to calculate statistical significance; p-values are shown.

3.2.9 PSF and p54nrb regulate telomere fragility in ALT cells

RNA:DNA hybrids and R-loop structures act as a great barrier to DNA replication fork progression and persistent replication stress can cause collapse of replication forks and consequent DSBs leading to chromosomal fragility (Gan W. et al. 2011; Aguilera A. and Garcia-Muse T. 2012). In addition, the stretch of exposed ssDNA of R-loops structures is unstable and more susceptible to transcription associated mutagenesis (TAM), recombination (TAR) and DSBs (Muers M. 2011; Wimberly H et al. 2013; Skourti-Stathaki K. et al. 2014).

Importantly, replication is particularly challenged at telomeres due to the heterochromatic structure, TERRA transcription and the propensity of G-rich sequences to form secondary structures (G-quadruplexes) (Blasco M.A. and Martinez P. 2015).

Consistent with this, proteins involved in preventing formation of RNA:DNA structures at telomeres could antagonize telomere fragility. In support of this, overexpression of RNase H1 reduced telomere fragility of ALT positive cells (Arora R. et al. 2014).

To address whether altered R-loops levels at telomeres induced by depletion of p54nrb or PSF correlates with telomere fragility, we performed Chromosome Orientation Fluorescent in Situ Hybridization (CO-FISH) analysis in p54nrb and PSF loss and gain of function experiments. CO-FISH technique uses two differencially labelled telomeric probes to specifically detect lagging strand telomere $(TTAGGG)_n$ or leading strand telomere $(CCCTAA)_n$ (Figure 3.2.8A-B). Fragile telomeres are visualized as multimeric telomere signals as shown in Figure 3.2.8C.

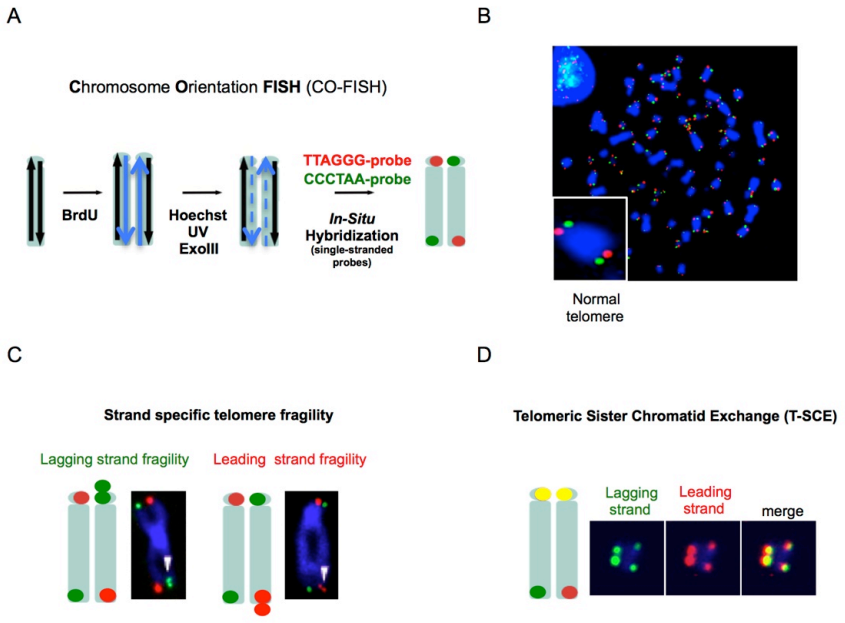

Figure 3.2.8. Chromosome-Orientation FISH (CO-FISH). **A**. Cells blocked in metaphase are collected after culture in BrdU (bromodeoxyuridine) for a single cell cycle. Fixed cells on microscope slides are stained with the DNA-binding fluorescent dye Hoechst 33258. Exposure to UV light nicks the substituted strand, and exonuclease III digests it. The process efficiently removes the newly synthesized DNA strand and leaves the two parental strands. The TTAGGG single-stranded probe hybridizes to complementary C-rich telomeric strand (leading strand telomere) on one chromatid of each chromosome arm producing a two-signal pattern. Reciprocally, the CCCTAA single-stranded probe hybridizes to G-rich telomeric strand (lagging strand telomere) (modified from Bailey S.M. et al. 2004). **B**. Representative image of CO-FISH on metaphase chromosomes and of normal telomere phenotype. **C**. CO-FISH detects strand specific telomere fragility. Fragile telomeres are visualized as multimeric telomere signals. **D**. CO-FISH detects events of T-SCE.

We found that depletion of p54nrb in U2-OS cells significantly increases lagging strand telomere fragility without affecting the leading strand (Figure 3.2.9A). In constrast, PSF knockdown strongly reduces basal fragility of the telomeric lagging strand telomere and does not impact on leading strand fragility (Figure 3.2.9C). In line with loss of function experiments, stable over-expression of p54nrb protects U2-OS cells from telomeric lagging strand fragility without any significant change in leading strand fragility (Figure 3.2.9E). Differently, stable over-expression of PSF in U2-OS cells does not have a significant impact on telomere fragility of neither the lagging or the leading strand (Figure 3.2.9G). Western blotting experiments confirmed p54nrb or PSF silencing/overexpression efficiency (Figure 3.2.9B, D, F, H).

Interestingly, only the G-rich lagging strand telomere that is also prone to form G-quadruplex secondary structures shows fragility in the absence of p54nrb. This is in line with the exposition of the G-rich strand in R-loop structures. Surprisingly, PSF acts in an opposite direction and appears to block a biological mechanism that resolves telomere fragility of lagging strand.

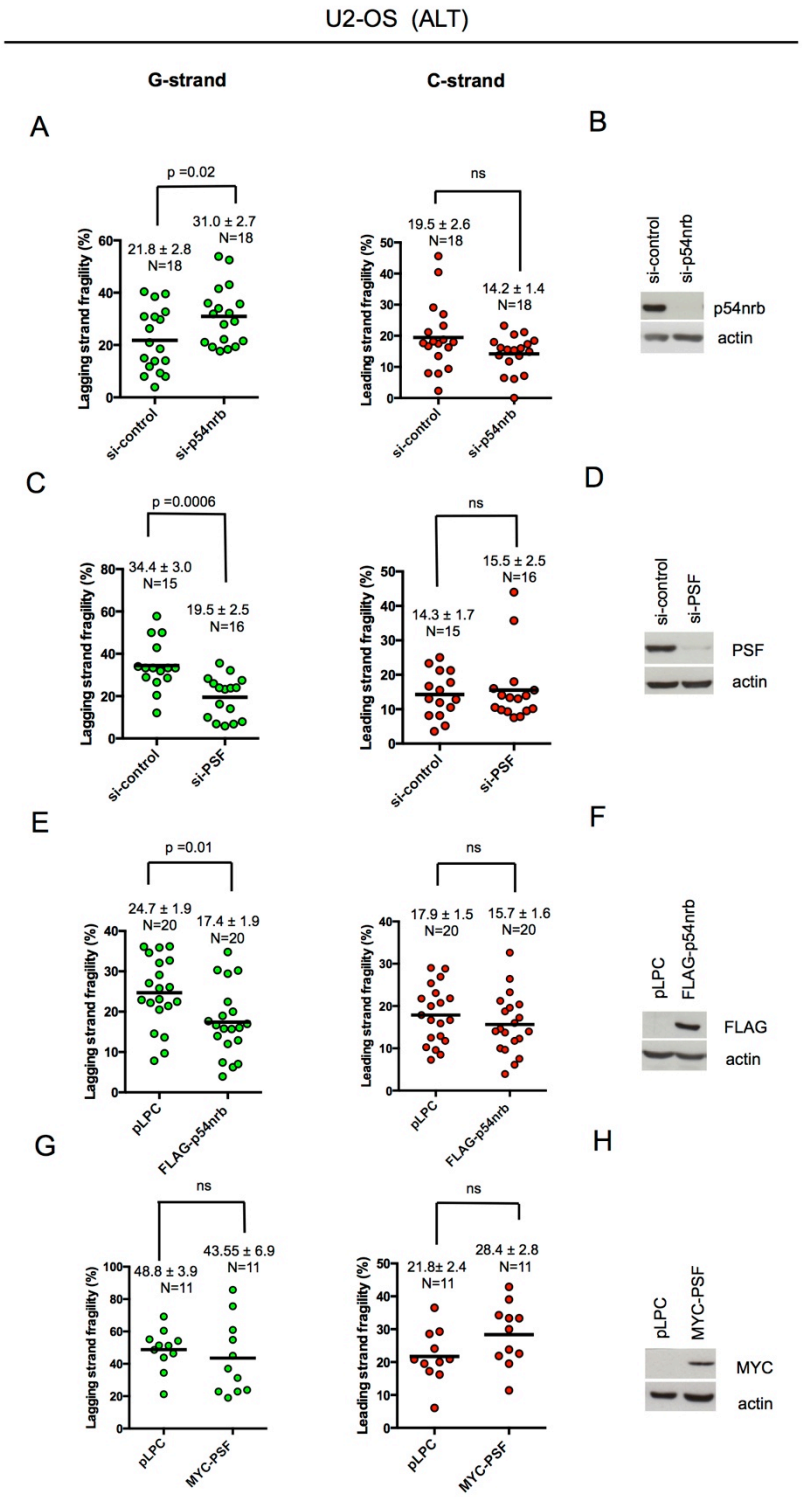

Figure 3.2.9. p54nrb and PSF regulate telomere fragility in U2-OS cells. A. Cells were transfected with p54nrb or control siRNAs and after 72 hours CO-FISH analysis was performed. Left panel shows frequency of lagging strand (G-strand) fragility; right panel shows frequency of leading strand (C-strand) fragility. **B**. Silencing efficiency is shown by western blotting. **C**. Cells were transfected with PSF or control siRNAs and after 72 hours CO-FISH analysis was performed. Left panel shows frequency of lagging strand (G-strand) fragility; right panel shows frequency of leading strand (C-strand) fragility. **D**. Silencing efficiency is shown by western blotting. **E**. CO-FISH analysis was performed in cells that stably overexpress FLAG-p54nrb or the empty vector, generated by retroviral transduction and cultured with antibiotic selection. Left panel shows frequency of lagging strand (G-strand) fragility; right panel shows frequency of leading strand (C-strand) fragility. **F**. FLAG-p54nrb overexpression is shown by western blot. **G**. CO-FISH analysis was performed in cells that stably overexpress MYC-PSF or the empty vector, generated by transfection and cultured with antibiotic selection. Left panel shows frequency of lagging strand (G-strand) fragility; right panel shows frequency of leading strand (C-strand) fragility. **F**. MYC-PSF overexpression is shown by western blot. Each dot represents the fraction of fragile telomeres per number of chromosomes in one metaphase. Metaphases from three independent experiments were analyzed. At least 1000 chromosome ends were analyzed for each condition. Bars indicate means. N= number of analyzed metaphases. P-values were computed using the Student's t-test.

3.2.10 PSF and p54nrb regulate telomere fragility in telomerase positive cells

To further validate the role of PSF and p54rnb in telomere homeostasis, we performed CO-FISH analysis in telomerase-positive H1299 cell line. We found that depletion of p54nrb increases telomere fragility from both telomeric strands (Figure 3.2.10A). In line with data from U2-OS cells we show that PSF depletion reduces fragility of lagging strand telomere without affecting leading strand (Figure 3.2.10C). In line with loss of function experiment, H1299 cells that stably overexpress p54nrb show decreased levels of global telomere fragility (Figure 3.2.10E). Again, stable PSF over-expression in H1299 has no impact on telomere fragility (Figure 3.2.10G). Western blotting experiments confirmed p54nrb or PSF silencing/overexpression efficiency (Figure 3.2.10B, D, F, H). We conclude that CO-FISH analysis of telomerase positive H1299 cells globally recapitulates data of ALT cells except for the p54nrb impact on the fragility of both lagging and leading strand telomere. Importantly, CO-FISH analysis in U2-OS and H1299 cells indicates a general relevance of p54nrb and PSF in controlling telomere structure and function in both ALT and telomerase positive cancer cells.

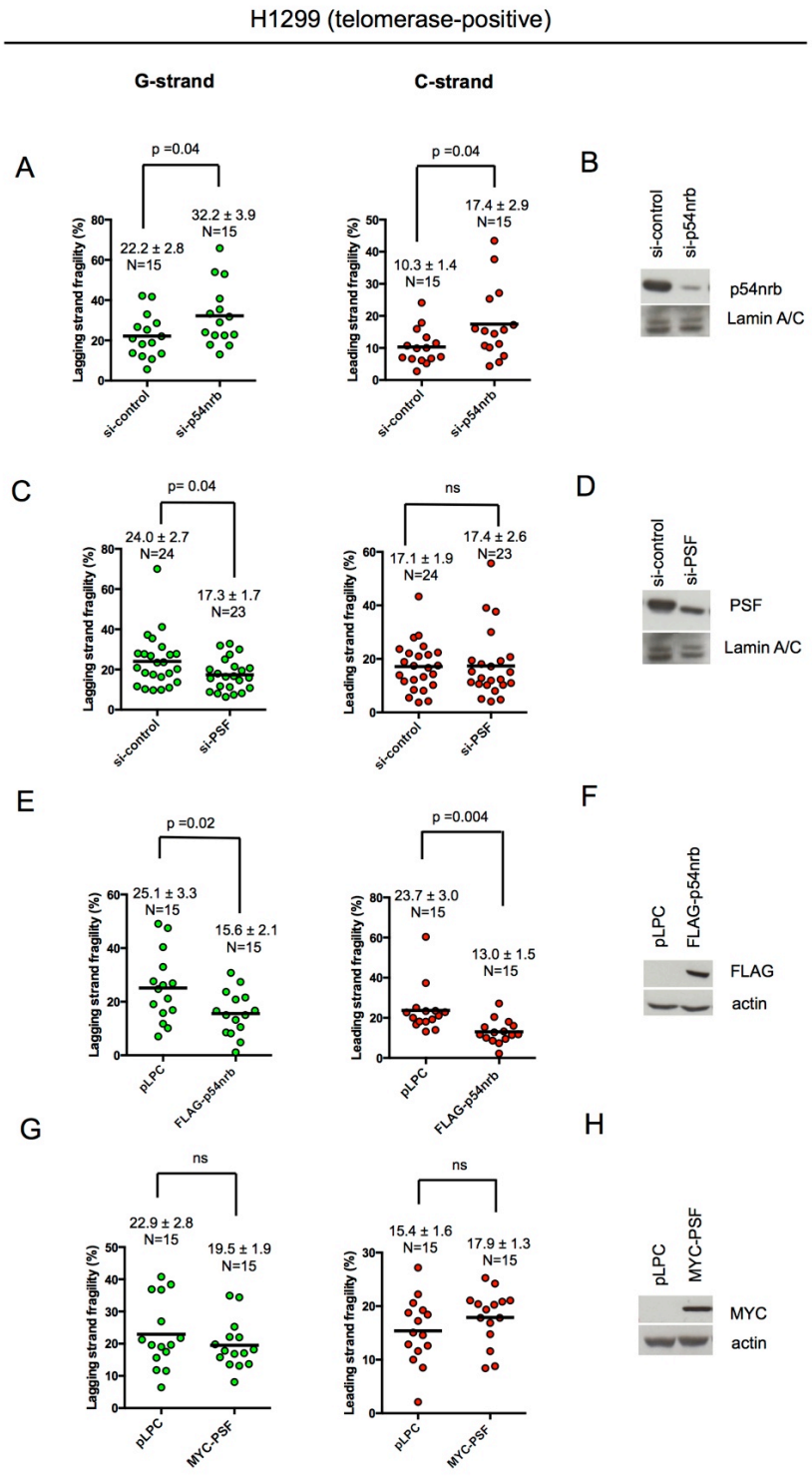

Figure 3.2.10. p54nrb and PSF regulate telomere telomere fragility in H1299 cells. A. Cells were transfected with p54nrb or control siRNAs and after 72 hours CO-FISH analysis was performed. Left panel shows frequency of lagging strand (G-strand) fragility; right panel shows frequency of leading strand (C-strand) fragility. **B**. Silencing efficiency is shown by western blotting. **C**. Cells were transfected with PSF or control siRNAs and after 72 hours CO-FISH analysis was performed. Left panel shows frequency of lagging strand (G-strand) fragility; right panel shows frequency of leading strand (C-strand) fragility. **D**. Silencing efficiency is shown by western blotting. **E**. CO-FISH analysis was performed in cells that stably overexpress FLAG-p54nrb or the empty vector, generated by retroviral transduction and cultured with antibiotic selection. Left panel shows frequency of lagging strand (G-strand) fragility; right panel shows frequency of leading strand (C-strand) fragility. **F**. FLAG-p54nrb overexpression is shown by western blot. **G**. CO-FISH analysis was performed in cells that stably overexpress MYC-PSF or the empty vector, generated by transfection and cultured with antibiotic selection. Left panel shows frequency of lagging strand (G-strand) fragility; right panel shows frequency of leading strand (C-strand) fragility. **F**. MYC-PSF overexpression is shown by western blot. Each dot represents the fraction of fragile telomeres per number of chromosomes in one metaphase. Metaphases from three independent experiments were analyzed. At least 1000 chromosome ends were analyzed for each condition. Bars indicate means. N= number of analyzed metaphases. p-values were computed using the Student's t-test.

3.2.11 PSF suppresses homologous recombination at telomeres

In addition to chromosome fragility, R-loops structures are prone to homologous recombination (HR) (Aguilera A. and Garcia-Muse T. 2012). In particular, telomeric hybrids have been demonstrated to sustain telomeric homologous recombination and synthesis of new telomeric DNA in ALT positive cells (Arora R. et al. 2014). Antagonizing with RNA:DNA hybrids formation by RNase H1 overexpression leads to diminished telomeric replication stress and reduced loading of phosphorylated RPA, impaired telomeric HR and consequent telomere shortening in ALT cells (Arora R. et al. 2014). To test whether telomeric R-loops accumulation induced by depletion of PSF and p54nrb stimulates homologous recombination at telomeres, we performed CO-FISH analysis in U2-OS and H1299 cells depleted for p54nrb or PSF. A merged signal (yellow) of the two telomeric probes used for CO-FISH indicates that a recombination event occurred between telomeric sister chromatids (Telomeric sister chromatid exchange or T-SCE) (Figure 3.2.8D). We found that depletion of p54nrb does not change T-SCE frequency in U2-OS and H1299 cells (Figure 3.2.11A,D). In contrast PSF depletion induces a ten-fold increase of T-SCE frequency in both U2-OS and H1299 cell lines (Figure 3.2.11B,E). Representative images of metaphase spreads of si-control and si-PSF conditions are shown in Figure 3.2.11C. These results demonstrate that PSF has a critical relevance in suppressing homologous recombination at telomeres.

In order to explain how loss of PSF reduces telomere fragility, we hypothesized that PSF depletion triggers T-SCE at fragile telomeres present at basal levels in normal conditions. To test this idea, we explored weather the combined depletion of PSF/p54nrb creates highly recombinogenic telomeres. We performed CO-FISH analysis using U2-OS cells depleted for p54nrb or p54nrb and PSF. As expected, increased overall fragility caused by p54nrb siRNA is rescued by PSF depletion (Figure 3.2.11F). Importantly, we found that combined p54nrb/PSF depletion induces a 60-fold increase of T-SCE frequency (Figure 3.2.11G). This suggests that loss of PSF unleashes homologous recombination at telomeres, thereby promoting the repair of fragile telomeres caused by si-p54nrb.

In conclusion, CO-FISH experiments demonstrate that p54nrb suppresses telomeric fragility and that PSF acts as a powerful suppressor of homologous recombination at telomeres.

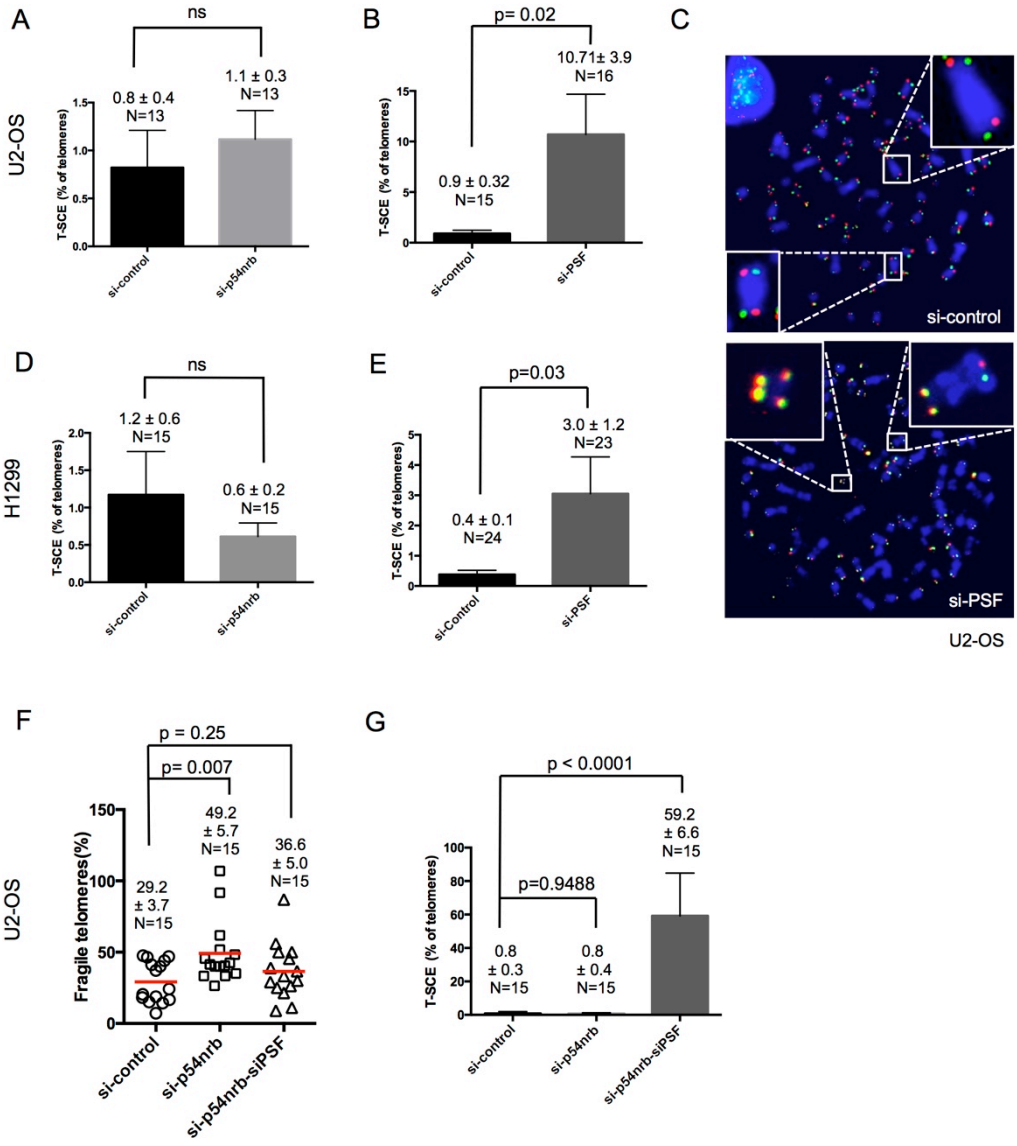

Figure 3.2.11 PSF/p54nrb complex suppresses homologous recombination at telomeres. CO-FISH analysis was performed in cells transfected with p54nrb or PSF siRNAs (A-E). **A**. Depletion of p54nrb does not significantly impact on T-SCE frequency in U2-OS cells. **B.** Knock-down of PSF induces a ten-fold increase of T-SCE frequency in U2-OS cells. **C**. Representative images of metaphase spreads; normal telomeres in si-control condition and recombinant telomeres in si-PSF cells are shown. **D**. Depletion of p54nrb does not significantly impact on T-SCE frequency in H1299 cells. **E**. Knock-down of PSF induces a ten-fold increase of T-SCE frequency in H1299 cells. CO-FISH analysis was performed in U2-OS cells depleted for p54nrb or p54nrb and PSF (F-G). **F**. Increased fragility caused by p54nrb siRNA is rescued by PSF depletion. Each dot represents the fraction of fragile telomeres per number of chromosomes in one metaphase. Metaphases from three independent experiments were analyzed. At least 1000 chromosome ends were analyzed for each condition. Red bars indicate means. **G**. Combined p54nrb/PSF depletion induces a 60-fold increase of T-SCE frequency. T-SCE frequency was measured as the percentage of T-SCE events per number of chromosome ends in one metaphase. Average of T-SCE frequency of metaphases from three independent experiments is represented. At least 1000 chromosome ends were analyzed for each condition. N= number of analyzed metaphases. SE (error bars) is reported. p-values were computed using the Student's t-test.

3.2.12 PSF suppresses telomeric recombination in ALT-associated promyelocytic leukaemia bodies

Increased levels of recombination at telomeres are reported to be one of the features of ALT cells (Londono-Vallejo J.A. et al. 2004). In these cells, homologous recombination is reported to take place the ALT-associated promyelocytic leukaemia bodies (APBs) (Cesare A.J. and Reddel R.R. 2010). To test whether depletion of PSF releasing homologous recombination at telomeres could increase the number of APBs in ALT cell, we performed co-staining with PML and TRF2 antibodies in U2-OS cells depleted of PSF or of both p54nrb and PSF (Figure 3.2.12A). In line with increased T-SCE frequency, loss of PSF or of PSF/p54nrb correlates with an increased number of co-localizations of TRF2 with PML (Number of APBs per nucleus) (Figure 3.2.12B). Together with CO-FISH results, this indicates that PSF impacts on two distinct features of ALT cells: T-SCE frequency and number of APBs. We further found that both, single depletion of PSF and combined PSF/p54nrb knockdown results in increased RAD51 loading at telomeres, indicative for increased abundance of recombinogenic DNA substrates (Figure 3.2.12C-D). In addition to homologous recombination factors, APBs also host DNA helicases (WRN and BLM) and topoisomerases (Topoisomerases IIα and IIIα) that contribute to formation/resolution of recombinational intermediates (Nabetani A. and Ishikawa F. 2010; Chung I. et al. 2012). As expected, depletion of PSF or both p54nrb and PSF induces a stronger recruitment of TopIIα into the APBs when compared to control cells (Figure 3.2.12E-F). Together these data suggest that PSF is important to suppress homologous recombination of telomeric DNA in ALT-associated promyelocytic leukaemia body (APBs).

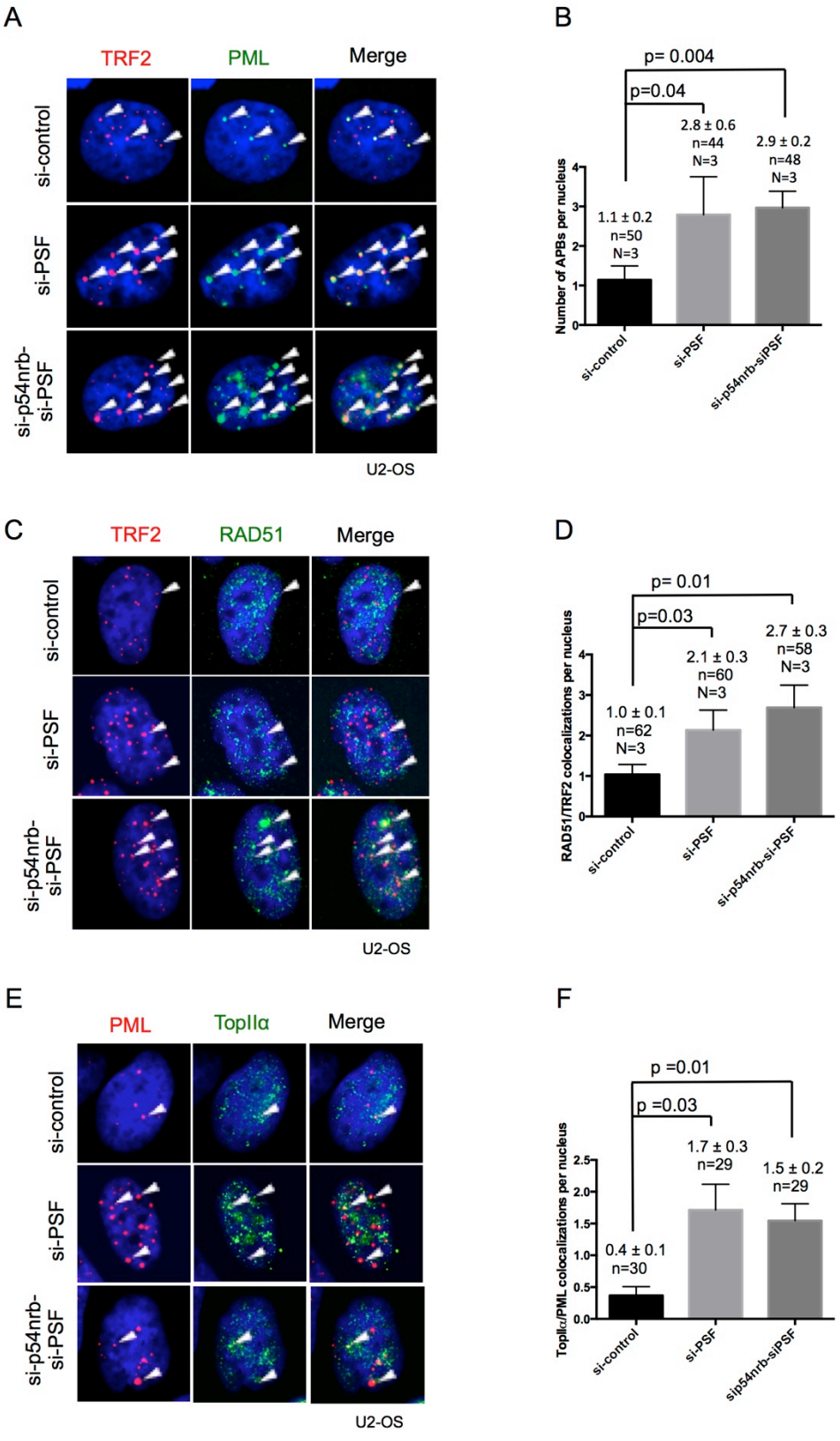

Figure 3.2.12. PSF/p54nrb complex suppresses recombination processes in ALT-associated promyelocytic leukaemia body (APBs). U2-OS cells were transfected with PSF or p54nrb and PSF specific siRNAs and immunofluorescence experiments were performed. **A**. Representative images of TRF2-PML co-staining. **B**. Knock-down of PSF or PSF and p54nrb significantly increases the number of co-localizations between TRF2 and PML (number of APBs per nucleus). N=number of independent experiments; n=number of analyzed nuclei. **C**. Representative images of TRF2-RAD51 co-staining**. D**. Knock-down of PSF or PSF and p54nrb significantly increases the loading of RAD51 at telomeres. N=number of independent experiments; n=number of analyzed nuclei. **E**. Representative images of PML-TopIIα co-staining. **F**. Depletion of PSF or PSF and p54nrb significantly increases the number of co-localizations between TopIIα and PML; n=number of analyzed nuclei. Means (bars) and SDs (error bars) are reported. A student t-test was used to calculate statistical significance; p-values are shown.

3.2.13 Loss of PSF and p54nrb impacts on telomere length of human cancer cells

Our data demonstrated that loss of p54nrb and PSF is associated with telomeric hybrids-induced replicative stress and consequent telomere fragility and recombination. To evaluate whether alteration of telomere stability induced by depletion of p54nrb and PSF has an impact on telomere length homeostasis, we performed telomere Q-FISH analysis to measure telomere length in U2-OS and H1299 cells depleted for p54nrb or PSF.

We found that depletion of p54nrb and PSF correlates with increased telomere length in ALT cells (U2-OS) (Figure 3.2.13A). Importantly, depletion of both p54nrb and PSF has an additive effect, resulting in a further increase of telomere length (Figure 3.2.13A). These results were reproduced when telomeric signals were divided into three categories based on telomeric fluorescence intensity. The category "A" indicates low telomere signals while "B" and "C" indicate medium and high signal, respectively. As expected we found increased number of high intensity telomere signals in si-p54nrb, si-PSF and si-p54nrb/si-PSF transfected cells compared to control cells (Figure 3.2.13A, right panel).

Q-FISH analysis in H1299 cells revealed that depletion of p54nrb results in a slight increase of telomere length and increased number of high intensity telomere signals (Figure 3.2.13B). In contrast PSF-depleted H1299 cells show a rapid and dramatic loss of telomeric repeats only three days post transfection that correlates with an increased proportion of short telomeres (Figure 3.2.12B, right panel). This suggests that increased T-SCE frequency induced by PSF depletion has a different outcome in ALT cells compared to telomerase-positive cells. In H1299 telomerase-positive cells that are not competent for recombination-dependent telomere elongation, increased T-SCE frequency induced by PSF-depletion leads to telomere repeats loss. In contrast telomerase negative ALT cells used increased abundance of recombinogenic sequences to elongate telomeres by homologous recombination.

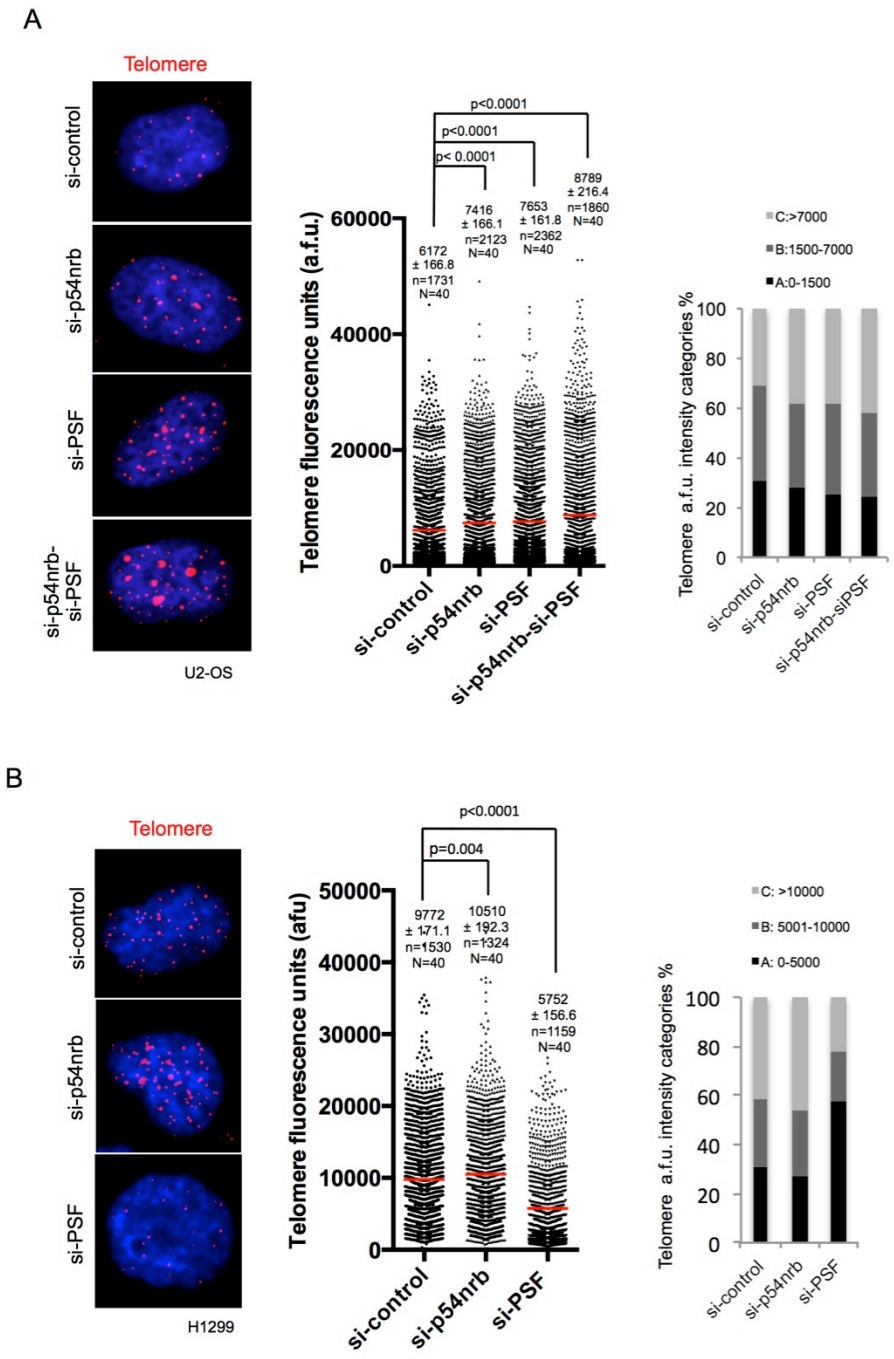

Figure 3.2.13. p54nrb and PSF regulate telomere length in human cancer cells. A. U2-OS cells were transfected with p54nrb, PSF or p54nrb and PSF siRNAs. After 72 hours, telomere length measurements were performed by quantitative telomere DNA FISH on interphase cells. Representative images are shown (left panel). Telomere fluorescence intensity analyzed for each telomere (central panel). Individual telomere signal intensities were categorized in three subgroups (right panel). **B**. H1299 cells were transfected with p54nrb or PSF siRNAs. After 72 hours, telomere length measurements were performed by quantitative telomere DNA FISH on interphase cells. Representative images are shown (left panel). Telomere fluorescence intensity analyzed for each telomere (central panel). Individual telomere signal intensities were categorized in three subgroups (right panel). p-values and SDs are indicated. N=number of independent experiments; n= total signals analyzed; 40 nuclei for each condition were analyzed. Arbitrary fluorescence units (a.f.u.).

3.2.14 Working model

Our work identified PSF and p54nrb as two novel TERRA interacting proteins and explored their role in telomere regulation. Given their interaction, we propose that p54nrb and PSF may work in the same complex at chromosome ends.

In particular, we propose that PSF/p54nrb complex interacting with telomeric chromatin and binding to TERRA transcripts, prevent accumulation of TERRA-telomere hybrids structures and consequent formation of unstable ssDNA or DNA breaks that can trigger recombination at telomeres (Figure 3.2.14A). In this way, PSF and p54nrb contribute to the maintenance of telomere stability.

Loss of PSF and p54nrb leads to the accumulation of TERRA-telomere hybrid structures and consequent displacement of the non-template strand (G-strand) that remains unpaired and exposed as ssDNA bound by RPA32pSer33 (Figure 3.2.14B). Formation of these structures (R-loops) is particularly favoured by formation of secondary structures (G4-quadruplexes) on G-rich telomeric strand. Telomeric R-loops induced by loss of p54nrb and PSF might be a source of fragility by two mechanisms. The exposed ssDNA of R-loop is unstable and prone to DNA lesions. In addition, R-loops form a barrier to DNA replication machinery progression, thus causing stalling of replication forks and consequent DNA breaks. In both cases, ssDNA lesions and DNA breaks might fuel recombination processes at telomeres mediated by RAD51. Uncontrolled telomere recombination leads to the loss of telomere length control and genomic instability that favour telomere elongation in ALT cells, but compromise telomere length in telomerase positive cancer cells (Figure 3.2.14B).

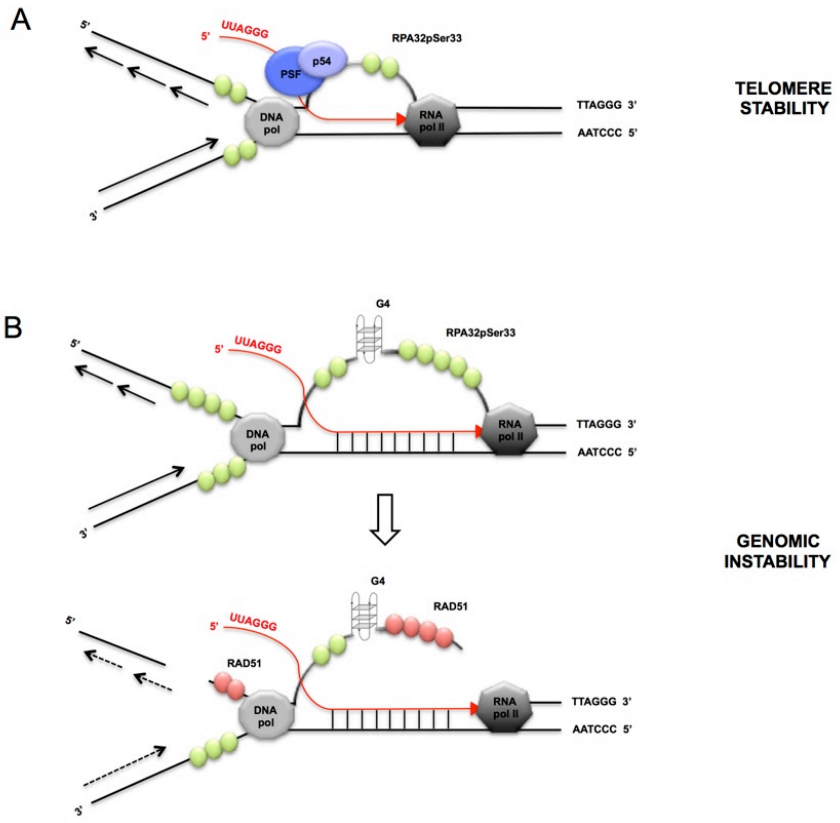

Figure 3.2.14 Working model. A. In normal conditions PSF and p54nrb interact with telomeric chromatin and bind to nascent TERRA transcript, thus allowing proper TERRA displacement from the template strand (C-strand telomere). In this way, PSF/p54nrb complex prevents stalling of DNA replication forks and consequent fragility as well as the formation of exposed ssDNA or DNA breaks that can trigger recombination processes at telomeres. **B**. Loss of PSF and p54nrb leads to formation of TERRA-RNA: telomeric-DNA hybrids structures and consequent displacement of the non-template strand (G-strand) that remains unpaired and exposed as ssDNA bound by RPA32pSer33. These structures named R-loops are particularly favoured by the propensity of G-rich telomeric strand to form secondary structures (G4-quadruplexes). The exposed ssDNA of R-loop is unstable and prone to DNA lesions. In addition, R-loops form a barrier to DNA replication machinery progression, thus causing stalling of replication forks and consequent DNA breaks. ssDNA lesions and DNA breaks might fuel recombination processes at telomeres mediated by RAD51. DNA pol, DNA polymerase; RNA pol II, RNA polymeraseII.

4. Discussion

Telomeres are specialized structures located at the physical ends of eukaryotic chromosomes that ensure genome integrity. Dynamic changes in telomere length and structure play key roles in replicative aging, genome stability and cancer. Critical telomere shortening or telomere dysfunction leads to the activation of DNA damage response at telomeres with subsequent activation of DNA damage repair driving increased genomic instability. In addition to classic telomere regulators such as the shelterin complex or telomerase, chromatin structure is critically involved in the regulation of telomere homeostasis.

Costitutive heterochromatin structure is a common feature of telomeric repeats from yeast to man and acts as negative regulator of telomere length and telomeric recombination (Blasco M.A. 2007). Although telomeres consist of constitutive heterochromatin, RNA polymerase II was found to transcribe telomeric repeats giving rise to a long non-coding RNA, called TERRA (telomeric repeat-containing RNA) (Azzalin C.M. et al. 2007; Schoeftner S. and Blasco M.A. 2008). TERRA has been demonstrated to integrate various pathways of telomere homeostasis including telomere length regulation, replication, recombination and the DNA damage response (Azzalin C.M. and Ligner J. 2014; Cusanelli E. and Chartrand P. 2015). Providing an assembly platform for a variety of proteins, TERRA may sustain additional pathways of telomere regulation.

My work aimed to give new insights into the epigenetic regulation of telomeres by exploring the role of the histone methyltransferase Suv39h1 on telomere homeostasis and carcinogenesis *in vivo* and by identifying novel TERRA interactors that impact on telomere function.

4.1 Project 1: altered telomere homeostasis and resistance to skin carcinogenesis in Suv39h1 transgenic mice

Suv39h1 and Suv39h2 are H3K9 specific histone methyltransferases (HTMases) that play a central role in the establishment of constitutive heterochromatin at pericentromeric and telomeric repeats (Rea S. et al. 2000; Lachner M. et al. 2001; Fodor B.D. et al. 2010). Importantly, Suv39h1 has been demonstrated to have an important role in gene silencing

and establishment of senescence in primary cells mediated by Retinoblastoma protein 1 (Rb1) (Nielsen S.J. et al. 2001). Interestingly, Suv39h1 also mediates oncogene-induced senescence in premalignant tumors (Narita M. et al. 2003; Braig M. et al. 2005; Reimann M. et al. 2010).

Lack of Suv39h1 and Suv39h2 in mice results in genomic instability and loss of telomeric heterochromatin leading to abnormal telomere elongation (Peters A.H. et al. 2001; García-Cao M. et al. 2004). In this study, we used a transgenic mouse model system to investigate the impact of Suv39h1 overexpression in telomere regulation, transformation and chemical carcinogenesis.

Deletion of the transcriptional stop cassette in Suv39h1ΔStop mice results in ectopic Suv39h1 expression. In line with this, primary MEFs derived from Suv39h1ΔStop embryos show increased global H3K9me3 levels as determined by western blotting. Consistent with pMEF data, we found that ectopic expression of Suv39h1 impacts on heterochromatin formation *in vivo*, as demonstrated by increased H3K9me3 levels in the nuclei of skin cells (tail sections) of Suv39h1ΔStop transgenic mice. Interestingly, elevated H3K9me3 levels are not paralleled by increased levels of nuclear HP1γ and HP1β, but by altered HP1β localization. This is in line with a previous study that showed that altered expression of Suv39h1 result in modulation of heterochromatic subdomains including the re-localization of HP1 proteins (Melcher M. et al. 2000; Czitkovich S. et al. 2001). Suv39h1 overexpression does not impact on HP1γ staining pattern.

We then investigated whether increased global H3K9me3 levels correlate with increased heterochromatin compaction specifically at telomeric and major satellite repeats. We observed increase in H3K9me3 at telomeric and pericentric regions without any effect on the abundance of HP1γ or H4K20me3. This is in line with the unaffected levels of global HP1γ. Our data suggest that the moderate increase of H3K9me3 in Suv39h1 transgenic mice is not sufficient to increase the recruitment of HP1 proteins to constitutive heterochromatin.

Several studies demonstrated that telomeric heterochromatin acts as potent regulator of telomere length in vertebrates (García-Cao M. et al. 2004; Benetti R. et al. 2007). In particular, in the absence of both HTMases Suv39h1 and Suv39h2 (Suv39h DN), lack of H3K9me3 at telomeres and subtelomeres drives recombination between telomeric sister chromatids and leads to strong telomere elongation (García-Cao M. et al. 2004; Benetti R. et al. 2007). Consistent with results from Suv39h DN pMEFs and mESCs, we found that

increased global and telomeric H3K9me3 levels drive telomere shortening in pMEFs derived from Suv39h1ΔStop embryos. This demonstrates that a modest increase of H3K9me3 abundance at telomeres is sufficient to impact on telomere length. Our results in line with previous studies confirmed that telomeric chromatin has a major role in the regulation of telomere length in vertebrates. This intimately connects telomere chromatin structure with human aging and cancer (Blasco M.A. 2007).

In addition to the role in the establishment of constitutive heterochromatin, Suv39h1 is recruited by Retinoblastoma protein 1 (Rb1) to impose repressive H3K9 methylation at the promoters of E2F target genes, thereby contributing to cellular senescence (Nielsen S.J. et al. 2001). The link between Suv39h1 and cellular senescence was further supported by the role of Suv39h1 in the establishment of foci enriched for H3K9me3 and HP1 in the periphery of senescent but not quiescent cells (Narita M. et al. 2003). Cellular senescence represents a crucial barrier to oncogene-mediated transformation in premalignant tumors (Serrano M. et al. 1997; Campisi J. et al. 2001). Recent studies identified H3K9me3-mediated senescence as a Suv39h1-dependent tumor suppressor mechanism in response to oncogenic stress induced by Ras (Braig M. et al. 2005). In particular, H3K9me3-mediated senescence has been demonstrated to be an efficient mechanism to abolish Ras-induced lymphomagenesis *in vivo* (Braig M. et al. 2005). In line with this, an independent work demonstrated that genetic inactivation of Suv39h1 accelerates Myc-driven lymphomagenesis, confirming the central role of Suv39h HMTases in oncogene-induced senescence (Reimann M. et al. 2010). Importantly, Suv39h1 overexpression has been reported to impair growth potential of cancer cells and to increase p53 expression (Melcher M. et al. 2000; Czitkovich S. et al. 2001). In our study, we found that ectopic Suv39h1 confers increased resistance to oncogenic stress conditions. Western blotting revealed that oncogene transduced Suv39h1ΔStop pMEFs show an activation of the p53 tumor suppressor pathway. In particular, we demonstrated that pMEFs obtained from Suv39h1ΔStop embryos show elevated p53 levels and upregulation of Puma and Bax transcriptional levels. PUMA is a critical mediator of p53-dependent apoptosis that acts on the Bcl-2 family members such as Bax by relieving apoptosis inhibition, thus increasing tumor suppression (Yu J. et al. 2008).

Increased tumor surveillance activity mediated by elevated basal p53 levels in Suv39h1ΔStop pMEFs provides an interesting model to explain the increased resistance of

Suv39h1ΔStop pMEFs to oncogenic transformation by E1A/H-*ras*. This is in line with previous studies that demonstrate that Ras-induced senescence is accompanied by accumulation of p53 and that loss of Suv39h1 or p53 impairs oncogene induced senescence, thus accelerating tumorigenesis (Serrano M. et al. 1997; Braig M. et al. 2005; Reimann M. et al. 2010).

After providing *in vitro* evidence of the tumor suppressive role of Suv39h1 in E1A/H-ras transduced Suv39h1ΔStop, we explore its role *in vivo*. Importantly, we found that Suv39h1ΔStop transgenic animals display a remarkable resistance to DMBA/TPA mediated skin carcinogenesis, a process that involves the acquisition of oncogenic H-*ras* mutations and consequent development of skin papillomas (Balmain A. et al. 1984). We propose that increased resistence to chemical carcinogenesis of Suv39h1ΔStop transgenic animals can be explained by increased tumor surveillance mediated by p53 pathway, as observed in Suv39h1ΔStop pMEFs. This is in line with the reported loss of oncogene induced senescence in the absence of p53 or Suv39h1 (Serrano M. et al. 1997; Braig M. et al. 2005; Reimann M. et al. 2010). In addition, this model is supported by the fact that a modest increase in p53 protein levels in Super-p53 mice is sufficient to mediate increased resistance to fibrosarcomas induced by exposure to 3MC (3-methyl-cholanthrene)(García-Cao I. et al. 2002).

In line with the role of telomeric heterochromatin in the regulation of telomere length, our transgenic mouse model demonstrates that Suv39h1 acts as a negative regulator of telomere length. Importantly, our study demonstrates that Suv39h1 modulates p53 tumorsuppressor activity and improves resistance to oncogene-induced transformation. Together this makes Suv39h1 an interesting target for future cancer therapeutic approaches.

4.2 Project 2: PSF/p54nrb complex safeguards telomere stability by preventing TERRA-telomere hybrids

Long non-coding RNAs (lncRNAs) have been demonstrated to play a central role in controlling genome function by diverse mechanisms. LncRNAs impact on chromatin structure through the recruitment of chromatin remodeling factors, regulating protein

activity and acting as a scaffold to target enzymatic activities to their sites of action (Morris K.V. et al. 2014). The telomeric repeat containing non-coding RNA (TERRA) performs all these activities at telomeres, thus regulating telomere homeostasis in a very dynamic manner.

In particular, associating with telomeric heterochromatin TERRA is able to target accessory factors to chromosome ends via RNA-protein interactions. In addition to shelterin factors (TRF1, TRF2) and telomeric heterochromatin components such as H3K9me3, Suv39h1, HP1α or HP1β, TERRA has been demonstrated to interact with the origin replication complex (ORC), the heterogeneous ribonucleoproteins (hnRNPs), the histone demethylase LSD1 and Fused in Sarcoma (FUS) (Deng Z. et al. 2009; Arnoult N. et al. 2012; Porro A. et al. 2014; de Silanes I.L. et al. 2010; Takahama K. et al. 2013; Sheibe M. et al. 2013). However, TERRA-interacting proteome might include multiple other factors. Identifying novel TERRA interactors is important to extend our insight into TERRA function and telomere regulation.

Using a TERRA RNA-affinity approach followed by mass spectrometry, we identified two novel TERRA interacting proteins: the polypyrimidine tract-binding protein-associated splicing factor (PSF) and the nuclear RNA-binding protein 54 kDa (p54nrb). PSF and p54nrb are members of the Drosophila Behavior Human Splicing (DBHS) family proteins and can form heterodimers (Shav-Tal Y. and Zipori D. 2002; Bond C.S. and Fox A.H. 2009; Passon D.M. et al. 2012). Initially identified as factors involved in splicing and transcription regulation, to date PSF and p54nrb have been demonstrated to act as a multifunctional regulator complex of RNA and DNA metabolism, including an important role in DNA damage response and repair (Patton J.G et al. 1991; Hallier M. et al. 1996; Basu A. et al. 1997; Salton M. et al. 2010; Rajesh C. et al. 2011; Li S. et al. 2014; Alfano L. et al. 2015; Yarosh C.A. et al. 2015).

In cultured human cells prolonged reduction of PSF expression leads to apoptosis (Heyd F. and Lynch K.W. 2010; Melton A.A. et al. 2007). Differently, murine embryonic fibroblast (MEFs) derived from NONO knockout mice show the same growth rates and cell cycle distribution compared to MEF derived from wild-type mice (Li S. et al. 2014). However, a very recent study showed that loss of p54nrb results in reduced cell proliferation (Alfano L. et al. 2015). p54nrb-silenced HeLa cells fail to trigger the intra-S-phase checkpoint in response to UV-induced DNA damage (Alfano L. et al. 2015). In particular, depletion of p54nrb in HeLa cells reduces the chromatin loading of TOBP1 and prevents full activation

of ATR. Despite DNA damage, p54nrb-depleted cells continue to synthesize DNA and fail to block new origin firing (Alfano L. et al. 2015). Importantly p54nrb silencing affects cell response to UV radiations also in a melanoma cell line. Very recently, a role of p54nrb in breast cancer has been demonstrated. p54nrb protein is highly expressed in breast cancer tissues as compared with the adjacent normal tissues in human patients. In addition, p54nrb is required for breast cancer cell grow *in vitro* and regulates SREBP-1A, thus impacting on lipid metabolism of breast cancer cells (Zhu Z. et al. 2015).

Mutation in PSF gene or gene fusion between PSF and other proteins have been linked with neurological diseases and cancer. PSF is included in a group of genes predicted to have differential alternative splicing (DAS) in Autism spectrum disorders (Stamova B.S. et al. 2013). In addition, PSF shows an altered nucleo-cytoplasmic distribution under neurodegenerative conditions. In particular, nuclear depletion and cytoplasmic accumulation of PSF is mediated by Tau in Alzheimer's and Pick's disease (Ke Y.D. et al. 2012). Importantly, commonly altered genomic regions in acute myeloid leukemia (AML) are enriched for somatic mutations in genes involved in chromatin remodeling and splicing that include PSF (Dolnik A. et al. 2012). Fusion of PSF with transcription factor E3 (TFE3) in papillary renal cell carcinoma inactivates TFE3 and p53 through cystoplasmic sequestration (Mathur M. et al. 2003). In addition, the translocation that causes the fusion between the proto-oncogene ABL1 and PSF is frequent in acute lymphoblastic leukemias (Duhoux F.P. et al. 2012).

Mutations in p54nrb have been recently linked to human disease. Loss of p54nrb function has been linked with human intellectual disability that correlates with macrocephaly, distinctive facial features, a thick corpus callosum and a small cerebellum. In line with this, NONO-deficient mice show flattened nose, a smaller cerebellum, cognitive and behavioral deficits. On the molecular level, NONO deficiency was shown to correlate with defects in the regulation of synaptic transcription regulation that ultimately result in structural defects of inhibitory synapse (Mircsof D. et al. 2015).

Together this underlines the functional relevance of PSF and p54nrb in regulating gene expression in human development and disease.

We found that the PSF/p54nrb complex associates with TERRA via PSF. In support of this, depletion of PSF abolishes TERRA-RNA affinity for p54nrb. TERRA is a nuclear RNA that

can localize in the nucleoplasm (polyA$^+$ TERRA) or associate with telomeres (polyA$^-$ TERRA) (Porro A. et al. 2010). To test whether our complex interacts with telomere-bound TERRA, we localized PSF and p54nrb at telomeres. Importantly, we found that PSF and p54nrb associate with telomeric heterochromatin as determined by ChIP and co-immunoprecipitate with the shelterin component TRF2. Telomeric localization of PSF and p54nrb offered the first evidence that they are candidate telomere regulators.

TERRA transcription is controlled by subtelomeric promoters. DNA methyl-transferases DNMT1 and DNMT3b, Suv39h HTMases and HP1α repress TERRA transcription (Nergadze S.G. et al. 2009; Arnoult N. et al. 2012). Conversely, the chromatin organizing factor CTCF and the cohesin Rad21 (radiation-sensitive 21) are reported to act as positive regulators of TERRA transcription in a particular subset of TERRA promoters (Deng Z. et al. 2012). However, TERRA is also regulated on the post-transcriptional level via regulation of TERRA-telomere hybrids and TERRA association with telomeres (Rippe K. and Luke B. 2015). Post-transcriptional regulation of TERRA at telomeres is mediated by members of the nonsense-mediated RNA decay (NMD) such as the RNA/DNA helicase and ATPase UPF1 and the RNA endonuclease SMG6 and by factors involved in R-loop metabolism such as the RNase H1 (Azzalin C.M. et al. 2007; Arora R. et al. 2014). Importantly, depletion of p54nrb and PSF induced a substantial increase in the number of TERRA foci per nucleus. Northern blotting and quantitative RT-PCR exclude that the observed accumulation of TERRA in the nuclei of p54nrb or PSF-depleted cells is the result of substantially increased steady state TERRA levels. Together this indicates a role of PSF and p54nrb in regulating TERRA at chromosome ends rather than TERRA metabolism.

Alterations of TERRA abundance at telomeres has been linked to telomere dysfunction and DNA damage response at telomeres (de Silanes L.I. et al. 2014; Porro A. et al. 2014). In addition, deficiency of p54nrb and PSF correlates with increased sensitivity to DNA-damaging agents and NONO-deficient MEFs show delayed DNA DSB repair (Rajesh C. et al. 2011; Li S. et al. 2014). Our results show that p54nrb and PSF are important to prevent DNA damage response activation at telomeres in U2-OS and H1299 human cancer lines. This underlines a general role of PSF and p54nrb in telomere protection of telomerase-negative ALT cells (U2-OS) and telomerase-positive (H1299) cancer cells. In particular, we found that depletion of p54nrb and PSF leads to an increase localization of DNA

damage marker γH2AX with nuclear TERRA foci and increased frequency of dysfunctional telomeres at metaphase chromosomes. Importantly, formation of γH2AX foci is a very early step in DNA damage activation and NONO-deficiency has been demonstrated to have not effect on this step (Li S. et al. 2014). Notably, telomere dysfunction induced by p54nrb or PSF depletion doesn't fuel a massive DNA damage response activation at a global level. We observed a modest ATR checkpoint activation in PSF-depleted H1299/U2-OS cells. The absence of ATR induction in p54nrb-depleted cells is in line with inefficient ATR DNA damage signalling in p54nrb-depleted HeLa cells (Alfano L. et al. 2015). Thus it is is likely that p54nrb or PSF depletion might impair subsequent steps in the DNA damage cascade thus preventing full activation of DNA damage checkpoints at a global level.
Summarizing, our results indicate that p54nrb and PSF prevent DNA damage activation at telomeres, thus indicating a role in stabilizing telomere function.

Telomere dysfunction has been reported to be the consequence of critical telomere shortening, loss of shelterin components or defective telomere replication (Palm W. and de Lange T. 2008; Martínez P. et al. 2009; Zimmermann M. et al. 2014). ATR activation in PSF knockdown cells suggests the formation of single-stranded DNA (ssDNA) ruptures at telomeres. ATR is activated by the presence of single-stranded DNA (ssDNA) coated by replication protein A (RPA) often generated at stalled replication forks that are susceptible to DNA breaks (Zhou B.B. and Elledge S.J. 2000; Jazayeri A. et al. 2006). We hypothesized that aberrant accumulation of TERRA transcripts at telomeres might impede progression of DNA replication fork resulting in ssDNA damage. This was confirmed by increased phosphorylated RPA32, marker of replicative stress at telomere in p54nrb- and PSF-depleted cells. Increased number of co-localizations of TERRA foci with phosphorylated RPA32 in U2-OS cells depleted for p54nrb and PSF suggest that replicative stress is associated with accumulation of TERRA at telomeres.

In addition to torsional stress generated in the DNA by concomitant replication and transcription, replicative stress is caused by the formation of R-loops (Helmirich A. et al. 2011). R-loops are structures triggered by RNA:DNA hybrid resulting in the displacement of the non-template strand. RNA:DNA hybrids are prone to be formed in genomic regions

with negative supercoiling and high G-content (Roy D. and Lieber M.R. 2009). In addition, the presence of nicks or G-quadruplexes in the displaced ssDNA favours R-loop formation (Duquette M.L. et al. 2004; Roy D. et al. 2010). The existence of telomeric R-loops have been demonstrated in both yeast and human cells (Balk B. et al. 2013; Pfeiffer V. et al. 2013; Arora R. et al. 2014). Importantly, we demonstrate that depletion of PSF and p54nrb increases accumulation of TERRA-telomere hybrids in U2-OS cells. Importantly, overexpression of RNAse H1 strongly reduces RPA32pSer33 loading at telomeres in U2-OS cells depleted for both p54nrb and PSF. This demonstrates that telomeric replicative stress induced by depletion of p54nrb and PSF is mediated by TERRA-telomere hybrids formation.

Mechanisms that control RNA:DNA hybrids formation regulate R-loops abundance. These include factors involved in RNA biogenesis and metabolism such as THO complex, the splicing factor SRSF1 and exoribonucleases exosome component 3 and 10 (EXOSC3 and EXOSC10) as well as DNA-RNA helicases such as senataxin (SETX) and topoisomerase 1 (TOP1) that resolve the negative supercoiling behind RNA pol II progression (Tuduri S. et al. 2009; Gomez-Gonzalez B. et al. 2011; Santos-Pereira J. M. and Aguilera A. 2015). In addition, resolution of R-loops is mediated by degradation activity of RNase H1 (Wahba L. et al. 2011). The mechanism by which p54nrb and PSF impinge on RNA:DNA hybrid management is currently under investigation.

Telomeric TTAGGG repeats are susceptible to DNA replication stress. In fact, DNA replication at telomeres is particularly challenged by the heterochromatic structure, TERRA transcription and G-quadruplexes formed by the G-rich telomere strand (Blasco M.A. and Martinez P. 2015). Importantly, telomeres have evolved complex mechanisms that involve shelterin and telomere-associated proteins to prevent telomeric fragility.

R-loops are a source of genomic instability and chromosome fragility by different mechanisms. The displaced single strand DNA of R-loops structures can act as a substrate to DNA-damaging agents, deaminases (activation-induced cytidine deaminase) and repair enzymes (base excision repair), leading to DNA lesions and nicks (Yu K. et al. 2003). In addition, R-loops can interfere with DNA replication by blocking the progression of replication forks, thus generating DNA lesions and DSBs (Gan W. et al. 2011; Aguilera A. and Garcia-Muse T. 2012; Skourti-Stathaki K. et al. 2014).

Importantly, telomeric RNA:DNA hybrids causing replicative stress at telomeres impacts

on telomere fragility as demonstrated by the fact that overexpression of RNase H1 was shown to reduce telomere fragility of ALT positive cells (Arora R. et al. 2014).
CO-FISH analysis in U2-OS and H1299 cells revealed that p54nrb and PSF have an opposite role in telomere fragility regulation. In fact, depletion of p54nrb significantly increases telomere fragility, while depletion of PSF induces telomere stabilization. Remarkably, our CO-FISH experiments in U2-OS cells highlight that the impact of PSF and p54nrb on telomere fragility is limited to the lagging strand telomere that represents the displaced unpaired DNA strand in telomeric R-loop structures. Recent works showed that factors involved in RNA:DNA hybrids resolution at telomeres such as the RNaseH1 or proteins that displace TERRA from telomeric chromatin such as UPF1, stabilize the telomeric leading strand (Arora R. et al. 2014; Chawla R. et al. 2011). In contrast, our data show that p54nrb overexpression or PSF depletion stabilizes the telomeric lagging strand. We consequently propose that p54nrb and PSF have a role in stabilizing the looped G-rich telomeric strand. This function could prevent the formation of G-quadruplex structures thereby limiting replication stress caused by R-loops. However, this function remains to be validated in future experiments.

DNA lesions formed on the ssDNA of the R-loop or DNA breaks generated by replication fork collisions with the transcription bubble could induce homologous recombination-directed repair mechanisms (Aguilera A. and Garcia-Muse T. 2012). In line with this, telomeric hybrids have been demonstrated to sustain telomeric homologous recombination and synthesis of new telomeric DNA in ALT positive cells (Arora R. et al. 2014).
Consistent with this, PSF depletion results a ten-fold increase of telomeric sister chromatid exchange (T-SCE) frequency in both U2-OS and H1299 cell lines, thus indicating that PSF acts as an important suppressor of homologous recombination at telomeres. Although p54nrb protects from fragility, depletion of p54nrb does not increase telomere recombination frequency. Importantly, combined depletion of p54nrb and PSF in U2-OS cells rescues telomere fragility observed in cells exclusively depleted of p54nrb. This effect is paralleled by a massive increase (60-fold) of T-SCE frequency. We hypothesize that depletion of PSF unleashes homologous recombination machinery at telomere and allows the repair of fragile telomeres, thus inducing telomere stabilization.
Taken together, our results demonstrated that together p54nrb and PSF suppress fragility

and aberrant recombination caused by DNA breaks generated at R-loops.

Increased levels of T-SCE is a classical feature of ALT cells (Londono-Vallejo J.A. et al. 2004). In these cells, telomeric DNA and associated binding proteins are found in a subset of promyelocytic leukaemia nuclear bodies (PML bodies) defined as ALT-associated PML bodies (APBs) (Yeager T.R. et al. 1999). Additional HR proteins such as RAD51, RAD52, RPA, NBS1, SLX4, BLM, MRN, BRCA1, BRIT1 are enriched in APBs and are required for telomere maintenance in ALT cells. Therefore, ALT activity is thought to take place in these nuclear domains (Cesare A.J. and Reddel R.R. 2010). Accordingly, in conditions in which ALT activity is inhibited, the number of APB-positive cells often decreases and is paralleled by decreased T-SCE frequency (Perrem K. et al. 2001; Jiang W.Q. et al. 2005; Fynn R.L. et al. 2015). In addition, the homologous recombination-associated MRN complex is required for APB formation (Wu G. et al. 2000; Jiang W.Q. et al. 2007).
Consistent with these reports, we demonstrated that increased T-SCE frequency in U2-OS induced by single depletion of PSF or combined depletion of p54nrb and PSF cells is paralleled by an increased number of nuclear APBs and increased RAD51 loading at telomeres. Together these data indicate that loss of the PSF/p54nrb complex impacts on distinct features of ALT cells: T-SCE frequency, number of APBs and recruitment of homologous recombination factors.
In addition to telomeric DNA and homologous recombination factors, APBs also host DNA helicases such as Werner and Bloom (WRN and BLM) and topoisomerases (Topoisomerases IIα and IIIα) that contribute to resolution of recombinational intermediates as well as DNA damage and repair factors (RPA, γH2AX, ATR) (Wang J.C. et al. 1990; Nabetani A. and Ishikawa F. 2010; Chung I. et al. 2012; Flynn R.L. et al. 2015).
The amount of Topoisomerase IIα and IIβ at telomeres is negatively regulated by TRF2 and Apollo to relive topological stress during telomere replication (Jing Y. et al. 2010). Consistent with this, Topoisomerase IIα depletion correlates with telomere fragility at both telomeric strands, thus suggesting that Topo IIα is important to resolve DNA replication intermediates at telomeres (d'Alcontres M.S. et al. 2014). Importantly, in human ALT positive cells, topoisomerase IIα and IIβ knockdown decreases APBs number, increases telomere dysfunction-induced foci (TIFs) and triggers telomere shortening (Meng-Hsun H. et al. 2015). This highlights that topoisomerase II is involved in the ALT pathway, contributing to maintenance of ALT cell proliferation.

Consistent with the involvement of Topoisomerase IIα in ALT pathway, our results demonstrate that knockdown of PSF or both PSF and p54nrb induces a stronger recruitment of TopIIα into the APBs. Thus we propose that accumulation of TERRA-telomere hybrids, increased replication stress and enhanced homologous recombination activity induced by depletion of PSF or both PSF and p54nrb may recruit increased levels of topoisomerases in order to resolve homologous recombination structures in APBs.

Telomeric hybrids have been demonstrated to allow telomere length maintenance in ALT positive cells by promoting telomeric homologous recombination (Arora R. et al. 2014; Yu T.Y. et al. 2014). In line with this, our Q-FISH results demonstrate that depletion of p54nrb or PSF increases telomere length in U2-OS cells. Increased telomere length induced by PSF depletion appears as a direct consequence of increased ALT activity. Differently, increased telomere length induced by depletion of p54nrb is not paralleled by increased T-SCE frequency. However, the additive effect on T-SCE frequency increase induced by combined depletion of p54nrb and PSF suggest that depletion of p54nrb impact on telomeric recombination. Telomere elongation in si-p54nrb condition might be mediated by intrastrand recombination mechanisms in which telomeric sequences could copy themselves looping out or looping back on themselves (Pickett H.A. and Reddel R.R. 2015). However, this remains to be demonstrated.
Taken together these data suggest that PSF/p54nrb complex is important to regulate ALT activity and telomere length, thus preventing telomere instability in telomerase–negative U2-OS cells.
Our telomere length analysis in H1299 cells demonstrates that p54nrb and PSF also have a role in telomere length regulation of telomerase-positive cells. In particular, si-p54nrb mediated slight telomere length changes can be considered not biologically relevant. Remarkably, telomere length analysis in H1299 cells depleted for PSF shows a rapid and dramatic loss of telomeric repeats three days post transfection. This suggests that aberrant telomeric recombination induced by PSF depletion has a dramatic outcome in non ALT-competent H1299 cells. We propose that telomeric R-loops initiate homologous recombination at telomeres in H1299, however recombination intermediates cannot be resolved, finally leading to telomere breakage.

In conclusion, our work identified a new TERRA interacting complex composed by

p54nrb and PSF that acts as novel regulator of telomere homeostasis. Importantly, we demonstrated that the PSF/p54nrb complex is essential to suppress TERRA-telomere hybrids formation thereby preventing telomere fragility (via p54nrb) and telomere recombination (via PSF). This represents a new molecular mechanism that is essential to safeguard telomere stability in human cancer cells.

Telomere maintenance and genomic instability represent two hallmarks of cancer. Importantly, our data demonstrate that the PSF/p54nrb complex strongly impacts on telomere length homeostasis, fragility and recombination, thus ensuring telomere stability. Genomic instability induced by replication stress is considered an early step in cancer formation (Gailard H. et al. 2015). High levels of p54nrb and PSF might protect cells from telomeric replication stress, fragility and uncontrolled recombination, thus promoting cancer cell proliferation, allowing tumor progression. In contrast, low levels of p54nrb and PSF may increase cell sentitivity to replication stress and DNA damaging agents. In this scenario, tumor cells with low p54nrb and PSF might be more susceptible to inhibitors of DNA synthesis, including PCNA (proliferating cell nuclear antigen) and BLM (Bloom helicase) inhibitors or G-quadruplexes stabilizer agents (Punchihewa C. et al. 2012; Nguyen G.H. et al. 2013; Zimmer J. et al. 2016).

Interestingly, our complex acquires a great importance in the context of ALT tumors where telomere length maintenance depends on the activation of telomere recombination. ALT telomeres require a balance of pro- and anti-recombinogenic signals. In fact, inhibition of recombination would lead to loss of telomere sequence and block of cell proliferation. Alternatively, shifting the equilibrium towards recombination could lead to further genomic instability due to the excessive accumulation of recombination intermediates and cell lethality. Importantly our work demonstrates that PSF/p54nrb complex influences recombination balance of ALT cells via the regulation of TERRA-telomere hybrids. New mechanistic insights into the regulation of ALT activity by p54nrb/PSF may highlight vulnerabilities of ALT cells in order to develop therapeutic strategies. Given that ALT activity is prevalent in cancers arising from mesenchymal tissues such as bone, soft tissues and neuroendocrine systems (Dilley R.L. et al. 2015), we suggest that PSF/p54nrb may have an important role in these defined tumor types.

References

Aguilera A, García-Muse T. R Loops: From Transcription Byproducts to Threats to Genome Stability. Mol. Cell. 2012; **46**: 115–124.

Ajuh P, Kuster B, Panov K, Zomerdijk J, Mann M, Lamond AI. Functional analysis of the human CDC5L complex and identification of its components by mass spectrometry. *EMBO J* 2000; **19**: 6569–6581.

Akhmedov a T, Lopez BS. Human 100-kDa homologous DNA-pairing protein is the splicing factor PSF and promotes DNA strand invasion. *Nucleic Acids Res* 2000; **28**: 3022–30.

Alfano L, Costa C, Caporaso A, Altieri A, Indovina P, Macaluso M *et al.* NONO regulates the intra-S-phase checkpoint in response to UV radiation. *Oncogene* 2015; : 1–10.

Amiard S, Doudeau M, Pinte S, Poulet A, Lenain C, Faivre-Moskalenko C *et al.* A topological mechanism for TRF2-enhanced strand invasion. *Nat Struct Mol Biol* 2007; **14**: 147–154.

Armanios M, Blackburn EH. The telomere syndromes. *Nat Rev Genet* 2012; **13**: 693–704.

Arnoult N, Van Beneden A, Decottignies A. Telomere length regulates TERRA levels through increased trimethylation of telomeric H3K9 and HP1α. *Nat Struct Mol Biol* 2012; **19**: 948–956.

Arora R, Lee Y, Wischnewski H, Brun CM, Schwarz T, Azzalin CM. RNaseH1 regulates TERRA-telomeric DNA hybrids and telomere maintenance in ALT tumour cells. *Nat Commun* 2014; **5**: 5220.

Artandi SE, DePinho RA. Telomeres and telomerase in cancer. Carcinogenesis. 2009; **31**: 9–18.

Azzalin CM, Lingner J. Telomere functions grounding on TERRA firma. Trends Cell Biol. 2015; **25**: 29–36.

Azzalin CM, Reichenbach P, Khoriauli L, Giulotto E, Lingner J. Telomeric repeat containing RNA and RNA surveillance factors at mammalian chromosome ends. *Science* 2007; **318**: 798–801.

Bailey SM, Goodwin EH, Cornforth MN. Strand-specific fluorescence in situ hybridization: The CO-FISH family. *Cytogenetic and Genome Research* 2004; **107**: 14–17.

Bailey SM, Brenneman MA, Goodwin EH. Frequent recombination in telomeric DNA may extend the proliferative life of telemerase-negative cells. *Nucleic Acids Res* 2004; **32**: 3743–3751.

Baird DM, Coleman J, Rosser ZH, Royle NJ. High levels of sequence polymorphism and linkage disequilibrium at the telomere of 12q: implications for telomere biology and human evolution. *Am J Hum Genet* 2000; **66**: 235–50.

Baird DM, Jeffreys a J, Royle NJ. Mechanisms underlying telomere repeat turnover, revealed by hypervariable variant repeat distribution patterns in the human Xp/Yp telomere. *EMBO J* 1995; **14**: 5433–5443.

Balk B, Maicher A, Dees M, Klermund J, Luke-Glaser S, Bender K *et al.* Telomeric RNA-DNA hybrids affect telomere-length dynamics and senescence. *Nat Struct Mol Biol* 2013; **20**: 1199–1205.

Ball HL, Myers JS, Cortez D. ATRIP binding to replication protein A-single-stranded DNA promotes ATR-ATRIP localization but is dispensable for Chk1 phosphorylation. *Mol Biol Cell* 2005; **16**: 2372–81.

Balmain A, Ramsden M, Bowden GT, Smith J. Activation of the mouse cellular Harvey-ras gene in chemically induced benign skin papillomas. *Nature* 1984; **307**: 658–660.

Barlow JH, Faryabi RB, Callen E, Wong N, Malhowski A, Chen HT *et al.* Identification of early replicating fragile sites that contribute to genome instability. *Cell* 2013; **152**: 620–632.

Bartek J, Lukas C, Lukas J. Checking on DNA damage in S phase. *Nat Rev Mol Cell Biol* 2004; **5**: 792–804.

Bartek J, Lukas J. DNA damage checkpoints: from initiation to recovery or adaptation. *Curr Opin Cell Biol* 2007; **19**: 238–245.

Basu a, Dong B, Krainer a R, Howe CC. The intracisternal A-particle proximal enhancer-binding protein activates transcription and is identical to the RNA- and DNA-binding protein p54nrb/NonO. *Mol Cell Biol* 1997; **17**: 677–686.

Baur JA, Zou Y, Shay JW, Wright WE. Telomere position effect in human cells. *Science* 2001; **292**: 2075–7.

Begus-Nahrmann Y, Hartmann D, Kraus J, Eshraghi P, Scheffold A, Grieb M *et al.* Transient telomere dysfunction induces chromosomal instability and promotes carcinogenesis. *J Clin Invest* 2012; **122**: 2283–2288.

Beier F, Martinez P, Blasco MA. Chronic replicative stress induced by CCl4 in TRF1 knockout mice recapitulates the origin of large liver cell changes. *J Hepatol* 2015; **63**: 446–455.

Benetti R, García-Cao M, Blasco MA. Telomere length regulates the epigenetic status of mammalian telomeres and subtelomeres. *Nat Genet* 2007; **39**: 243–50.

Benetti R, Gonzalo S, Jaco I, Schotta G, Klatt P, Jenuwein T *et al.* Suv4-20h deficiency results in telomere elongation and derepression of telomere recombination. *J Cell Biol* 2007; **178**: 925–936.

Bermejo R, Lai MS, Foiani M. Preventing Replication Stress to Maintain Genome Stability: Resolving Conflicts between Replication and Transcription. Mol. Cell. 2012; **45**: 710–718.

Blackburn EH, Gall JG. A tandemly repeated sequence at the termini of the extrachromosomal ribosomal RNA genes in Tetrahymena. *J Mol Biol* 1978; **120**: 33–53.

Blackburn EH, Greider CW, Szostak JW. Telomeres and telomerase: the path from maize, Tetrahymena and yeast to human cancer and aging. *Nat Med* 2006; **12**: 1133–1138.

Blanco R, Munoz P, Flores JM, Klatt P, Blasco MA. Telomerase abrogation dramatically accelerates TRF2-induced epithelial carcinogenesis. *Genes Dev* 2007; **21**: 206–220.

Blasco MA, Lee HW, Hande MP, Samper E, Lansdorp PM, DePinho RA *et al.* Telomere shortening and tumor formation by mouse cells lacking telomerase RNA. *Cell* 1997; **91**: 25–34.

Blasco MA. Telomeres and human disease: ageing, cancer and beyond. *Nat Rev Genet* 2005; **6**: 611–22.

Blasco MA. The epigenetic regulation of mammalian telomeres. *Nat Rev Genet* 2007; **8**: 299–309.

Blumrich A, Zapatka M, Brueckner LM, Zheglo D, Schwab M, Savelyeva L. The FRA2C common fragile site maps to the borders of MYCN amplicons in neuroblastoma and is associated with gross chromosomal rearrangements in different cancers. *Hum Mol Genet* 2011; **20**: 1488–1501.

Bond CS, Fox AH. Paraspeckles: Nuclear bodies built on long noncoding RNA. *J Cell Biol* 2009; **186**: 637–644.

Braig M, Lee S, Loddenkemper C, Rudolph C, Peters AH, Schlegelberger B *et al.* Oncogene-induced senescence as an initial barrier in lymphoma development. *Nature* 2005; **436**: 660–665.

Brosh RM, Majumdar A, Desai S, Hickson ID, Bohr VA, Seidman MM. Unwinding of a DNA Triple Helix by the Werner and Bloom Syndrome Helicases. *J Biol Chem* 2001; **276**: 3024–3030.

Brown EJ, Baltimore D. ATR disruption leads to chromosomal fragmentation and early embryonic lethality. *Genes Dev* 2000; **14**: 397–402.

Brown EJ, Baltimore D. Essential and dispensable roles of ATR in cell cycle arrest and genome maintenance. *Genes Dev* 2003; **17**: 615–628.

Bryan TM, Englezou A, Dalla-Pozza L, Dunham MA, Reddel RR. Evidence for an alternative mechanism for maintaining telomere length in human tumors and tumor-derived cell lines. *Nat Med* 1997; **3**: 1271–4.

Bryan TM, Englezou A, Gupta J, Bacchetti S, Reddel RR. Telomere elongation in immortal human cells without detectable telomerase activity. *EMBO J* 1995; **14**: 4240–8.

Bunting SF, Callen E, Wong N, Chen HT, Polato F, Gunn A *et al.* 53BP1 inhibits homologous recombination in brca1-deficient cells by blocking resection of DNA breaks. *Cell* 2010; **141**: 243–254.

Burrow A a, Williams LE, Pierce LCT, Wang Y-H. Over half of breakpoints in gene pairs involved in cancer-specific recurrent translocations are mapped to human chromosomal fragile sites. *BMC Genomics* 2009; **10**: 59.

Campisi, J. Cellular senescence as a tumor-suppressor mechanism. *Trends in Cell Biology* 2001; **11:** 27-31.

Carty MP, Zernik-Kobak M, McGrath S, Dixon K. UV light-induced DNA synthesis arrest in HeLa cells is associated with changes in phosphorylation of human single-stranded DNA-binding protein. *EMBO J* 1994; **13**: 2114–2123.

Caslini C, Connelly JA, Serna A, Broccoli D, Hess JL. MLL associates with telomeres and regulates telomeric repeat-containing RNA transcription. *Mol Cell Biol* 2009; **29**: 4519–4526.

Cayuela ML, Flores JM, Blasco MA. The telomerase RNA component Terc is required for the tumour-promoting effects of Tert overexpression. *EMBO Rep* 2005; **6**: 268–74.

Cea V, Cipolla L, Sabbioneda S. Replication of Structured DNA and its implication in epigenetic stability. Front. Genet. 2015; **6**. doi:10.3389/fgene.2015.00209.

Celli GB, de Lange T. DNA processing is not required for ATM-mediated telomere damage response after TRF2 deletion. *Nat Cell Biol* 2005; **7**: 712–8.

Celli GB, Denchi EL, de Lange T. Ku70 stimulates fusion of dysfunctional telomeres yet protects chromosome ends from homologous recombination. *Nat Cell Biol* 2006; **8**: 885–90.

Cesare AJ, Kaul Z, Cohen SB, Napier CE, Pickett HA, Neumann AA *et al.* Spontaneous occurrence of telomeric DNA damage response in the absence of chromosome fusions. *Nat Struct Mol Biol* 2009; **16**: 1244–1251.

Cesare AJ, Reddel RR. Alternative lengthening of telomeres: models, mechanisms and implications. *Nat Rev Genet* 2010; **11**: 319–330.

Chan SRWL, Blackburn EH. Telomeres and telomerase. *Philos Trans R Soc Lond B Biol Sci* 2004; **359**: 109–21.

Chang S, Khoo CM, Naylor ML, Maser RS, DePinho RA. Telomere-based crisis: Functional differences between telomerase activation and ALT in tumor progression. *Genes Dev* 2003; **17**: 88–100.

Chatziantoniou VD. Telomerase: biological function and potential role in cancer management. *Pathol Oncol Res* 2001; **7**: 161–170.

Chawla R *et al*. Human UPF1 interacts with TPP1 and telomerase and sustains telomere leading-strand replication. *EMBO J* 2011*;* **30**: 4047–4058.

Chen JJ-L, Blasco MA, Greider CW. Secondary structure of vertebrate telomerase RNA. *Cell* 2000; **100**: 503–14.

Chen JL, Greider CW. Determinants in mammalian telomerase RNA that mediate enzyme processivity and cross-species incompatibility. *EMBO J* 2003; **22**: 304–314.

Chen LL, Carmichael GG. Altered Nuclear Retention of mRNAs Containing Inverted Repeats in Human Embryonic Stem Cells: Functional Role of a Nuclear Noncoding RNA. *Mol Cell* 2009; **35**: 467–478.

Chiang YJ, Kim SH, Tessarollo L, Campisi J, Hodes RJ. Telomere-associated protein TIN2 is essential for early embryonic development through a telomerase-independent pathway. *Mol Cell Biol* 2004; **24**: 6631–6634.

Cho NW, Dilley RL, Lampson MA, Greenberg RA. Interchromosomal homology searches drive directional ALT telomere movement and synapsis. *Cell* 2014; **159**: 108–121.

Cho S, Moon H, Loh TJ, Oh HK, Williams DR, Liao DJ *et al*. PSF contacts exon 7 of SMN2 pre-mRNA to promote exon 7 inclusion. *Biochim Biophys Acta - Gene Regul Mech* 2014; **1839**: 517–525.

Chung I, Osterwald S, Deeg KI, Rippe K. PML body meets telomere: The beginning of an ALTernate ending? Nucleus 2012; **3**: 263-275.

Cimprich KA, Cortez D. ATR: an essential regulator of genome integrity. *Nat Rev Mol Cell Biol* 2008; **9**: 616–27.

Clynes D, Jelinska C, Xella B, Ayyub H, Scott C, Mitson M *et al*. Suppression of the alternative lengthening of telomere pathway by the chromatin remodelling factor ATRX. *Nat Commun* 2015; **6**: 7538.

Cohen SB, Graham ME, Lovrecz GO, Bache N, Robinson PJ, Reddel RR. Protein composition of catalytically active human telomerase from immortal cells. *Science* 2007; **315**: 1850–3.

Conomos D, Reddel RR, Pickett HA. NuRD–ZNF827 recruitment to telomeres creates a molecular scaffold for homologous recombination. *Nat Struct Mol Biol* 2014; **21**: 760–770.

Conomos D, Stutz MD, Hills M, Neumann AA, Bryan TM, Reddel RR *et al*. Variant repeats are interspersed throughout the telomeres and recruit nuclear receptors in ALT cells. *J Cell Biol* 2012; **199**: 893–906.

Cortez D, Guntuku S, Qin J, Elledge SJ. ATR and ATRIP: partners in checkpoint signaling. *Science* 2001; **294**: 1713–1716.

Costantino L, Koshland D. The Yin and Yang of R-loop biology. *Curr Opin Cell Biol* 2015; **34**: 39–45.

Crabbe L, Verdun RE, Haggblom CI, Karlseder J. Defective telomere lagging strand synthesis in cells lacking WRN helicase activity. *Science* 2004; **306**: 1951–1953.

Czvitkovich S, Sauer S, Peters a H, Deiner E, Wolf a, Laible G *et al*. Over-expression of the SUV39H1 histone methyltransferase induces altered proliferation and differentiation in transgenic mice. *Mech Dev* 2001; **107**: 141–153.

d'Adda di Fagagna F, Reaper PM, Clay-Farrace L, Fiegler H, Carr P, Von Zglinicki T *et al.* A DNA damage checkpoint response in telomere-initiated senescence. *Nature* 2003; **426**: 194–198.

d'Adda di Fagagna F. Living on a break: cellular senescence as a DNA-damage response. *Nat Rev Cancer* 2008; **8**: 512–522.

D'Alcontres MS, Palacios JA, Mejias D, Blasco MA. TopoIIα prevents telomere fragility and formation of ultra thin DNA bridges during mitosis through TRF1-dependent binding to telomeres. *Cell Cycle* 2014; **13**: 1463–1481.

Davies SL, North PS, Hickson ID. Role for BLM in replication-fork restart and suppression of origin firing after replicative stress. *Nat Struct Mol Biol* 2007; **14**: 677–679.

De Klein A, Muijtjens M, Van Os R, Verhoeven Y, Smit B, Carr AM *et al.* Targeted disruption of the cell-cycle checkpoint gene ATR leads to early embryonic lethality in mice. *Curr Biol* 2000; **10**: 479–482.

de Lange T. How telomeres solve the end-protection problem. *Science* 2009; **326**: 948–52.

Denchi EL, Celli G, de Lange T. Hepatocytes with extensive telomere deprotection and fusion remain viable and regenerate liver mass through endoreduplication. *Genes Dev* 2006; **20**: 2648–2653.

Denchi EL, de Lange T. Protection of telomeres through independent control of ATM and ATR by TRF2 and POT1. *Nature* 2007; **448**: 1068–71.

Deng Y, Guo X, Ferguson DO, Chang S. Multiple roles for MRE11 at uncapped telomeres. *Nature* 2009; **460**: 914–8.

Deng Z, Norseen J, Wiedmer A, Riethman H, Lieberman PM. TERRA RNA Binding to TRF2 Facilitates Heterochromatin Formation and ORC Recruitment at Telomeres. *Mol Cell* 2009; **35**: 403–413.

Deng Z, Wang Z, Stong N, Plasschaert R, Moczan A, Chen HS *et al.* A role for CTCF and cohesin in subtelomere chromatin organization, TERRA transcription, and telomere end protection. *EMBO J* 2012; **31**: 4165–4178.

Dilley RL, Greenberg RA. ALTernative Telomere Maintenance and Cancer. *Trends in Cancer* 2015; **1**: 145–156.

Dimitrova N, de Lange T. Cell cycle-dependent role of MRN at dysfunctional telomeres: ATM signaling-dependent induction of nonhomologous end joining (NHEJ) in G1 and resection-mediated inhibition of NHEJ in G2. *Mol Cell Biol* 2009; **29**: 5552–63.

Dimitrova N, de Lange T. MDC1 accelerates nonhomologous end-joining of dysfunctional telomeres. *Genes Dev* 2006; **20**: 3238–3243.

Ding Z, Wu CJ, Jaskelioff M, Ivanova E, Kost-Alimova M, Protopopov A *et al.* Telomerase reactivation following telomere dysfunction yields murine prostate tumors with bone metastases. *Cell* 2012; **148**: 896–907.

Diotti R, Loayza D. Shelterin complex and associated factors at human telomeres. *Nucleus* 2011; **2**: 119–135.

Doksani Y, de Lange T. The role of double-strand break repair pathways at functional and dysfunctional telomeres. *Cold Spring Harb Perspect Biol* 2014; **6**. doi:10.1101/cshperspect.a016576.

Doksani Y, Wu JY, Lange T De, Zhuang X. Super-Resolution Fluorescence Imaging of Telomeres Reveals TRF2- Dependent T-loop Formation. *Cell* 2013; **155**: 345–356.

Dolnik A, Engelmann JC, Scharfenberger-Schmeer M, Mauch J, Kelkenberg-Schade S, Haldemann B, Fries T, Kronke J, Kuhn MW, Paschka P, et al. Commonly altered genomic regions in acute myeloid leukemia are enriched for somatic mutations involved in chromatin remodeling and splicing. *Blood* 2012; **120**: 83–92.

Dong X, Sweet J, Challis JRG, Brown T, Lye SJ. Transcriptional activity of androgen receptor is modulated by two RNA splicing factors, PSF and p54nrb. *Mol Cell Biol* 2007; **27**: 4863–4875.

Dunham MA, Neumann AA, Fasching CL, Reddel RR. Telomere maintenance by recombination in human cells. *Nat Genet* 2000; **26**: 447–50.

Duhoux FP, Auger N, De Wilde S, Wittnebel S, Ameye G, Bahloula K, Van den Berg C, Libouton JM, Saussoy P, Grand FH, et al. The t(1;9)(p34;q34) fusing ABL1 with SFPQ, a pre-mRNA processing gene, is recurrent in acute lymphoblastic leukemias. *Leuk Res* 2012; **35**: 114–117.

Duong H a, Robles MS, Knutti D, Weitz CJ. A molecular mechanism for circadian clock negative feedback. *Science* 2011; **332**: 1436–1439.

Duquette ML, Handa P, Vincent JA, Taylor AF, Maizels N. Intracellular transcription of G-rich DNAs induces formation of G-loops, novel structures containing G4 DNA. *Genes Dev* 2004; **18**: 1618–1629.

Edwards DN, Orren DK, Machwe A. Strand exchange of telomeric DNA catalyzed by the Werner syndrome protein (WRN) is specifically stimulated by TRF2. *Nucleic Acids Res* 2014; **42**: 7748–7761.

Emili A, Shales M, McCracken S, Xie W, Tucker PW, Kobayashi R *et al.* Splicing and transcription-associated proteins PSF and p54nrb/nonO bind to the RNA polymerase II CTD. *RNA* 2002; **8**: 1102–11.

Episkopou H, Draskovic I, Van Beneden A, Tilman G, Mattiussi M, Gobin M *et al.* Alternative Lengthening of Telomeres is characterized by reduced compaction of telomeric chromatin. *Nucleic Acids Res* 2014; **42**: 4391–4405.

Farnung BO, Brun CM, Arora R, Lorenzi LE, Azzalin CM. Telomerase efficiently elongates highly transcribing telomeres in human cancer cells. *PLoS One* 2012; **7**. doi:10.1371/journal.pone.0035714.

Feng J, Funk W, Wang S, Weinrich S. The RNA component of human telomerase. *Science (80-)* 1995; **269**: 1236–1241.

Ferrón S, Mira H, Franco S, Cano-Jaimez M, Bellmunt E, Ramírez C *et al.* Telomere shortening and chromosomal instability abrogates proliferation of adult but not embryonic neural stem cells. *Development* 2004; **131**: 4059–4070.

Flores I, Cayuela ML, Blasco MA. Effects of telomerase and telomere length on epidermal stem cell behavior. *Science* 2005; **309**: 1253–1256.

Flynn RL, Centore RC, O'Sullivan RJ, Rai R, Tse A, Songyang Z *et al.* TERRA and hnRNPA1 orchestrate an RPA-to-POT1 switch on telomeric single-stranded DNA. *Nature* 2011; **471**: 532–536.

Flynn RL, Cox KE, Jeitany M, Wakimoto H, Bryll AR, Ganem NJ *et al.* Alternative lengthening of telomeres renders cancer cells hypersensitive to ATR inhibitors. *Science* 2015; **347**: 273–277.

Fodor BD, Shukeir N, Reuter G, Jenuwein T. Mammalian Su(var) genes in chromatin control. *Annu Rev Cell Dev Biol* 2010; **26**:471-501.

Fouche N, Cesare AJ, Willcox S, Ozzgur S, Compton SA, Griffith JD. The basic domain of TRF2 directs binding to DNA junctions irrespective of the presence of TTAGGG repeats. *J Biol Chem* 2006; **281**: 37486–37495.

Fox AH, Lam YW, Leung AKL, Lyon CE, Andersen J, Mann M *et al.* Paraspeckles: A novel nuclear domain. *Curr Biol* 2002; **12**: 13–25.

Fox AH, Lamond AI. Paraspeckles. Cold Spring Harb. Perspect. Biol. 2010; **2**. doi:10.1101/cshperspect.a000687.

Fraga MF, Ballestar E, Villar-Garea A, Boix-Chornet M, Espada J, Schotta G *et al.* Loss of acetylation at Lys16 and trimethylation at Lys20 of histone H4 is a common hallmark of human cancer. *Nat Genet* 2005; **37**: 391–400.

Fu X-D, Ares M. Context-dependent control of alternative splicing by RNA-binding proteins. *Nat Rev Genet* 2014; **15**: 689–701.

Gaillard H, García-Muse T, Aguilera A. Replication stress and cancer. *Nat Rev Cancer* 2015; **15**: 276–289.

Gall JG. Free ribosomal RNA genes in the macronucleus of Tetrahymena. *Proc Natl Acad Sci* 1974; **71**: 3078–3081.

Gan W, Guan Z, Liu J, Gui T, Shen K, Manley JL *et al.* R-loop-mediated genomic instability is caused by impairment of replication fork progression. *Genes Dev* 2011; **25**: 2041–2056.

García-Cao I, García-Cao M, Tomás-Loba A, Martín-Caballero J, Flores JM, Klatt P *et al.* Increased p53 activity does not accelerate telomere-driven ageing. *EMBO Rep* 2006; **7**: 546–552.

García-Cao M, Gonzalo S, Dean D, Blasco MA. A role for the Rb family of proteins in controlling telomere length. *Nat Genet* 2002; **32**: 415–9.

García-Cao M, O'Sullivan R, Peters AHFM, Jenuwein T, Blasco MA. Epigenetic regulation of telomere length in mammalian cells by the Suv39h1 and Suv39h2 histone methyltransferases. *Nat Genet* 2004; **36**: 94–99.

Gillis AJ, Schuller AP, Skordalakes E. Structure of the Tribolium castaneum telomerase catalytic subunit TERT. *Nature* 2008; **455**: 633–637.

Glousker G, Touzot F, Revy P, Tzfati Y, Savage S a. Unraveling the pathogenesis of Hoyeraal-Hreidarsson syndrome, a complex telomere biology disorder. *Br J Haematol* 2015; : n/a–n/a.

Gómez-González B, García-Rubio M, Bermejo R, Gaillard H, Shirahige K, Marín A *et al.* Genome-wide function of THO/TREX in active genes prevents R-loop-dependent replication obstacles. *EMBO J* 2011; **30**: 3106–3119.

González-Suárez E, Samper E, Flores JM. Telomerase-deficient mice with short telomeres are resistant to skin tumorigenesis. *Nat Genet* 2000; **26**: 114–7.

Gonzalez-Suarez E, Samper E, Ramirez A, Flores JM, Martin-Caballero J, Jorcano JL *et al.* Increased epidermal tumors and increased skin wound healing in transgenic mice overexpressing the catalytic subunit of telomerase, mTERT, in basal keratinocytes. *EMBO J* 2001; **20**: 2619–2630.

Gonzalo S, Blasco MA. Role of Rb family in the epigenetic definition of chromatin. *Cell Cycle* 2005; **4**: 752–755.

Gonzalo S, Jaco I, Fraga MF, Chen T, Li E, Esteller M *et al.* DNA methyltransferases control telomere length and telomere recombination in mammalian cells. *Nat Cell Biol* 2006; **8**: 416–24.

Gottschling DE, Aparicio OM, Billington BL, Zakian VA. Position effect at S. cerevisiae telomeres: Reversible repression of Pol II transcription. *Cell* 1990; **63**: 751–762.

Gozani O, Patton JG, Reed R. A novel set of spliceosome-associated proteins and the essential splicing factor PSF bind stably to pre-mRNA prior to catalytic step II of the splicing reaction. *EMBO J* 1994; **13**: 3356–3367.

Greider CW, Blackburn EH. Identification of a specific telomere terminal transferase activity in tetrahymena extracts. *Cell* 1985; **43**: 405–413.

Greider CW. Wnt Regulates TERT--Putting the Horse Before the Cart. Science (80-.). 2012; **336**: 1519–1520.

Griffith JD, Comeau L, Rosenfield S, Stansel RM, Bianchi A, Moss H *et al.* Mammalian telomeres end in a large duplex loop. *Cell* 1999; **97**: 503–514.

Ha K, Takeda Y, Dynan WS. Sequences in PSF/SFPQ mediate radioresistance and recruitment of PSF/SFPQ-containing complexes to DNA damage sites in human cells. *DNA Repair (Amst)* 2011; **10**: 252–259.

Hackett JA, Greider CW. Balancing instability: dual roles for telomerase and telomere dysfunction in tumorigenesis. *Oncogene* 2002; **21**: 619–26.

Hallier M, Tavitian A, Moreau-Gachelin F. The transcription factor Spi-1/PU.1 binds RNA and interferes with the RNA-binding protein p54nrb. *J Biol Chem* 1996; **271**: 11177–11181.

Hanada K, Budzowska M, Davies SL, van Drunen E, Onizawa H, Beverloo HB *et al.* The structure-specific endonuclease Mus81 contributes to replication restart by generating double-strand DNA breaks. *Nat Struct Mol Biol* 2007; **14**: 1096–1104.

Hayflick L. The limited in vitro lifetime of human diploid cell strains. *Exp Cell Res* 1965; **37**: 614–636.

He H, Multani AS, Cosme-Blanco W, Tahara H, Ma J, Pathak S *et al.* POT1b protects telomeres from end-to-end chromosomal fusions and aberrant homologous recombination. *EMBO J* 2006; **25**: 5180–5190.

Heaphy CM, de Wilde RF, Jiao Y, Klein AP, Edil BH, Shi C *et al.* Altered telomeres in tumors with ATRX and DAXX mutations. *Science* 2011; **333**: 425.

Hellman A, Zlotorynski E, Scherer SW, Cheung J, Vincent JB, Smith DI *et al.* A role for common fragile site induction in amplification of human oncogenes. *Cancer Cell* 2002; **1**: 89–97.

Helmrich A, Ballarino M, Tora L. Collisions between Replication and Transcription Complexes Cause Common Fragile Site Instability at the Longest Human Genes. *Mol Cell* 2011; **44**: 966–977.

Helmrich A, Ballarino M, Tora L. Collisions between Replication and Transcription Complexes Cause Common Fragile Site Instability at the Longest Human Genes. *Mol Cell* 2011; **44**: 966–977.

Hemann MT, Strong MA, Hao LY, Greider CW. The shortest telomere, not average telomere length, is critical for cell viability and chromosome stability. *Cell* 2001; **107**: 67–77.

Henson JD, Cao Y, Huschtscha LI, Chang AC, Au AYM, Pickett H a *et al.* DNA C-circles are specific and quantifiable markers of alternative-lengthening-of-telomeres activity. *Nat Biotechnol* 2009; **27**: 1181–1185.

Henson JD, Reddel RR. Assaying and investigating Alternative Lengthening of Telomeres activity in human cells and cancers. FEBS Lett. 2010; **584**: 3800–3811.

Herrera E, Samper E, Martin-Caballero J, Flores JM, Lee HW, Blasco MA. Disease states associated with telomerase deficiency appear earlier in mice with short telomeres. *EMBO J* 1999; **18**: 2950–2960.

Heyd F, Lynch KW. Phosphorylation-dependent regulation of PSF by GSK3 controls CD45 alternative splicing. *Mol Cell* 2010; **40**: 126–137.

Heyd F, Lynch KW. PSF controls expression of histone variants and cellular viability in thymocytes. *Biochem Biophys Res Commun* 2011; **414**: 743–749.

Hockemeyer D, Daniels JP, Takai H, de Lange T. Recent Expansion of the Telomeric Complex in Rodents: Two Distinct POT1 Proteins Protect Mouse Telomeres. *Cell* 2006; **126**: 63–77.

Hockemeyer D, Palm W, Else T, Daniels J-P, Takai KK, Ye JZ-S *et al.* Telomere protection by mammalian Pot1 requires interaction with Tpp1. *Nat Struct Mol Biol* 2007; **14**: 754–761.

Hodskinson MRG, Silhan J, Crossan GP, Garaycoechea JI, Mukherjee S, Johnson CM *et al.* Mouse SLX4 Is a Tumor Suppressor that Stimulates the Activity of the Nuclease XPF-ERCC1 in DNA Crosslink Repair. *Mol Cell* 2014; **54**: 472–484.

Hoffmeyer K, Raggioli A, Rudloff S, Anton R, Hierholzer A, Del Valle I *et al.* Wnt/β-catenin signaling regulates telomerase in stem cells and cancer cells. *Science* 2012; **336**: 1549–54.

Horn S, Figl A, Rachakonda PS, Fischer C, Sucker A, Gast A *et al.* TERT promoter mutations in familial and sporadic melanoma. *Science* 2013; **339**: 959–61.

Hsiao SJ, Smith S. Sister telomeres rendered dysfunctional by persistent cohesion are fused by NHEJ. *J Cell Biol* 2009; **184**: 515–526.

Hsieh MH *et al.* Topoisomerase II inhibition suppresses the proliferation of telomerase-negative cancers. *Cell Mol Life Sci* 2015; **72**: 1825-1837.

Hsu LC-L, Chen H-Y, Lin Y-W, Chu W-C, Lin M-J, Yan Y-T *et al.* DAZAP1, an hnRNP protein, is required for normal growth and spermatogenesis in mice. *RNA* 2008; **14**: 1814–22.

Hu J, Hwang SS, Liesa M, Gan B, Sahin E, Jaskelioff M *et al.* Antitelomerase therapy provokes ALT and mitochondrial adaptive mechanisms in cancer. *Cell* 2012; **148**: 651–663.

Huang FW, Hodis E, Xu MJ, Kryukov G V, Chin L, Garraway L a. Highly recurrent TERT promoter mutations in human melanoma. *Science* 2013; **339**: 957–9.

Jacobs SA, Podell ER, Cech TR. Crystal structure of the essential N-terminal domain of telomerase reverse transcriptase. *Nat Struct Mol Biol* 2006; **13**: 218–25.

Jazayeri A, Falck J, Lukas C, Bartek J, Smith G, Lukas J *et al.* ATM- and cell cycle-dependent regulation of ATR in response to DNA double-strand breaks. *Nat Cell Biol* 2006; **8**: 37–45.

Jiang WQ *et al.* Suppression of alternative lengthening of telomeres by Sp100-mediated sequestration of MRE11/RAD50/NBS1 complex. *Mol Cell Biol* 2005; **25**: 2708–2721.

Jiang WQ, Zhong ZH, Henson JD, Reddel RR. Identification of candidate alternative lengthening of telomeres genes by methionine restriction and RNA interference. *Oncogene* 2007; **26**: 4635–4647.

Johnson JE, Cao K, Ryvkin P, Wang LS, Johnson FB. Altered gene expression in the Werner and Bloom syndromes is associated with sequences having G-quadruplex forming potential. *Nucleic Acids Res* 2009; **38**: 1114–1122.

Jones B, Su H, Bhat A, Lei H, Bajko J, Hevi S *et al.* The histone H3K79 methyltransferase Dot1L is essential for mammalian development and heterochromatin structure. *PLoS Genet* 2008; **4**. doi:10.1371/journal.pgen.1000190.

Jurica MS, Moore MJ. Pre-mRNA splicing: Awash in a sea of proteins. Mol. Cell. 2003; **12**: 5–14.

Kaneko S, Rozenblatt-Rosen O, Meyerson M, Manley JL. The multifunctional protein p54nrb/PSF recruits the exonuclease XRN2 to facilitate pre-mRNA 3′ processing and transcription termination. *Genes Dev* 2007; **21**: 1779–1789.

Karlseder J, Broccoli D, Dai Y, Hardy S, de Lange T. p53- and ATM-dependent apoptosis induced by telomeres lacking TRF2. *Science* 1999; **283**: 1321–1325.

Karlseder J, Kachatrian L, Takai H, Mercer K, Hingorani S, Jacks T *et al.* Targeted deletion reveals an essential function for the telomere length regulator Trf1. *Mol Cell Biol* 2003; **23**: 6533–41.

Kastan MB, Bartek J. Cell-cycle checkpoints and cancer. *Nature* 2004; **432**: 316–323.

Ke YD, Dramiga J, Schutz U, Kril JJ, Ittner LM, Schroder H, Gotz J. Tau-mediated nuclear depletion and cytoplasmic accumulation of SFPQ in Alzheimer's and Pick's disease. *PLoS One* 2012; **7**: e35678.

Kibe T, Osawa GA, Keegan CE, de Lange T. Telomere protection by TPP1 is mediated by POT1a and POT1b. *Mol Cell Biol* 2010; **30**: 1059–1066.

Kim KK, Kim YC, Adelstein RS, Kawamoto S. Fox-3 and PSF interact to activate neural cell-specific alternative splicing. *Nucleic Acids Res* 2011; **39**: 3064–3078.

Kim NW, Piatyszek MA, Prowse KR, Harley CB, West MD, Ho PL *et al.* Specific association of human telomerase activity with immortal cells and cancer. *Science* 1994; **266**: 2011–5.

Koering CE, Pollice A, Zibella MP, Bauwens S, Puisieux A, Brunori M *et al.* Human telomeric position effect is determined by chromosomal context and telomeric chromatin integrity. *EMBO Rep* 2002; **3**: 1055–1061.

Konishi A, de Lange T. Cell cycle control of telomere protection and NHEJ revealed by a ts mutation in the DNA-binding domain of TRF2. *Genes Dev* 2008; **22**: 1221–1230.

Kyo S, Inoue M. Complex regulatory mechanisms of telomerase activity in normal and cancer cells: how can we apply them for cancer therapy? *Oncogene* 2002; **21**: 688–697.

Lachner M, O'Carroll D, Rea S, Mechtler K, Jenuwein T. Methylation of histone H3 lysine 9 creates a binding site for HP1 proteins. *Nature* 2001; **410**: 116–120.

Lai CK, Miller MC, Collins K. Roles for RNA in telomerase nucleotide and repeat addition processivity. *Mol Cell* 2003; **11**: 1673–1683.

Laud PR, Multani AS, Bailey SM, Wu L, Ma J, Kingsley C *et al.* Elevated telomere-telomere recombination in WRN-deficient, telomere dysfunctional cells promotes escape from senescence and engagement of the ALT pathway. *Genes Dev* 2005; **19**: 2560–2570.

Lavin MF. Ataxia-telangiectasia: from a rare disorder to a paradigm for cell signalling and cancer. *Nat Rev Mol Cell Biol* 2008; **9**: 759–769.

Law MJ, Lower KM, Voon HPJ, Hughes JR, Garrick D, Viprakasit V *et al.* ATR-X syndrome protein targets tandem repeats and influences allele-specific expression in a size-dependent manner. *Cell* 2010; **143**: 367–378.

Lee HW, Gottlieb GJ, Horner JW, Greider CW, DePinho RA, Blasco MA. Essential role of mouse telomerase in highly proliferative organs. *Nature* 1998; **392**: 569–74.

Lee J, Kumagai A, Dunphy WG. Claspin, a Chk1-regulatory protein, monitors DNA replication on chromatin independently of RPA, ATR, and Rad17. *Mol Cell* 2003; **11**: 329–340.

Lee JC, Jeng YM, Liau JY, Tsai JH, Hsu HH, Yang CY. Alternative lengthening of telomeres and loss of ATRX are frequent events in pleomorphic and dedifferentiated liposarcomas. *Mod Pathol* 2015; **28**: 1064–1073.

Lee M, Hills M, Conomos D, Stutz MD, Dagg RA, Lau LMS *et al.* Telomere extension by telomerase and ALT generates variant repeats by mechanistically distinct processes. *Nucleic Acids Res* 2014; **42**: 1733–1746.

Lee MS, Edwards RA, Thede GL, Glover JNM. Structure of the BRCT repeat domain of MDC1 and its specificity for the free COOH-terminal end of the γ-H2AX histone tail. *J Biol Chem* 2005; **280**: 32053–32056.

Lee SS, Bohrson C, Pike AM, Wheelan SJ, Greider CW. ATM Kinase Is Required for Telomere Elongation in Mouse and Human Cells. *Cell Rep* 2015; **13**: 1623–1632.

Lempiäinen H, Halazonetis TD. Emerging common themes in regulation of PIKKs and PI3Ks. *EMBO J* 2009; **28**: 3067–73.

Leri A, Franco S, Zacheo A, Barlucchi L, Chimenti S, Limana F *et al.* Ablation of telomerase and telomere loss leads to cardiac dilatation and heart failure associated with p53 upregulation. *EMBO J* 2003; **22**: 131–139.

Leung JWC, Ghosal G, Wang W, Shen X, Wang J, Li L *et al.* Alpha thalassemia/mental retardation syndrome X-linked gene product ATRX is required for proper replication restart and cellular resistance to replication stress. *J Biol Chem* 2013; **288**: 6342–6350.

Levis R, Hazelrigg T, Rubin GM. Effects of genomic position on the expression of transduced copies of the white gene of Drosophila. *Science* 1985; **229**: 558–561.

Li B, Jog SP, Reddy S, Comai L. WRN controls formation of extrachromosomal telomeric circles and is required for TRF2DeltaB-mediated telomere shortening. *Mol Cell Biol* 2008; **28**: 1892–904.

Li S, Li Z, Shu F-J, Xiong H, Phillips AC, Dynan WS. Double-strand break repair deficiency in NONO knockout murine embryonic fibroblasts and compensation by spontaneous upregulation of the PSPC1 paralog. *Nucleic Acids Res* 2014; **42**: 1–10.

Liang S, Lutz CS. p54nrb is a component of the snRNP-free U1A (SF-A) complex that promotes pre-mRNA cleavage during polyadenylation. *RNA* 2006; **12**: 111–121.

Lin Y, Dent SYR, Wilson JH, Wells RD, Napierala M. R loops stimulate genetic instability of CTG.CAG repeats. *Proc Natl Acad Sci U S A* 2010; **107**: 692–697.

Liu Q, Guntuku S, Cui XS, Matsuoka S, Cortez D, Tamai K *et al.* Chk1 is an essential kinase that is regulated by Atr and required for the G2/M DNA damage checkpoint. *Genes Dev* 2000; **14**: 1448–1459.

Liu S, Shiotani B, Lahiri M, Marechal A, Tse A, Leung CCY *et al.* ATR Autophosphorylation as a Molecular Switch for Checkpoint Activation. *Mol Cell* 2011; **43**: 192–202.

Liu Y, Kao H-I, Bambara R a. Flap endonuclease 1: a central component of DNA metabolism. *Annu Rev Biochem* 2004; **73**: 589–615.

Liu Y, Masson J-Y, Shah R, O'Regan P, West SC. RAD51C is required for Holliday junction processing in mammalian cells. *Science* 2004; **303**: 243–246.

Londono-Vallejo JA, Der-Sarkissian H, Cazes L, Bacchetti S, Reddel RR. Alternative Lengthening of Telomeres Is Characterized by High Rates of Telomeric Exchange. *Cancer Res* 2004; **64**: 2324–2327.

Lopez de Silanes I, Grana O, De Bonis ML, Dominguez O, Pisano DG, Blasco MA. Identification of TERRA locus unveils a telomere protection role through association to nearly all chromosomes. *Nat Commun* 2014; **5**: 4723.

Lopez de Silanes I, Stagno d'Alcontres M, Blasco MA. TERRA transcripts are bound by a complex array of RNA-binding proteins. *Nat Commun* 2010; **1**: 33.

Lossaint G, Larroque M, Ribeyre C, Bec N, Larroque C, Décaillet C *et al*. FANCD2 Binds MCM Proteins and Controls Replisome Function upon Activation of S Phase Checkpoint Signaling. *Mol Cell* 2013; **51**: 678–690.

Lou Z, Minter-Dykhouse K, Franco S, Gostissa M, Rivera MA, Celeste A *et al*. MDC1 maintains genomic stability by participating in the amplification of ATM-dependent DNA damage signals. *Mol Cell* 2006; **21**: 187–200.

Lovejoy CA, Cortez D. Common mechanisms of PIKK regulation. *DNA Repair (Amst)* 2009; **8**: 1004–1008.

Lovejoy CA, Li W, Reisenweber S, Thongthip S, Bruno J, de Lange T *et al*. Loss of ATRX, genome instability, and an altered DNA damage response are hallmarks of the alternative lengthening of Telomeres pathway. *PLoS Genet* 2012; **8**. doi:10.1371/journal.pgen.1002772.

MacHwe A, Karale R, Xu X, Liu Y, Orren DK. The Werner and Bloom syndrome proteins help resolve replication blockage by converting (regressed) Holliday junctions to functional replication forks. *Biochemistry* 2011; **50**: 6774–6788.

Maizels N, Gray LT. The G4 Genome. *PLoS Genet* 2013; **9**. doi:10.1371/journal.pgen.1003468.

Makarov VL, Lejnine S, Bedoyan J, Langmore JP. Nucleosomal organization of telomere-specific chromatin in rat. *Cell* 1993; **73**: 775–787.

Maloisel L, Fabre F, Gangloff S. DNA polymerase δ is preferentially recruited during homologous recombination to promote heteroduplex DNA extension. *Mol Cell Biol* 2008; **28**: 1373–1382.

Martinez P, Blasco MA. Replicating through telomeres: A means to an end. *Trends Biochem Sci* 2015; **40**: 504–515.

Martinez P, Thanasoula M, Carlos AR, Gómez-López G, Tejera AM, Schoeftner S *et al*. Mammalian Rap1 controls telomere function and gene expression through binding to telomeric and extratelomeric sites. *Nat Cell Biol* 2010; **12**: 768–780.

Martinez P, Thanasoula M, Munoz P, Liao C, Tejera A, McNees C *et al*. Increased telomere fragility and fusions resulting from TRF1 deficiency lead to degenerative pathologies and increased cancer in mice. *Genes Dev* 2009; **23**: 2060–2075.

Mathur M, Tucker PW, Samuels HH. PSF is a novel corepressor that mediates its effect through Sin3A and the DNA binding domain of nuclear hormone receptors. *Mol Cell Biol* 2001; **21**: 2298–311.

Mathur M, Das S, Samuels HH. PSF-TFE3 oncopro- tein in papillary renal cell carcinoma inactivates TFE3 and p53 through cytoplasmic sequestration. *Oncogene* 2003; **22**: 5031–5044.

Matsuoka S, Ballif BA, Smogorzewska A, McDonald ER, Hurov KE, Luo J *et al*. ATM and ATR substrate analysis reveals extensive protein networks responsive to DNA damage. *Science* 2007; **316**: 1160–1166.

McClintock, B. (1939). "The Behavior in Successive Nuclear Divisions of a Chromosome Broken at Meiosis." ProcNatl Acad Sci U S A **25**(8): 405-416.

McElligott R, Wellinger RJ. The terminal DNA structure of mammalian chromosomes. *EMBO J* 1997; **16**: 3705–3714.

McNees CJ, Tejera AM, Martínez P, Murga M, Mulero F, Fernandez-Capetillo O *et al*. ATR suppresses telomere fragility and recombination but is dispensable for elongation of short telomeres by telomerase. *J Cell Biol* 2010; **188**: 639–652.

Meier A, Fiegler H, Munoz P, Ellis P, Rigler D, Langford C *et al*. Spreading of mammalian DNA-damage response factors studied by ChIP-chip at damaged telomeres. *EMBO J* 2007; **26**: 2707–2718.

Meier UT. The many facets of H/ACA ribonucleoproteins. Chromosoma. 2005; **114**: 1–14.

Melcher M, Schmid M, Aagaard L, Selenko P, Laible G, Jenuwein T. Structure-function analysis of SUV39H1 reveals a dominant role in heterochromatin organization, chromosome segregation, and mitotic progression. *Mol Cell Biol* 2000; **20**: 3728–3741.

Melton AA, Jackson J, Wang J, Lynch KW. Combi- natorial control of signal-induced exon repression by hnRNP L and PSF. *Mol Cell Biol* 2007; **27**: 6972–6984.

Metcalfe JA, Parkhill J, Campbell L, Stacey M, Biggs P, Byrd PJ *et al*. Accelerated telomere shortening in ataxia telangiectasia. *Nat Genet* 1996; **13**: 350–3.

Meyne J, Ratliff RL, Moyzis RK. Conservation of the human telomere sequence (TTAGGG)n among vertebrates. *Proc Natl Acad Sci U S A* 1989; **86**: 7049–53.

Michishita E, McCord RA, Berber E, Kioi M, Padilla-Nash H, Damian M *et al*. SIRT6 is a histone H3 lysine 9 deacetylase that modulates telomeric chromatin. *Nature* 2008; **452**: 492–6.

Mircsof D. *et al*. Mutations in NONO lead to syndromic intellectual disability and inhibitory synaptic defects. *Nat Neurosci* 2015; **18**: 1731-1736.

Mitchell M, Gillis A, Futahashi M, Fujiwara H, Skordalakes E. Structural basis for telomerase catalytic subunit TERT binding to RNA template and telomeric DNA. *Nat Struct Mol Biol* 2010; **17**: 513–518.

Mohaghegh P, Hickson ID. DNA helicase deficiencies associated with cancer predisposition and premature ageing disorders. *Hum Mol Genet* 2001; **10**: 741–746.

Morozumi Y, Takizawa Y, Takaku M, Kurumizaka H. Human PSF binds to RAD51 and modulates its homologous-pairing and strand-exchange activities. *Nucleic Acids Res* 2009; **37**: 4296–4307.

Morris, KV, Mattick, JS. The rise of regulatory RNA. *Nat Rev Genet* 2014; **15**: 423–37.

Mortusewicz O, Herr P, Helleday T. Early replication fragile sites: where replication-transcription collisions cause genetic instability. *EMBO J* 2013; **32**: 493–495.

Muers M. Mutation: the perils of transcription. *Nat Rev Genet* 2011; **12**: 156.

Muñoz P, Blanco R, de Carcer G, Schoeftner S, Benetti R, Flores JM *et al*. TRF1 controls telomere length and mitotic fidelity in epithelial homeostasis. *Mol Cell Biol* 2009; **29**: 1608–25.

Muñoz P, Blanco R, Flores JM, Blasco MA. XPF nuclease-dependent telomere loss and increased DNA damage in mice overexpressing TRF2 result in premature aging and cancer. *Nat Genet* 2005; **37**: 1063–71.

Muntoni A, Neumann AA, Hills M, Reddel RR. Telomere elongation involves intra-molecular DNA replication in cells utilizing alternative lengthening of telomeres. *Hum Mol Genet* 2009; **18**: 1017–1027.

Murnane JP, Sabatier L, Marder BA, Morgan WF. Telomere dynamics in an immortal human cell line. *EMBO J* 1994; **13**: 4953–62.

Nabel CS, Schutsky EK, Kohli RM. Molecular targeting of mutagenic AID and APOBEC deaminases. *Cell Cycle* 2014; **13**: 171–172.

Nabel CS, Schutsky EK, Kohli RM. Molecular targeting of mutagenic AID and APOBEC deaminases. *Cell Cycle* 2014; **13**: 171–172.

Nabetani A, Ishikawa F. Unusual telomeric DNAs in human telomerase-negative immortalized cells. *Mol Cell Biol* 2009; **29**: 703–13.

Napier CE, Huschtscha LI, Harvey A, Bower K, Noble JR, Hendrickson EA *et al.* ATRX represses alternative lengthening of telomeres. *Oncotarget* 2015; **6**: 16543–58.

Narita M, Nunez S, Heard E, Narita M, Lin AW, Hearn SA, Spector DL, Hannon GJ, Lowe SW. Rb-mediated heterochromatin formation and silencing of E2F target genes during cellular senescence. *Cell* 2003; **113**:703-16.

Naro C, Bielli P, Pagliarini V, Sette C. The interplay between DNA damage response and RNA processing: The unexpected role of splicing factors as gatekeepers of genome stability. *Front Genet* 2015; **6**. doi:10.3389/fgene.2015.00142.

Nergadze SG, Farnung BO, Wischnewski H, Khoriauli L, Vitelli V, Chawla R *et al.* CpG-island promoters drive transcription of human telomeres. *RNA* 2009; **15**: 2186–94.

Neumann AA, Watson CM, Noble JR, Pickett HA, Tam PPL, Reddel RR. Alternative lengthening of telomeres in normal mammalian somatic cells. *Genes Dev* 2013; **27**: 18–23.

Nguyen GH, Dexheimer TS, Rosenthal AS, Chu WK, Singh DK, Mosedale G *et al.* A small molecule inhibitor of the BLM helicase modulates chromosome stability in human cells. *Chem Biol* 2013; **20**: 55–62.

Nielsen SJ, Schneider R, Bauer UM, Bannister AJ, Morrison A, O'Carroll D, Firestein R, Cleary M, Jenuwein T, Herrera RE, *et al*. Rb targets histone H3 methylation and HP1 to promoters. *Nature* 2001; **412**:561- 5.

Niida H, Shinkai Y, Hande MP, Matsumoto T, Takehara S, Tachibana M *et al.* Telomere maintenance in telomerase-deficient mouse embryonic stem cells: characterization of an amplified telomeric DNA. *Mol Cell Biol* 2000; **20**: 4115–4127.

Nikitina T, Woodcock CL. Closed chromatin loops at the ends of chromosomes. *J Cell Biol* 2004; **166**: 161–165.

Nora GJ, Buncher NA, Opresko PL. Telomeric protein TRF2 protects Holliday junctions with telomeric arms from displacement by the werner syndrome helicase. *Nucleic Acids Res* 2010; **38**: 3984–3998.

O'Connor MS, Safari A, Xin H, Liu D, Songyang Z. A critical role for TPP1 and TIN2 interaction in high-order telomeric complex assembly. *Proc Natl Acad Sci U S A* 2006; **103**: 11874–9.

O'Sullivan RJ, Almouzni G. Assembly of telomeric chromatin to create ALTernative endings. *Trends Cell Biol* 2014; **24**: 675–685.

Ohta M, Inoue H, Cotticelli MG, Kastury K, Baffa R, Palazzo J *et al*. The FHIT gene, spanning the chromosome 3p14.2 fragile site and renal carcinoma-associated t(3;8) breakpoint, is abnormal in digestive tract cancers. *Cell* 1996; **84**: 587–597.

Okamoto K, Bartocci C, Ouzounov I, Diedrich JK, Yates JR, Denchi EL. A two-step mechanism for TRF2-mediated chromosome-end protection. *Nature* 2013; **494**: 502–5.

Olovnikov AM. A theory of marginotomy. The incomplete copying of template margin in enzymic synthesis of polynucleotides and biological significance of the phenomenon. *J Theor Biol* 1973; **41**: 181–190.

Paeschke K, Bochman ML, Garcia PD, Cejka P, Friedman KL, Kowalczykowski SC *et al*. Pif1 family helicases suppress genome instability at G-quadruplex motifs. *Nature* 2013; **497**: 458–462.

Palm W, de Lange T. How shelterin protects mammalian telomeres. *Annu Rev Genet* 2008; **42**: 301–34.

Palm W, Hockemeyer D, Kibe T, de Lange T. Functional dissection of human and mouse POT1 proteins. *Mol Cell Biol* 2009; **29**: 471–82.

Pamidi A, Cardoso R, Hakem A, Matysiak-Zablocki E, Poonepalli A, Tamblyn L *et al*. Functional interplay of p53 and Mus81 in DNA damage responses and cancer. *Cancer Res* 2007; **67**: 8527–8535.

Pandita TK. ATM function and telomere stability. *Oncogene* 2002; **21**: 611–8.

Passon DM, Lee M, Rackham O, Stanley WA, Sadowska A, Filipovska A *et al*. Structure of the heterodimer of human NONO and paraspeckle protein component 1 and analysis of its role in subnuclear body formation. *Proc Natl Acad Sci U S A* 2012; **109**: 4846–4850.

Patton JG, Mayer SA, Tempst P, Nadal-Ginard B. Characterization and molecular cloning of polypyrimidine tract-binding protein: A component of a complex necessary for pre-mRNA splicing. *Genes Dev* 1991; **5**: 1237–1251.

Perrem K, Colgin LM, Neumann AA, Yeager TR, Reddel RR. Coexistence of alternative lengthening of telomeres and telomerase in hTERT-transfected GM847 cells. *Mol Cell Biol* 2001; **21**: 3862–75.

Peters AH, O'Carroll D, Scherthan H, Mechtler K, Sauer S, Scho€fer C, Weipoltshammer K, Pagani M, Lachner M, Kohlmaier A, et al. Loss of the Suv39h histone methyltransferases impairs mammalian heterochromatin and genome stability. *Cell* 2001; **107**:323- 37.

Peters AHFM, Kubicek S, Mechtler K, O'Sullivan RJ, Derijck AAHA, Perez-Burgos L *et al*. Partitioning and Plasticity of Repressive Histone Methylation States in Mammalian Chromatin. *Mol Cell* 2003; **12**: 1577–1589.

Peters AHFM, O'Carroll D, Scherthan H, Mechtler K, Sauer S, Schöfer C *et al*. Loss of the Suv39h histone methyltransferases impairs mammalian heterochromatin and genome stability. *Cell* 2001; **107**: 323–337.

Petersen S, Saretzki G, von Zglinicki T. Preferential accumulation of single-stranded regions in telomeres of human fibroblasts. *Exp Cell Res* 1998; **239**: 152–60.

Petti E, Jordi F, Buemi V, Dinami R, Benetti R, Blasco MA *et al*. Altered telomere homeostasis and resistance to skin carcinogenesis in Suv39h1 transgenic mice. *Cell Cycle* 2015; **14**: 1438–1446.

Pfeiffer V, Crittin J, Grolimund L, Lingner J. The THO complex component Thp2 counteracts telomeric R-loops and telomere shortening. *EMBO J* 2013; **32**: 2861–71.

Pichierri P, Franchitto a, Mosesso P, Palitti F. Werner's syndrome protein is required for correct recovery after replication arrest and DNA damage induced in S-phase of cell cycle. *Mol Biol Cell* 2001; **12**: 2412–2421.

Pickett HA, Reddel RR. Molecular mechanisms of activity and derepression of alternative lengthening of telomeres. *Nat Struct Mol Biol* 2015; **22**: 875–880.

Pogacić V, Dragon F, Filipowicz W. Human H/ACA small nucleolar RNPs and telomerase share evolutionarily conserved proteins NHP2 and NOP10. *Mol Cell Biol* 2000; **20**: 9028–9040.

Porro A, Feuerhahn S, Delafontaine J, Riethman H, Rougemont J, Lingner J. Functional characterization of the TERRA transcriptome at damaged telomeres. *Nat Commun* 2014; **5**: 5379.

Porro A, Feuerhahn S, Lingner J. TERRA-Reinforced Association of LSD1 with MRE11 Promotes Processing of Uncapped Telomeres. *Cell Rep* 2014; **6**: 765–776.

Porro A, Feuerhahn S, Reichenbach P, Lingner J. Molecular dissection of telomeric repeat-containing RNA biogenesis unveils the presence of distinct and multiple regulatory pathways. *Mol Cell Biol* 2010; **30**: 4808–4817.

Poulet A, Buisson R, Faivre-Moskalenko C, Koelblen M, Amiard S, Montel F *et al.* TRF2 promotes, remodels and protects telomeric Holliday junctions. *EMBO J* 2009; **28**: 641–651.

Punchihewa C, Inoue A, Hishiki A, Fujikawa Y, Connelly M, Evison B *et al.* Identification of small molecule proliferating cell nuclear antigen (PCNA) inhibitor that disrupts interactions with PIP-box proteins and inhibits DNA replication. *J Biol Chem* 2012; **287**: 14289–14300.

Rajesh C, Baker DK, Pierce AJ, Pittman DL. The splicing-factor related protein SFPQ/PSF interacts with RAD51D and is necessary for homology-directed repair and sister chromatid cohesion. *Nucleic Acids Res* 2011; **39**: 132–145.

Ray P, Kar A, Fushimi K, Havlioglu N, Chen X, Wu JY. PSF suppresses tau exon 10 inclusion by interacting with a stem-loop structure downstream of exon 10. In: *Journal of Molecular Neuroscience*. 2011, pp 453–466.

Rea S, Eisenhaber F, O'Carroll D, Strahl BD, Sun ZW, Schmid M, Opravil S, Mechtler K, Ponting CP, Allis CD, *et al*. Regulation of chromatin structure by site- specific histone H3 methyltransferases. *Nature* 2000; **406**:593-9.

Recolin B, van der Laan S, Tsanov N, Maiorano D. Molecular mechanisms of DNA replication checkpoint activation. Genes (Basel). 2014; **5**: 147–175.

Redon S, Reichenbach P, Lingner J. The non-coding RNA TERRA is a natural ligand and direct inhibitor of human telomerase. *Nucleic Acids Res* 2010; **38**: 5797–5806.

Redon S, Zemp I, Lingner J. A three-state model for the regulation of telomerase by TERRA and hnRNPA1. *Nucleic Acids Res* 2013; **41**: 9117–9128.

Reimann M, Lee S, Loddenkemper C, Dorr JR, Tabor V, Aichele P *et al.* Tumor Stroma-Derived TGF-β Limits Myc-Driven Lymphomagenesis via Suv39h1-Dependent Senescence. *Cancer Cell* 2010; **17**: 262–272.

Riethman HC, Moyzis RK, Meyne J, Burke DT, Olson M V. Cloning human telomeric DNA fragments into Saccharomyces cerevisiae using a yeast-artificial-chromosome vector. *Proc Natl Acad Sci U S A* 1989; **86**: 6240–4.

Riley T, Sontag E, Chen P, Levine A. Transcriptional control of human p53-regulated genes. *Nat Rev Mol Cell Biol* 2008; **9**: 402–412.

Rippe K, Luke B. TERRA and the state of the telomere. *Nat Struct {&} Mol Biol* 2015; **22**: 853–858.

Ritchie K, Seah C, Moulin J, Isaac C, Dick F, B??rub?? NG. Loss of ATRX leads to chromosome cohesion and congression defects. *J Cell Biol* 2008; **180**: 315–324.

Roberts RW, Crothers DM. Stability and properties of double and triple helices: dramatic effects of RNA or DNA backbone composition. *Science* 1992; **258**: 1463–1466.

Robison JG, Elliott J, Dixon K, Oakley GG. Replication protein A and the Mre11·Rad50·Nbs1 complex co-localize and interact at sites of stalled replication forks. *J Biol Chem* 2004; **279**: 34802–34810.

Roepcke S, Stahlberg S, Klein H, Schulz MH, Theobald L, Gohlke S *et al.* A tandem sequence motif acts as a distance-dependent enhancer in a set of genes involved in translation by binding the proteins NonO and SFPQ. *BMC Genomics* 2011; **12**: 624.

Rouda S, Skordalakes E. Structure of the RNA-Binding Domain of Telomerase: Implications for RNA Recognition and Binding. *Structure* 2007; **15**: 1403–1412.

Roy D, Lieber MR. G clustering is important for the initiation of transcription-induced R-loops in vitro, whereas high G density without clustering is sufficient thereafter. *Mol Cell Biol* 2009; **29**: 3124–3133.

Roy D, Zhang Z, Lu Z, Hsieh CL, Lieber MR. Competition between the RNA transcript and the nontemplate DNA strand during R-loop formation *in vitro:* a nick can serve as a strong R-loop initiation site. *Mol Cell Biol* 2010; **30**: 146–159.

Saharia A, Guittat L, Crocker S, Lim A, Steffen M, Kulkarni S *et al.* Flap Endonuclease 1 Contributes to Telomere Stability. *Curr Biol* 2008; **18**: 496–500.

Saharia A, Teasley DC, Duxin JP, Dao B, Chiappinelli KB, Stewart SA. FEN1 ensures telomere stability by facilitating replication fork re-initiation. *J Biol Chem* 2010; **285**: 27057–27066.

Salton M, Lerenthal Y, Wang SY, Chen DJ, Shiloh Y. Involvement of Matrin 3 and SFPQ/NONO in the DNA damage response. *Cell Cycle* 2010; **9**: 1568–1576.

Samper E, Fernández P, Eguía R, Martín-Rivera L, Bernad A, Blasco MA *et al.* Long-term repopulating ability of telomerase-deficient murine hematopoietic stem cells. *Blood* 2002; **99**: 2767–2775.

Samper E, Goytisolo FA, Murcia JMD, González-Suárez E, Cigudosa JC, De Murcia G *et al.* Normal telomere length and chromosomal end capping in poly(ADP-ribose) polymerase-deficient mice and primary cells despite increased chromosomal instability. *J Cell Biol* 2001; **154**: 49–60.

Santos-Pereira JM, Aguilera A. R loops: new modulators of genome dynamics and function. *Nat Rev Genet* 2015; **16**: 583–597.

Sarek G, Vannier JB, Panier S, Petrini HJ, Boulton SJ. TRF2 recruits RTEL1 to telomeres in s phase to promote t-loop unwinding. *Mol Cell* 2015; **57**: 622–635.

Sasaki T, Gilbert DM. The many faces of the origin recognition complex. Curr. Opin. Cell Biol. 2007; **19**: 337–343.

Sasaki YTF, Hirose T. How to build a paraspeckle. *Genome Biol* 2009; **10**: 227.

Savic V, Yin B, Maas NL, Bredemeyer AL, Carpenter AC, Helmink BA *et al*. Formation of Dynamic γ-H2AX Domains along Broken DNA Strands Is Distinctly Regulated by ATM and MDC1 and Dependent upon H2AX Densities in Chromatin. *Mol Cell* 2009; **34**: 298–310.

Scheibe M, Arnoult N, Kappei D, Buchholz F, Decottignies A, Butter F *et al*. Quantitative interaction screen of telomeric repeatcontaining RNA reveals novel TERRA regulators. *Genome Res* 2013; **23**: 2149–2157.

Schlacher K, Christ N, Siaud N, Egashira A, Wu H, Jasin M. Double-strand break repair-independent role for BRCA2 in blocking stalled replication fork degradation by MRE11. *Cell* 2011; **145**: 529–542.

Schlacher K, Wu H, Jasin M. A Distinct Replication Fork Protection Pathway Connects Fanconi Anemia Tumor Suppressors to RAD51-BRCA1/2. *Cancer Cell* 2012; **22**: 106–116.

Schoeftner S, A BM. Developmentally regulated transcription of mammalian telomeres by DNA-dependent RNA polymerase II. *Nat Cell Biol* 2008; **10**: 228–36.

Schoeftner S, Blasco MA. Chromatin regulation and non-coding RNAs at mammalian telomeres. Semin. Cell Dev. Biol. 2010; **21**: 186–193.

Schotta G, Lachner M, Sarma K, Ebert A, Sengupta R, Reuter G *et al*. A silencing pathway to induce H3-K9 and H4-K20 trimethylation at constitutive heterochromatin. *Genes Dev* 2004; **18**: 1251–1262.

Schwartz EK, Heyer WD. Processing of joint molecule intermediates by structure-selective endonucleases during homologous recombination in eukaryotes. Chromosoma. 2011; **120**: 109–127.

Sen D, Gilbert W. Formation of parallel four-stranded complexes by guanine-rich motifs in DNA and its implications for meiosis. *Nature* 1988; **334**: 364–6.

Serrano M, Lin AW, McCurrach ME, Beach D, Lowe SW. Oncogenic ras provokes premature cell senescence associated with accumulation of p53 and p16(INK4a). *Cell* 1997; **88**: 593–602.

Sfeir A, Kosiyatrakul ST, Hockemeyer D, MacRae SL, Karlseder J, Schildkraut CL *et al*. Mammalian Telomeres Resemble Fragile Sites and Require TRF1 for Efficient Replication. *Cell* 2009; **138**: 90–103.

Sfeir A, Kabir S, van Overbeek M, Celli GB and de lange T. Loss of Rap1 induces telomere recombination in absence of NHEJ or a DNA damage signal. *Science* 2010; **18**: 1199–1216.

Shampay J, Szostak JW, Blackburn EH. DNA sequences of telomeres maintained in yeast. *Nature* 1984; **310**: 154–7.

Sharma NK, Reyes A, Green P, Caron MJ, Bonini MG, Gordon DM *et al*. Human telomerase acts as a hTR-independent reverse transcriptase in mitochondria. Nucleic Acids Res. 2012; **40**: 712–725.

Sharma S, Sommers JA, Gary RK, Friedrich-Heineken E, Hubscher U, Brosh RM. The interaction site of Flap Endonuclease-1 with WRN helicase suggests a coordination of WRN and PCNA. *Nucleic Acids Res* 2005; **33**: 6769–6781.

Sharma S, Hicks JK, Chute CL, Brennan JR, Ahn JY, Glover TW, Canman CE. REV1 and polymerase ζ facilitate homologous recombination repair. *Nucleic Acids Res* 2012; **40**: 682–691.

Shav-Tal Y, Zipori D. PSF and p54(nrb)/NonO--multi-functional nuclear proteins. *FEBS Lett* 2002; **531**: 109–114.

Shay JW, Bacchetti S. A survey of telomerase activity in human cancer. *Eur J Cancer* 1997; **33**: 787–791.

Shay JW, Wright WE. Senescence and immortalization: Role of telomeres and telomerase. *Carcinogenesis* 2005; **26**: 867–874.

Shiloh Y. ATM and related protein kinases: safeguarding genome integrity. *Nat Rev Cancer* 2003; **3**: 155–168.

Shiotani B, Zou L. Single-Stranded DNA Orchestrates an ATM-to-ATR Switch at DNA Breaks. *Mol Cell* 2009; **33**: 547–558.

Skourti-Stathaki K, Proudfoot NJ. A double-edged sword: R loops as threats to genome integrity and powerful regulators of gene expression. Genes Dev. 2014; **28**: 1384–1396.

Smilenov LB, Morgan SE, Mellado W, Sawant SG, Kastan MB, Pandita TK. Influence of ATM function on telomere metabolism. *Oncogene* 1997; **15**: 2659–65.

Smogorzewska A, de Lange T. Regulation of telomerase by telomeric proteins. *Annu Rev Biochem* 2004; **73**: 177–208.

Smogorzewska A, Karlseder J, Holtgreve-Grez H, Jauch A, de Lange T. DNA ligase IV-dependent NHEJ of deprotected mammalian telomeres in G1 and G2. *Curr Biol* 2002; **12**: 1635–1644.

Sollier J, Stork CT, Garcia-Rubio ML, Paulsen RD, Aguilera A, Cimprich KA. Transcription-Coupled Nucleotide Excision Repair Factors Promote R-Loop-Induced Genome Instability. *Mol Cell* 2014; **56**: 777–785.

Stamova BS, Tian Y, Nordahl CW, Shen MD, Rogers S, Amaral DG, Sharp FR. Evidence for differential alternative splicing in blood of young boys with autism spectrum disorders. *Mol Autism* 2013;: 4-30.

Stewart GS, Wang B, Bignell CR, Taylor AMR, Elledge SJ. MDC1 is a mediator of the mammalian DNA damage checkpoint. *Nature* 2003; **421**: 961–966.

Stucki M, Clapperton JA, Mohammad D, Yaffe MB, Smerdon SJ, Jackson SP. MDC1 directly binds phosphorylated histone H2AX to regulate cellular responses to DNA double-strand breaks. *Cell* 2005; **123**: 1213–1226.

Szostak JW, Blackburn EH. Cloning yeast telomeres on linear plasmid vectors. *Cell* 1982; **29**: 245–255.

Takahama K, Takada A, Tada S, Shimizu M, Sayama K, Kurokawa R *et al.* Regulation of telomere length by G-quadruplex telomere DNA- and TERRA-binding protein TLS/FUS. *Chem Biol* 2013; **20**: 341–350.

Takai H, Smogorzewska A, de Lange T. DNA damage foci at dysfunctional telomeres. *Curr Biol* 2003; **13**: 1549–1556.

Takai KK, Kibe T, Donigian JR, Frescas D, de Lange T. Telomere Protection by TPP1/POT1 Requires Tethering to TIN2. *Mol Cell* 2011; **44**: 647–659.

Thorslund T, McIlwraith MJ, Compton S a, Lekomtsev S, Petronczki M, Griffith JD *et al.* The breast cancer tumor suppressor BRCA2 promotes the specific targeting of RAD51 to single-stranded DNA. *Nat Struct {&} Mol Biol* 2010; **17**: 1263–1265.

Toledo LI, Altmeyer M, Rask MB, Lukas C, Larsen DH, Povlsen LK *et al.* ATR prohibits replication catastrophe by preventing global exhaustion of RPA. Cell. 2014; **156**: 374.

Tomas-Loba A, Flores I, Fernandez-Marcos PJ, Cayuela ML, Maraver A, Tejera A *et al.* Telomerase Reverse Transcriptase Delays Aging in Cancer-Resistant Mice. *Cell* 2008; **135**: 609–622.

Tommerup H, Dousmanis A, de Lange T. Unusual chromatin in human telomeres. *Mol Cell Biol* 1994; **14**: 5777–85.

Tong AS, Stern JL, Sfeir A, Kartawinata M, de Lange T, Zhu XD *et al.* ATM and ATR Signaling Regulate the Recruitment of Human Telomerase to Telomeres. *Cell Rep* 2015; **13**: 1633–1646.

Tsantoulis PK, Kotsinas a, Sfikakis PP, Evangelou K, Sideridou M, Levy B *et al.* Oncogene-induced replication stress preferentially targets common fragile sites in preneoplastic lesions. A genome-wide study. *Oncogene* 2008; **27**: 3256–3264.

Tuduri S, Crabbé L, Conti C, Tourrière H, Holtgreve-Grez H, Jauch A *et al.* Topoisomerase I suppresses genomic instability by preventing interference between replication and transcription. *Nat Cell Biol* 2009; **11**: 1315–1324.

Udugama M, M Chang FT, Chan FL, Tang MC, Pickett HA, R McGhie JD *et al.* Histone variant H3.3 provides the heterochromatic H3 lysine 9 tri-methylation mark at telomeres. *Nucleic Acids Res* 2015; **43**: 10227–37.

Uringa E-J, Lisaingo K, Pickett HA, Brind'Amour J, Rohde J-H, Zelensky A *et al.* RTEL1 contributes to DNA replication and repair and telomere maintenance. *Mol Biol Cell* 2012; **23**: 2782–2792.

Vannier JB, Pavicic-Kaltenbrunner V, Petalcorin MIR, Ding H, Boulton SJ. RTEL1 dismantles T loops and counteracts telomeric G4-DNA to maintain telomere integrity. *Cell* 2012; **149**: 795–806.

Vannier JB, Sandhu S, Petalcorin MIR, Wu X, Nabi Z, Ding H *et al.* RTEL1 is a replisome-associated helicase that promotes telomere and genome-wide replication. *Science* 2013; **342**: 239–42.

Vega LR, Mateyak MK, Zakian V a. Getting to the end: telomerase access in yeast and humans. *Nat Rev Mol Cell Biol* 2003; **4**: 948–959.

Venteicher AS, Abreu EB, Meng Z, McCann KE, Terns RM, Veenstra TD *et al.* A human telomerase holoenzyme protein required for Cajal body localization and telomere synthesis. *Science* 2009; **323**: 644–8.

Vera E, Canela A, Fraga MF, Esteller M, Blasco MA. Epigenetic regulation of telomeres in human cancer. *Oncogene* 2008; **27**: 6817–6833.

Wahba L, Amon JD, Koshland D, Vuica-Ross M. RNase H and Multiple RNA Biogenesis Factors Cooperate to Prevent RNA:DNA Hybrids from Generating Genome Instability. *Mol Cell* 2011; **44**: 978–988.

Wahba L, Gore SK, Koshland D. The homologous recombination machinery modulates the formation of RNA-DNA hybrids and associated chromosome instability. *Elife* 2013; **2013**. doi:10.7554/eLife.00505.

Walne AJ, Dokal I. Advances in the understanding of dyskeratosis congenita. Br. J. Haematol. 2009; **145**: 164–172.

Walsh KM, Rice T, Decker PA, Kosel ML, Kollmeyer T, Hansen HM *et al.* Genetic variants in telomerase-related genes are associated with an older age at diagnosis in glioma patients: Evidence for distinct pathways of gliomagenesis. *Neuro Oncol* 2013; **15**: 1041–1047.

Wang J, Gong Z, Chen J. MDC1 collaborates with TopBP1 in DNA replication checkpoint control. *J Cell Biol* 2011; **193**: 267–273.

Wang JC, Caron PR, Kim RA. The role of DNA topoisomerases in recombination and genome stability: A double-edged sword? *Cell* 1990; **62**: 403–406.

Wang RC, Smogorzewska A, De Lange T. Homologous recombination generates t-loop-sized deletions at human telomeres. *Cell* 2004; **119**: 355–368.

Wang Y, Ghosh G, Hendrickson E a. Ku86 represses lethal telomere deletion events in human somatic cells. *Proc Natl Acad Sci U S A* 2009; **106**: 12430–12435.

Wang Y, Putnam CD, Kane MF, Zhang W, Edelmann L, Russell R *et al.* Mutation in Rpa1 results in defective DNA double-strand break repair, chromosomal instability and cancer in mice. *Nat Genet* 2005; **37**: 750–5.

Ward IM, Chen J. Histone H2AX Is Phosphorylated in an ATR-dependent Manner in Response to Replicational Stress. *J Biol Chem* 2001; **276**: 47759–47762.

Watson JD. Origin of concatemeric T7 DNA. *Nat New Biol* 1972; **239**: 197–201.

Wechsler T, Newman S, West SC. Aberrant chromosome morphology in human cells defective for Holliday junction resolution. *Nature* 2011; **471**: 642–646.

Wimberly H, Shee C, Thornton PC, Sivaramakrishnan P, Rosenberg SM, Hastings PJ. R-loops and nicks initiate DNA breakage and genome instability in non-growing Escherichia coli. *Nat Commun* 2013; **4**: 2115.

Wong LH, McGhie JD, Sim M, Anderson MA, Ahn S, Hannan RD *et al.* ATRX interacts with H3.3 in maintaining telomere structural integrity in pluripotent embryonic stem cells. *Genome Res* 2010; **20**: 351–360.

Wu G, Lee WH, Chen PL. NBS1 and TRF1 colocalize at promyelocytic leukemia bodiesduring late S/G2 phases in immortalized telomerase- negative cells. Implication of NBS1 in alternative lengthening of telomeres. *J Biol Chem* 2000; **275**: 30618–30622.

Wu KJ, Grandori C, Amacker M, Simon-Vermot N, Polack a, Lingner J *et al.* Direct activation of TERT transcription by c-MYC. *Nat Genet* 1999; **21**: 220–224.

Wu L, Multani AS, He H, Cosme-Blanco W, Deng Y, Deng JM *et al.* Pot1 Deficiency Initiates DNA Damage Checkpoint Activation and Aberrant Homologous Recombination at Telomeres. *Cell* 2006; **126**: 49–62.

Wu Y, Kazuo SY, Brosh Jr RM. FANCJ helicase defective in Fanconia anemia and breast cancer unwinds G-quadruplex DNA to defend genomic stability. *Mol Cell Biol* 2008; **28**: 4116–4128.

Wyatt HDM, West SC, Beattie TL. InTERTpreting telomerase structure and function. *Nucleic Acids Res* 2010; **38**: 5609–5622.

Yao MC, Blackburn EH, Gall J. Tandemly repeated C-C-C-C-A-A hexanucleotide of Tetrahymena rDNA is present elsewhere in the genome and may be related to the alteration of the somatic genome. *J Cell Biol* 1981; **90**: 515–520.

Yarosh CA, Iacona JR, Lutz CS, Lynch KW. PSF: nuclear busy-body or nuclear facilitator? *Wiley Interdiscip Rev RNA* 2015; **6**. doi:10.1002/wrna.1280.

Yeager TR, Neumann AA, Englezou A, Huschtscha LI, Noble JR, Reddel RR. Telomerase-negative immortalized human cells contain a novel type of promyelocytic leukemia (PML) body. *Cancer Res* 1999; **59**: 4175–4179.

Yehezkel S, Segev Y, Viegas-Péquignot E, Skorecki K, Selig S. Hypomethylation of subtelomeric regions in ICF syndrome is associated with abnormally short telomeres and enhanced transcription from telomeric regions. *Hum Mol Genet* 2008; **17**: 2776–2789.

Yehezkel S, Shaked R, Sagie S, Berkovitz R, Shachar-Bener H, Segev Y *et al*. Characterization and rescue of telomeric abnormalities in ICF syndrome type I fibroblasts. *Front Oncol* 2013; **3**: 35.

Yu K, Chedin F, Hsieh C-L, Wilson TE, Lieber MR. R-loops at immunoglobulin class switch regions in the chromosomes of stimulated B cells. *Nat Immunol* 2003; **4**: 442–451.

Yu TY, Kao YW, Lin JJ. Telomeric transcripts stimulate telomere recombination to suppress senescence in cells lacking telomerase. *Proc Natl Acad Sci U S A* 2014; **111**: 3377–3382.

Zhang Z, Carmichael GG. The fate of dsRNA in the Nucleus: A p54nrb-containing complex mediates the nuclear retention of promiscuously A-to-I edited RNAs. *Cell* 2001; **106**: 465–475.

Zhou BB, Elledge SJ. The DNA damage response: putting checkpoints in perspective. *Nature* 2000; **408**: 433–439.

Zhu XD, Niedernhofer L, Kuster B, Mann M, Hoeijmakers JHJ, de Lange T. ERCC1/XPF Removes the 3′ Overhang from Uncapped Telomeres and Represses Formation of Telomeric DNA-Containing Double Minute Chromosomes. *Mol Cell* 2003; **12**: 1489–1498.

Zhu Z *et al*. p54(nrb)/NONO regulates lipid metabolism and breast cancer growth through SREBP-1A. *Oncogene* 2015; : 1- 12.

Zimmer J, Tacconi EMC, Folio C, Badie S, Porru M, Klare K *et al*. Targeting BRCA1 and BRCA2 Deficiencies with G-Quadruplex-Interacting Compounds. *Mol Cell* 2015. doi:10.1016/j.molcel.2015.12.004.

Zimmermann M, Kibe T, Kabir S, de Lange T. TRF1 negotiates TTAGGG repeatassociated replication problems by recruiting the BLM helicase and the TPP1/POT1 repressor of ATR signaling. *Genes Dev* 2014; **28**: 2477–2491.

Zinyk DL, Mercer EH, Harris E, Anderson DJ, Joyner AL. Fate mapping of the mouse midbrain-hindbrain constriction using a site-specific recombination system. *Curr Biol* 1998; **8**: 665-8.

Zou L, Elledge SJ. Sensing DNA damage through ATRIP recognition of RPA-ssDNA complexes. *Science* 2003; **300**: 1542–1548.

Aknowledgements

Desidero ringraziare il Prof. Stefan Schoeftner per essere stato uno straordinario mentore.
Lo ringrazio per avermi spinto ogni giorno un passo più avanti rispetto alle mie possibilità, stimolando così la mia crescita professionale.
Soprattutto lo ringrazio per avermi indicato, con il suo esempio, l'unica via che permette di diventare un bravo ricercatore: passione e lavoro quotidiano, curiosità insaziabile e grande entusiasmo.

Vorrei ringraziare il Dott. Sabbioneda per aver accettato l'invito del Prof. Schoeftner ed essersi mostrato disponibile a valutare e discutere questa tesi.

Ringrazio i miei co-autori. In particolare, Fabian Jordi e Maria Blasco per aver generato il modello murino transgenico Suv39h1 e per il loro grande contributo al primo progetto di questa tesi.

Ringrazio inoltre Silvia Matteoni (Proteomic Unit, Istituto Regina Elena, Roma) per la spettrometria di massa e le ex-colleghe Rosanna Sestito e Carmen Vico (Istituto Regina Elena, Roma) per la disponibilità e collaborazione.

Grazie al Laboratorio Nazionale CIB, in particolare a Roberta Benetti ed il suo gruppo per la collaborazione.

Ringrazio i miei colleghi Valentina e Roberto per aver contribuito ad entrambi i progetti di questa tesi, ma soprattutto per il confronto e l'incoraggiamento costante. Saper di poter contare su di voi in ogni momento è stato di enorme aiuto in questi anni come durante la stesura della tesi. Un grazie anche alla new entry Annie con cui sono certa amplieremo il progetto di p54nrb and PSF.

Infine desidero ringraziare i miei affetti più cari che supportano le mie scelte e che nonostante la distanza sono stati sempre presenti in questi anni come in questi ultimi faticosi mesi.